Author Manuscript

Author Manuscript

Author Manuscript

Author Manuscript

HHS Public Access

Author manuscript

Chem Soc Rev. Author manuscript; available in PMC 2023 October 31.

Published in final edited form as:

Chem Soc Rev. ; 51(21): 9127–9173. doi:10.1039/d2cs00618a.

Bio-Macromolecular Design Roadmap towards Tough Bioadhesives

Hossein Montazerian[a,b,c], **Elham Davoodi**[a,b,c,d], **Avijit Baidya**[e], **Maryam Badv**[b,g,h], **Reihaneh Haghniaz**[c], **Arash Dalili**[f], **Abbas S. Milani**[f], **Mina Hoorfar**[f], **Nasim Annabi**[a,e,*], **Ali Khademhosseini**[c,*], **Paul S. Weiss**[a,b,g,i,*]

[a]Department of Bioengineering, University of California, Los Angeles, California 90095, United States

[b]California NanoSystems Institute, University of California, Los Angeles, Los Angeles, California 90095, United States

[c]Terasaki Institute for Biomedical Innovation, Los Angeles, California 90024, United States

[d]Multi-Scale Additive Manufacturing Lab, Mechanical and Mechatronics Engineering Department, University of Waterloo, Waterloo, Ontario N2L 3G1, Canada

[e]Chemical and Biomolecular Engineering, University of California, Los Angeles, Los Angeles, California 90095, United States

[f]School of Engineering, University of British Columbia, Kelowna, BC, Canada

[g]Department of Chemistry and Biochemistry, University of California, Los Angeles, Los Angeles, California 90095, United States

[h]Department of Biomedical Engineering, Schulich School of Engineering, University of Calgary, Calgary, Alberta T2N 1N4, Canada

[i]Department of Materials Science and Engineering, University of California, Los Angeles, Los Angeles, California 90095, United States

Abstract

Emerging sutureless wound-closure techniques have led to paradigm shifts in wound management. State-of-the-art biomaterials offer biocompatible and biodegradable platforms enabling high cohesion (toughness) and adhesion for rapid bleeding control as well as robust attachment of implantable devices. Tough bioadhesion stems from the synergistic contributions of cohesive and adhesive interactions. This Review provides a biomacromolecular design roadmap for the development of tough adhesive surgical sealants. We discuss a library of materials and methods

[*]**Corresponding Authors** Prof. Paul S. Weiss, California NanoSystems Institute (CNSI), University of California, Los Angeles, Los Angeles, California 90095, United States; Department of Chemistry & Biochemistry, University of California, Los Angeles, Los Angeles, California 90095, United States; Department of Bioengineering, University of California, Los Angeles, Los Angeles, California 90095, United States; Department of Materials Science and Engineering, University of California, Los Angeles, Los Angeles, California 90095, United States; psw@cnsi.ucla.edu, Prof. Ali Khademhosseini, Terasaki Institute for Biomedical Innovation, Los Angeles, California 90024, United States; khademh@terasaki.org, Prof. Nasim Annabi, Chemical and Biomolecular Engineering, University of California, Los Angeles, Los Angeles, California 90095, United States; nannabi@ucla.edu.

The authors declare no competing financial interest.

Author Manuscript Author Manuscript Author Manuscript Author Manuscript

to introduce toughness and adhesion to biomaterials. Intrinsically tough and elastic polymers are leveraged primarily by introducing strong but dynamic inter- and intramolecular interactions either through polymer chain design or using crosslink regulating additives. In addition, many efforts have been made to promote underwater adhesion *via* covalent/noncovalent bonds, or through micro/macro-interlock mechanisms at the tissue interfaces. The materials settings and functional additives for this purpose and the related characterization methods are reviewed. Measurements and reporting needs for fair comparisons of different materials and their properties are discussed. Finally, future directions and further research opportunities for developing tough bioadhesive surgical sealants are highlighted.

Graphical Abstract

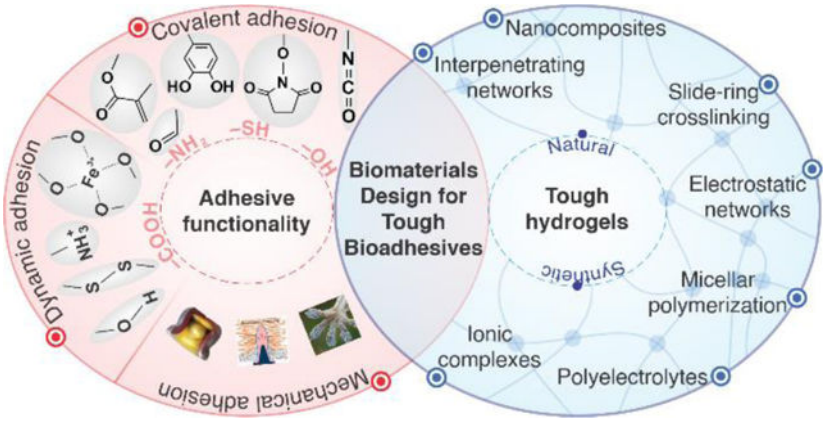

Bioadhesive hydrogels are promising candidates for sealing wounds as replacements for suturing and stapling techniques. Design of biomaterials involves introducing adhesive functionality into tough hydrogel networks.

Keywords

Surgical sealant; bioadhesives; hydrogel; tough; adhesive

Over ~129 million surgical procedures were performed in the US alone in 2018 (with a market value of over $14 billion); this figure is expected to rise to ~144 million procedures per year by 2023 according to MarketsandMarkets™.[1] Current techniques used for surgical wound closure rely heavily on suturing and stapling. These methods are time consuming, require technical skills, cause traumatic tissue damage, and cannot immediately and effectively seal wounds.[2] In particular, in organs with dynamic movement, such as the heart, wound closure is more difficult to perform.[3] As such, there are increased risks of post-operation complications, such as infection. Due to the limitations associated with existing wound-closure techniques, there are unmet needs for developing new methods to manage wounds[4] and lacerations of various types (*i.e.*, surgical, incident, *etc.*).[5]

Tissue sealants and bioadhesives have gained tremendous attention due to their potential for effective wound closure and reducing post-surgery complications.[6] In general, bioadhesives consist of a polymeric matrix (a hydrogel network) that are available either as a wound

Author Manuscript Author Manuscript Author Manuscript Author Manuscript

dressing patch,[7] dry cryogel,[8] or as an injectable glue. Bioadhesive patches are growing rapidly as substrates for smart bandages.[9–13] Hydrogel-based sealants maintain moisture on the skin lacerations.[14,15] They can offer biodegradable platforms for wound-closure purposes.[16] Injectable bio-glues are fit-to-shape sealants that can conform easily to the double-curved tissue surfaces.[17,18] They can interlock mechanically with the tissue in addition to providing adhesion. They can be loaded with antimicrobial and hemostatic agents, to prevent infection, to promote tissue healing, and to control hemorrhage.[19] In addition, the gelation times of injectable bioadhesives are tuned simply by processing parameters based on the relevant surgical time scales. Despite the numerous advantages offered by current surgical sealants, there remain many obstacles to overcome. Recent Food and Drug Administration (FDA)-approved commercial sealants based on fibrin (Tisseel®, Evicel®, Vitagel™, *etc.*)[20] are used for lung incisions,[21] hernia repair,[22] treatment of refractory chylous ascites,[23] skin grafts in burn surgery,[24] and cleft palate repair.[24] Most commercial sealants lack sufficient adhesion strength and durability, and they are prone to induce immune responses *in vivo*.[25]

Achieving strong adhesion to wet tissue surfaces using hydrogels is a major challenge and requires deep understanding of the mechanisms involved. In general, bioadhesion in hydrogels can fail, either due to rupture in their crosslinking network (cohesive failure) or detachment at the tissue interface (adhesive failure).[26] A number of studies have focused on improving cohesion in adhesive networks in terms of toughness, to prevent failure in bioadhesives.[27] Bioadhesives are required to mimic the mechanical properties of native tissues and are therefore required to be strong yet stretchable and elastic. For instance, photocrosslinked biodegradable hydrogels based on gelatin derivatives such as gelatin methacryloyl (GelMA) can stretch only ~30%, whereas this figure reaches ~150–200% for collagen in skin tissue.[28] Failure of bioadhesion in hydrogels can be exacerbated in wet environments due to significant loss of mechanical strength caused by water absorption.[29] Several strategies have been used to toughen hydrogel networks, but they have yet to be adapted for applications in wounds.

Adhesion failure due to insufficient interactions between the hydrogel and tissue surfaces is a major obstacle in the development of bioadhesives. Many attempts have been made to endow hydrogels with durable wet adhesiveness.[30,31] Efforts thus far have been focused primarily on taking advantage of mechanical interlocks as well as introducing covalent and/or noncovalent bonds with the underlying substrates.[26] Nevertheless, most studies have reported adhesive strengths on the order of 10^1–10^2 kPa for hydrogel-based bioadhesives,[32] which is significantly lower than the intrinsic strength of most native tissues in the human body (*e.g.,* up to 15 MPa for skin).[28] The lack of appropriate adhesion strength in recently developed bioadhesives has motivated research to explore novel biomaterials for stronger adhesion.[33]

Conflicting bioadhesive design requirements result in compromising one property when optimizing others.[34] For instance, a high swelling ratio is desired to induce hemostasis, and thereby, stop hemorrhage rapidly,[35,36] whereas the augmented swelling in hydrogels usually deteriorates adhesion strength.[19,37] In many cases, enhancing cohesion decreases adhesion and *vice versa*.[38] Hence, to choose the proper polymer network, crosslinking strategy, and

Author Manuscript Author Manuscript Author Manuscript Author Manuscript

adhesion mechanism for a cohesive (tough) and adhesive network, a rational design map is required to meet the specific requirements based on the intended application. As the field progresses, additional capabilities, such as monitoring biological function will be built into bioadhesive materials.[39,40]

In this Review, we discuss a broad range of biomaterials and fabrication methods that serve to enhance cohesion and adhesion, along with their advantages and shortcomings. As illustrated in Figure 1, the design of bioadhesives begins with the selection of a polymer backbone and a crosslinking mechanism that supports cohesion and toughness in the material. Hence, we first cover the macromolecular strategies and various crosslinking chemistries used to engineer tough and stretchable hydrogels. Then, a variety of chemical and physical mechanisms can be used to introduce interfacial interactions for adhesion. Therefore, the subsequent sections are devoted to biomaterial types and modification procedures leveraging their bioadhesion. We discuss the measurements used to compare materials and their properties. Finally, current challenges and targets for future research and development in tough bioadhesives are highlighted.

Cohesive biomaterials: Tough stretchable polymers

Tuning intra- and intermolecular chemical and physical interactions are essential for bioadhesives, to enhance their cohesion and adhesion. Cohesive failure refers to the early failure of polymer matrix that occurs before the tissue/hydrogel interface is damaged.[41] The mechanical mismatch between the sealant and tissue is a major cause of cohesive failure. This issue is particularly observed in brittle hydrogels, as they fail to comply with the tissue deformation.[42] To address this issue, bioadhesives with high stretchability and strain recovery are favored. These characteristics are reflected in so-called “tough” hydrogels.[43]

Most organs and tissues in the body, such as the myocardium, undergo continuous dynamic deformation. However, hydrogels, if not processed and designed properly, are rather brittle (mainly due to uncontrollable and inhomogeneous crosslinking distributions)[44,45] and are thereby susceptible to failure in response to dynamic loads. Therefore, they fail mostly at much lower fracture energies than natural tissue (*e.g.*, two orders of magnitude lower than cartilage).[46] Hence, considerable effort has been devoted to tuning the mechanical properties of bioadhesives to minimize mechanical mismatches with underlying tissue.[47] Soft, compliant hydrogels are of great interest to avoid early adhesion failure.[42] Failure in adhesion stems primarily from the deformation resistance in stiff hydrogels. The advances made for creating tough, yet compliant and stretchable hydrogels are inspired largely by efforts made in the field of flexible electronics and stretchable wearable devices[48–50] such as ultrasonic devices.[51] Similar principles can be implemented for the development of mechanically robust tissue adhesives. Below, methodologies to fabricate tough and stretchable hydrogels are highlighted.

Interpenetrating multi-network hydrogels

One common approach to enhance toughness in hydrogels is to support covalent polymer networks with secondary networks that can dissipate the deformation energy *via* non-

Author Manuscript Author Manuscript Author Manuscript Author Manuscript

covalent reversible attractions. In these so-called “interpenetrating polymer networks (IPN)”, reversible dynamic bonds reform continuously once polymer chains start to break off under tensile mechanical loads.[41] These double networks can also be formed *via* crosslinking two separate polymers with different chain lengths.[52] In these networks, when mechanical loads are applied, initially, the short-chain bridging networks are first ruptured irreversibly under tension, and thereafter, the long-chain macromolecule-based networks bear larger deformations.[53] Alginate, hyaluronic acid (HA), and chitosan are among the natural biomolecules used to introduce such short-chain energy dissipative networks in these hydrogel systems. Poly(acrylamide) (PAM) and poly(ethylene glycol)diacrylate (PEGDA) are the most commonly used long-chain polymer backbones used as elastic covalent networks.[46,53,54]

Incorporating chemical functionality that enables different crosslinking possibilities, such as covalent and ionic interactions, has leveraged tough hydrogels. The ionic crosslinks between the chains are broken reversibly during tensile deformation, whereas the covalently crosslinked network provides additional support by bridging the cracks through the dynamic molecular rearrangements.[52] For example, a maximum stretchability of 23× was obtained in a PAM-alginate hydrogel due to the synergistic effects of covalent and ionic crosslinked networks. This stretchability was significantly higher than that of its constitutive components (alginate and PAM with 1.2× and 6.6× stretchability, respectively).[52] Similarly, the addition of ionically crosslinked alginate within a poly(ethylene glycol) (PEG) network enhanced the stretchability of the hydrogel from ~300% to ~400% compared to control PEG samples.[55] One possible drawback associated with tough double network hydrogels is the permanent rupture of the short chains and thereby high mechanical hysteresis in response to cyclic loads.[56] This issue was addressed in the alginate-PEG crosslinked network, where alginate re-associates after removing the load, enabling the hydrogel to self-heal after each loading cycle.

In combination with covalent networks, hydrogen bonding between two polymers also improves toughness. This effect was demonstrated in a PAM and poly(ethylene oxide) (PEO)-based hydrogel (see Figure 1A).[57] The stretchability of the composite material was controlled by changing the concentration of PEO. At 8 wt.% PEO, approximately 5× improvement in stretchability was observed, compared to pure PAM. This effect was more prominent for lower molecular weight PEO due to the fewer polymer entanglements. In addition, the hydrogels were also characterized by high tear resistance (Figure 1B–D).

Copolymerization of different monomers is another simple approach to design multi-network tough hydrogels. Recently, a polymeric matrix with a pH-sensitive swelling was prepared through copolymerization of acrylamide (Aam) and acrylic acid (AA) monomers within an agar network.[58] Agar is a thermosensitive linear polysaccharide that forms a gel below 35 °C. Integration of agar within poly(Aam-*co*-AA) network led to a pH-sensitive tough hydrogel (stretchability on the order of 1500%) with tunable mechanical properties.

Interactions between two oppositely charged polymers drive another class of double-networked stretchable and tough hydrogels. For instance, strong electrostatic complexation of positively charged poly(diallyldimethylammonium chloride) (PDDA)/

Author Manuscript Author Manuscript Author Manuscript Author Manuscript

branched poly(ethylenimine) (PEI) and negatively charged polyelectrolyte mixture of poly(sodium 4-styrenesulfonate) (PSS)/poly(acrylic acid) (PAA), led to tough and stretchable (the maximum strain at the break of ~2400%) hydrogels (Figure 1E–G).[59] The stretchability of the hybrid hydrogel was tunable by modifying the concentrations of the chemical constituents (*i.e.*, the PDDA-PSS to PEI-PAA ratio). In addition to electrostatic interactions, *in situ* formation of PDDA-PSS nanoparticles within the PEI-PAA crosslinked chains introduces dynamic hydrogen bonding, which improves the mechanical properties of the synthesized biomaterial (Figure 1G). In another study, coacervation of natural bio-polyelectrolytes, such as the mixture of chitosan and HA in NaCl solution (due to syneresis, the expulsion of liquid) led to highly stretchable hydrogels.[60] The hydrogels were developed by desalting the mixture of chitosan and HA under different dialysis pH conditions. Changing the pH from the pK_a of amine groups in chitosan (6.3) to the pK_a of carboxylic acid in HA (2.9) during the dialysis process led to improvement in hydrogel stretchability (Figure 1H). At low pH (<3), HA molecules fold due to strong intra- and intermolecular interactions, while chitosan chains form extended conformations (Figure 1I,J). Thus, hydrogen-bonding interactions within the folded network of HA acted as energy-dissipating components improving the cohesive strength of the hydrogel.

Ionic hydrogels

Electrolytes have shown improvements in the stretchability of hydrogels by introducing dynamic ionic and dipole-dipole interactions. Such ionic hydrogels are electrically conductive, in addition to their mechanical stretchability, which is important in wearable and implantable devices.[61–63] Improved stretchability in ionic hydrogels is attained due to dynamic ionic interactions.[64] For example, poly(vinylidene fluoride-*co*-hexafluoropropylene) (PVDF)-*co*-hexafluoropropylene (HFP) polymers with high HFP content (*i.e.*, 45 wt.%) served as highly polar polymers that can be easily crosslinked upon the addition of an ionic liquid (*i.e.*, imidazolium).[64] The strong, reversible interactions between the polar groups on the polymeric chain and the ionic salt resulted in polymeric matrices with stretchability on the order of 5500%, while the lower ionic liquid concentrations showed stretchability of *ca.* 1000%. Here, the deformation of the material was fully reversible for strains smaller than 50%. Higher levels of strain reversibility (up to 100% strain) were obtained in ionic hydrogel systems composed of physically crosslinked poly(vinyl alcohol) (PVA) in NaCl solution.[65] In this hydrogel, hydroxypropyl cellulose (HPC) drew in Na^+ and Cl^- ions, leading to high ionic conductivity. The addition of HPC (16 wt.%) led to lower PVA crosslinking density. Hence, an ion-rich, porous PVA network with improved stretchability up to ~800% (from ~550%) was achieved. Variation of the NaCl concentration, from 0 to 5 M, increased the hydrogel stretchability from 300% to 850%. Stretchable hydrogels enabled by ion-dipole and dipole-dipole interactions were synthesized by using an ionic liquid (*i.e.*, 1-ethyl-3-methylimidazolium dicyanamide ([EMIm][DCA])) that also led to high electrical conductivity in the hydrogels.[66,67] The ionic liquids composed of [EMI][DCA] were used to develop a new type of hydrogel matrix where polymerization of 3-dimethyl and AA monomers was propagated in the presence of methacryloyloxyethyl ammonium propane sulfonate (DMAPS). This process resulted in dipole-dipole interactions between pendant zwitterionic functional groups and resulted in stretchability on the order

Author Manuscript Author Manuscript Author Manuscript Author Manuscript

of ~800%. Copolymerization of AAm and AA in the presence of $CoCl_2$ demonstrated a similar effect (see Figure 3A).[68] In this case, the hydrogel showed stretchability of greater than 1200%. Additionally, increasing the Co^{2+} concentration led to increased stretchability, from 300% to 700% (see Figure 3B,C). This stretchability was due to strong ionic interactions between Co^{2+} ions and the carboxylic groups present in the polymeric backbone that act as dynamic crosslinking points. The addition of Co^{2+} also enhanced the self-healing of the hydrogels (Figure 3D). Integration of other ionic liquids (*e.g.,* 1-ethyl-3-methylimidazolium ethyl sulfate) with PAA and a polyzwitterionic macromolecule, poly(3-dimethyl(methacryloyloxyethyl) ammonium propane sulfonate) (PDMAPS) has been shown to form strong hydrogel networks.[69] In this study, the hydrogel was reinforced by the ion-dipole interactions due to the ionic liquid, leading to stretchability ranging from 2000% to 100,000%, at different ionic-liquid-to-PDMAPS ratios. We attribute the low stretchability and the high elastic modulus in the absence of IL to dipole-dipole interactions (due to the ion-rich sites of the polyzwitterionic chain). Here, the addition of ionic liquids reduced Coulombic interactions, which results in enhanced stretchability (at 1:2 molar ratio of ionic liquid:PDMAPS). However, excess ionic liquid content leads to imperfect binding and uncontrolled interactions between the ionic liquid and polyzwitterionic macromolecules, degrading mechanical properties.

Recently, a physically crosslinked PVA-based hydrogel was crosslinked through hydrogen bonding between hydroxyl groups on the polymer chains.[70] Here, crosslinking in the presence of H_2SO_4 increased stretchability up to 380%. To enhance the stretchability of the synthesized PVA-based hydrogel, salts of a weak acid (*e.g.*, borax), were introduced to the system to interact with the tetrafunctional borate ions and hydroxyl groups of PVA macromolecular chains (Figure 3E,F).[71] The hydrogels showed stretchability of up to 1000% at 4 wt.% PVA concentration (Figure 3G).

Macromolecular modulation of crosslinkers and monomers

The chemical structures of the monomer units in single-component hydrogel systems play key roles in their mechanical properties. Many studies have examined the effects of polymerization processing parameters and monomer structure on mechanical properties. Chemical functionalization of the macromolecules, *e.g.*, with allyl and methacryloyl groups, enables crosslinking through radical polymerization reactions in the presence of chemical initiators.[72] For instance, modification of cellulosic biomaterials with allyl glycidyl ether led to crosslinkable allyl cellulose.[73] Polymerization of allyl cellulose in NaOH/urea solution using an ammonium persulfate (APS) initiator led to the stretchability of 126% (as opposed to <100% for those of unmodified cellulose hydrogels).[74]

The tertiary amine groups present in aliphatic amines such as *N,N,N',N'*-tetramethylethylenediamine (TEMED) can catalyze the chemical reaction with APS through electron transfer, producing free radicals for polymerization at room temperature. Redox polymerization enabled by introducing the tertiary amine on the monomer itself enhances stretchability.[75] By conjugating aliphatic amine functionality on the monomer backbone or the crosslinker, the crosslinking sites can be distributed more homogenously, leading to tough hydrogels. Figure 4A shows a polymeric network containing polyetheramine (PEA)

Author Manuscript Author Manuscript Author Manuscript Author Manuscript

and a linear epoxy with covalently grafted tertiary amines. The grafted tertiary amines enable the polymer molecule to act as an initiator during the radical polymerization process. Finally, polymerization of PEA along with PAM leads to a highly stretchable (up to 2000%) hydrogel and strain recovery for strains smaller than 1000% (Figure 4B, C), which was significantly larger than that of PAM hydrogels.

As discussed above, the chemical structure of the crosslinker is a key factor in the hydrogel toughness and elasticity. Changing the lengths of polymer chains and crosslinkers can significantly affect the stretchability of hydrogels. Stretchable PAM-based hydrogels crosslinked using PEGDA with different chain lengths show significant increases in swelling and stretchability when longer chains of PEGDA are used.[58] Similarly, a linear epoxy polymer with multiple tertiary amine sites (*i.e.,* PEA) was designed (initiating polymerization) to synthesize a PAM-based hydrogel with stretchability as high as 2000%.[75] Figure 4D illustrates a PAA polymer-based crosslinked hydrogel network synthesized with Pluronic F127 (F127DA) molecules.[66] Both stretchability and strength were enhanced with increased crosslinker concentration. Although at concentrations higher than 36 mg/ml, the stretchability was found to decrease with F127DA, the strength continued to increase.

Liquid metals are employed as additives for tuning the polymerization rates and mechanical properties of hydrogels.[76] Liquid metals act as redox catalysts and therefore accelerate the radical generation in APS-based radical-generation systems.[77,78] Gallium indium eutectic (EGaln) (composed of 75 v/v% gallium and 25 v/v% indium) is an example of a gallium-based liquid metal, which can be introduced in hydrogel systems to enhance toughness. Encapsulation of EGaln in graphene oxide (GO) nanoparticles through coordination with Ga^{3+} led to crosslinking complexes that can form hydrogen-bonding and covalent interactions with polymer matrices composed of alginate and polyacrylamide. These interactions resulted in over 4× improvement in stretchability.[77] Solutions of liquid metals are generally unstable in water; however, when mixed with polar monomers (*i.e.,* AAm and 2-hydroxyethyl acrylate, HEA), they can enhance surface interactions and form stable dispersions that favor polymerization of tough hydrogel materials (Figure 4E).[79] Co-gelation of the abovementioned monomers occurred within 20 s, once potassium persulfate (KPS) was added at room temperature. Tensile tests demonstrated that the hydrogels could stretch up to 1500%, as shown in Figure 4F–H (~4× higher than the control samples with no liquid metal content), confirming the potential use of liquid metals as an effective strategy for toughening the hydrogel network.

Slide-ring crosslinking

Slide-ring crosslinking is a relatively new chemical platform for introducing toughness into hydrogels.[80] These hydrogels are formed of a series of pulley-shaped molecules that pass through linear polymeric chains, which can slide freely along those chains.[81] This crosslinking approach reduces the stress concentration at the crosslinking sites when external deformations are applied.[81] Polyrotaxane (PR) derivatives, composed of cyclodextrin polysaccharide units, are one such moiety that can slide freely along linear chains, such as PEG.[81] Low concentrations (2–3 wt.%) of these pulley-shaped cyclodextrin

Author Manuscript Author Manuscript Author Manuscript Author Manuscript

molecules improve the stretchability of PVA hydrogels (up to ~1600% elongation at break).[82]

One of the main limitations of the unmodified PR however, is its poor water solubility, due to the hydroxyl-induced aggregation of the cyclodextrin molecules limiting the sliding effect of cyclodextrin along the chains.[81] High pH can be used to ionize the hydroxyl groups to avoid cyclodextrin aggregation; however, it is not always practical to polymerize hydrogels at high pH. Recently, a tough slide-ring hydrogel with enhanced water solubility was synthesized using carboxyl-functionalized hydroxypropylated PR (HPR) crosslinkers.[81] In this ionic PR-based crosslinker, PR molecules are in their expanded form at the neutral pH. As shown in Figure 5A,B, PR was modified with isocyanates (to form bonds with carboxyl groups) and vinyl groups to crosslink a poly(*N*-Isopropyl acrylamide) (PNIPAM) and PAA copolymer. This approach led to the slide-ring hydrogels with a maximum stretchability of ~1500%, which was significantly higher than the hydrogels crosslinked conventionally using *N,N′*-methylene-bis(acrylamide) (MBAA), (29% elongation at failure) as seen in Figure 5C,D.

Different types of pulley-shaped molecules have been designed to tune their toughening effects. In one example, a molecule with a hydrophobic cavity and inward-facing complementary polar groups formed slide-rings with hydrophilic linear chains, such as PEG.[83] The pseudo-polyrotaxane molecules can crosslink PEG networks with Cu(II) metal ions due to their chelation with carboxyl groups (Figure 5E–G).[84] Gelation was triggered upon vigorous shaking (for ~30 s) because of the applied shear forces. However, the gel was transformed into the sol state for hours or days after formation, depending on the compositions of the different components. These shear-induced hydrogels showed fast self-healing and excellent stretchability (~25–30× more), when compared to controls (Figure 5H).

Micellar polymers

Micellar copolymerization has provided new opportunities to develop different types of stretchable hydrogels where the dynamic hydrophobic interactions between the surfactant micelles and polymer chains define crosslinking points.[85] Reversible bond formation in micelles can deform, break, and reform continuously during mechanical deformation. These dynamic interactions in covalent networks lead to high stretchability in micellar polymers.[86] Stable dispersions of micelles in aqueous solutions are another advantage, as they provide homogeneous and uniform crosslinking distributions throughout the polymeric backbones. Recently, highly stretchable PAM-based hydrogels (with higher than 10000% failure strain) were fabricated using a crosslinker based on hydrogen-bonding and hydrophobic associations (Figure 6A).[87] The synthesized crosslinker consisted of a hydrophobic alkyl spacer that bridged a 2-ureido-4-pyrimidone (UPy) tail to an acrylic head. The crosslinker molecules were encapsulated into sodium dodecyl sulfate (SDS) micelles enabling micellar polymerization of acrylamide through the SDS emulsion. The obtained hydrogels exhibited stretchability over ~100× (Figure 6B).

Author Manuscript Author Manuscript Author Manuscript Author Manuscript

Other studies have revealed the potential mechanical improvements enabled by a combination of hydrophobic interactions and secondary dynamic networks, *e.g.*, using additives such as GO[88] and PVA.[89] The addition of GO in a hydrophobically associated hydrogel increased the crosslinking density through the formation of new hydrogen bonds, which further improved the toughness of the hydrogel matrix as demonstrated in Figure 6C.[88] The synthesized hydrogel showed high stretchability, on the order of ~30×, and could undergo extensive deformations, (*i.e.*, bending, knotting, *etc.*, see Figure 6D,E).

2,4,6-Trimethylbenzoyl-diphenylphosphine oxide (TPO) is a highly efficient photoinitiator for UV crosslinking of polymers. However, the poor water solubility of TPO has limited its use. To address this issue, SDS was used to form stable TPO nanoparticle dispersions in water.[90] The TPO emulsion was further used for 3D printing highly stretchable hydrogels (~1300% stretchability) from PAM-PEGDA hydrogels, which were far larger than conventionally processed hydrogels (*e.g.*, PEGDA with ~150% stretchability). In this study, the TPO nanoparticle-dispersed emulsion improved the polymerization kinetics significantly as compared to commercially available photoinitiator, *i.e.*, Irgacure 2959 (I2959).

Nanocomposite hydrogels

The incorporation of inorganic nanoparticles can enhance dynamic crosslinking and thereby, toughness in hydrogels.[91] The high specific surface area of nanoparticles and the presence of active functional groups on their surface, facilitate their dynamic interaction with the polymer matrix. The stretchability of the polymeric nanocomposite hydrogels depends on the concentration and dispersibility of the nanoparticles, as well as the particle sizes and their chemical structures.[92] The main challenge in the synthesis of nanoparticle-reinforced hydrogels is poor dispersion stability during polymerization.[45] For instance, GO has a large surface area with exposed hydroxyl, carboxyl, and epoxide functional groups that facilitate various physiochemical interactions with the PAM molecules.[44] Recently, hybrid nanocomposite hydrogels based on traces of GO/PAM were observed to exhibit maximum elongation at failure of greater than 3400% (*i.e.*, a 10-fold increase compared to unmodified PAM hydrogels).[44] This improvement is attributed to a variety of molecular interactions, including the combination of the hydrogen-bonding, ionic bonds, and physical interactions between the nanocomposite components. A similar combination of interactions was observed in a PAA and reduced graphene oxide (rGO)-based nanocomposite, where GO sheets functionalized with polydopamine (PDA) introduced a secondary strong ionic crosslinking point upon the addition of Fe^{3+} ions.[93] The mechanical properties of the hydrogel were highly dependent on the concentration of Fe^{3+} and GO. For example, increasing the concentrations of Fe^{3+} and GO to 0.25 and 0.05 wt.%, respectively, resulted in reduced stretchability of the materials from a maximum of ~1250% to ~500%.

Hydrophobic interactions and plastic deformation of the micellar particles play important roles in dissipating deformation energy. Recently, a tough hydrogel was synthesized where the deformation energy dissipated through the frictional forces between the micelles (Figure 7A–D).[94] In this case, casein additives, a milk-based protein molecule, formed micellar-structured nano/microparticles in water where the negatively charged hairy layer present on the surface caused repulsion and thereby a steric stabilization of the particles (Figure

Author Manuscript Author Manuscript Author Manuscript Author Manuscript

7D). Polymerization of these AAm molecules in the presence of casein showed significant improvement in stretchability of the hydrogels, from 1600% to over 3500%, and increased both stiffness and strain recoverability (Figure 7C).[94] In a similar study, a casein-reinforced hydrogel containing dopamine was synthesized to improve the adhesion of the material.[95] Similarly, high stretchability, on the order of 1600–2900%, was obtained when different concentrations of casein (up to 37.5 wt.%) were added to the hydrogel. In contrast to the previous study, although casein additives enhanced the mechanical strength, they compromised the overall stretchability of the hydrogels. Although nanoparticle-reinforced hydrogels have shown great promise with robust mechanical properties, their release can induce cytotoxicity and thrombosis, which require close attention, particularly when considered for internal use.

Hydroxide nanoparticles

The incorporation of hydroxide nanoparticles during the synthesis of hydrogels has proven to be a robust means to toughen hydrogels. Hydroxide nanoparticles introduce dynamic interactions within the polymeric macromolecules and produce reversible crosslinks within polymer networks. For instance, in a recent study, traces of $Ca(OH)_2$ nano-spherulites (40 ppm) were used as dynamic crosslinkers for synthesizing PAM hydrogel matrixes.[96] These particles were less than 5 nm in size and prepared through the hydration of Ca_3SiO_4. Here, the Ca^{2+} ions from the $Ca(OH)_2$ nanoparticles interacted with the $S_2O_8^{2-}$ ions released from APS (Figure 7E). Therefore, the persulfate initiator molecule (capping the chain end through free radical polymerization) favored the spontaneous ionic binding of the polymeric chains at the surface of $Ca(OH)_2$ particles, enabling the formation of a hydrogel network. The crosslinked hydrogel showed remarkable elongation at the break, up to ~12,100% (Figure 7F), along with excellent strain recovery. The improved mechanical properties of these hydrogels were related to (1) the aggregation-free, homogeneous dispersibility of the $Ca(OH)_2$ nanoparticles, (2) increased surface area resulting from single-digit size of $Ca(OH)_2$ nanoparticles, and (3) optimized concentrations of the nano-spherulites, which lowered the formation of connective filaments and thereby resulted in higher pore sizes and enhanced deformability.[96] In another study, the use of Portland cement, instead of Ca_3SiO_4 nanoparticles, enhanced the mechanical properties of the hybrid hydrogel with the maximum stretchability of PAM network, up to ~11,200%.[97] In this case, similar $Ca(OH)_2$ nanoparticles (<5 nm) were synthesized through the hydration reaction of $Ca(OH)_2$ in the presence of a polycarboxylate-ether superplasticizer (PCE) that restricted the precipitation of the cement. The addition of 2–3 nm-sized $Al(OH)_3$ particles instead of $Ca(OH)_2$ nanoparticles resulted in similar properties in the materials. In this case, the presence of inorganic nanoparticles with hydroxyl groups on the surface enhanced hydrogen bonding in PAM molecules, and 2-acrylamide-2-methylpropane sulfonic acid (AMPS)-based hydrogel materials,[98] and resulted in improved mechanical properties. The synthesized hydrogels were observed to have the highest stretchability, on the order of 2090% when 3 wt.% $Al(OH)_3$ was added.

Author Manuscript Author Manuscript Author Manuscript Author Manuscript

Nanoclays

One approach to improve toughness in hydrogels is to reinforce them with various nanoclays with strong surface charges. Recently, the addition of exfoliated Montmorillonite (MMT) clay particles ($[(Al,Mg)_4Si_8O_{20}(OH)_4]Na_{0.66}$) during the polymerization of PAM (Figure 7G) led to remarkable increases in the stretchability of hydrogels, on the order of 11,800%, compared to ~40% for the PAM hydrogels crosslinked by MBAA using APS/TEMED.[99] Another hydrogel with a similar chemical composition showed significantly reduced stretchability of 1290% when the polymerization reaction was carried out without TEMED.[100] The chemical reaction conditions play critical roles in the hydrogel mechanical properties. Laponite® nanoclay particles, ($[Mg_{5.34}Li_{0.66}Si_8O_{20}(OH)_4]Na_{0.66}$), enhanced the mechanical properties of hydrogels. *In situ* polymerization of PAM with Laponite® at ~4 wt.% improved the elongation at break (stretchability up to ~5000%).[101] Similar improvements were achieved through crosslinking PAM linear chains in the presence of a 60 nm double-layer hydroxide (DLH) with a chemical formula of $[Mg_{2.52}Al\ (OH)_7](HO\text{-}(CH_2)_2\text{-}SO_3)\cdot 1.27H_2O$.[102] In this study, ionic interactions between nanoparticles and initiators led to the formation of clay-brush particles, connecting the linear polymeric chains in an APS/TEMED crosslinking system. The electrostatic interactions involved in DLH/PAM nanocomposites were responsible for the improved mechanical properties (~3000% stretchability) of the developed hydrogel moiety at the optimum ~5 wt.% clay content. The hydrogen bonding between the clay and the initiator/catalyst system contributed to this improvement. In combination with dopamine, talc particles were well dispersed in water and facilitated the polymerization of dopamine molecules over the talc surface through partial oxidation.[103] The PDA-coated talc nanoparticles were embedded within the PAM network and enabled several dynamic interactions including physical attractions between the PDA and PAM molecules, **π**–**π** stacking, and hydrogen bonding between PDA and PAM. In this case, at dopamine:AAm and talc:AAm ratios of 0.5 and 0.75%, respectively, a maximum stretchability of over 1500% was reported.

Surface-functionalized nanoparticles

Apart from the non-covalent interactions discussed above, covalent bonds between the polymer molecules and various functionalized nanoparticles can also improve toughness in hydrogels. Copolymerization with these crosslinking regulating nanoparticles is achieved primarily by nanoparticle surface functionalization with reactive functional groups such as methacrylates. For instance, silica nanoparticles were modified chemically with vinyltriethoxysilane (VTES) through a sol-gel process and covalently crosslinked with PAM chains (Figure 7I,J);[104] as a result, stretchabilities over 3400% (Figure 7K,L) were reported.[105] A similar approach was demonstrated to polymerize AAc monomers. In this study, the incorporation of Fe^{3+} ions induced reversible ionic interactions and promoted interchain associations through the chelation of carboxylic groups.[106] These reversible interactions were further supported by hydrogen bonding and resulted in strain at break of 2300%,[106,107] while the control PAA crosslinked material showed stretchability of up to ~1500%. Similarly, gold nanoparticles were used to serve as a vehicle to carry surface-attached double bonds across the polymeric network. In this case, *N,N*-bis(acryloyl)cystamine (BAC) molecules with polymerizable alkyl groups were grafted

Author Manuscript Author Manuscript Author Manuscript Author Manuscript

chemically onto the gold nanoparticles. Because of chemical affinity between Au and S atoms, covalently crosslinked hydrogels were formed where crosslink points were cleavable due to the disulfide (S-S) bonds.[108]

Bioadhesive materials: Synthesis and characterization

After tough polymer networks are designed with a proper selection of backbone and crosslinking strategy through the methods discussed above, a variety of approaches can be employed to introduce adhesion (Figure 1). Long-lasting and strong adhesion to tissue surfaces is an essential requirement in bioadhesive sealants. The mechanical stability of the sealants depends on the synergy between the adhesion and cohesion.[30] Typically, adhesive failure occurs when the inter- and intramolecular interactions within the hydrogel network are stronger than the interactive forces between the tissue and sealant material.[26] This failure becomes even more of a concern when it comes to wet tissue surfaces. Furthermore, the gradual swelling of hydrogels, due to the absorption of biofluids, presents another challenge that needs to be taken into account.[29]

Although the underlying mechanisms of adhesion are not fully understood, adhesion is being explored rigorously through chemical covalent and non-covalent (such as hydrogen-bonding[109,110] and cation-π[111,112]) interactions as well as physical (mechanical interlocks, tissue fusion, and topological chain entanglement[113]) pathways. Nucleophilic functional groups present on the tissue surfaces drive chemical interactions of the bioadhesives to the underlying tissue substrates.[114,115] From a mechanical viewpoint, interlocking between the bioadhesives and uneven tissue surfaces can also favor bioadhesion.[116] In this regard, ultrasound-induced cavitation in hydrogels is emerging as a means to enhance polymer entanglement with tissues for tough bioadhesion.[117] In the following sections, we give a detailed overview of recent advances made in creating bioadhesive materials, and methods involved in their development. First, we introduce the testing methods used to characterize and to assess adhesion. Standard testing methods of key properties are critical to fair comparisons of materials prepared by different laboratories. Then, we discuss the chemistries involved in creating synthetic, natural,[118] and bio-inspired adhesives to enhance wet adhesion in bioadhesives.

Experimental characterization of adhesive strength

Several methods have been reported to quantify the adhesive strength of hydrogels. Despite having standardized procedures to demonstrate tissue adhesion, the lack of consistency seen in the testing instrumentation and its implementation makes it difficult to compare and to evaluate the adhesive characteristics of different hydrogels. Adhesion strength values are influenced by several handling and testing factors, including the loading rate, environmental temperature, humidity and dryness (which affect the hydrogel dimensions overtime), and substrate type.[30] Depending on the application and curing mechanism, a proper testing method should be selected to characterize adhesion strength. For example, photopolymerization requires illumination with light (with a certain wavelength), which may not be possible in testing adhesives that are applied between light-absorbing adherents (*i.e.*, in a lap shear test).

Author Manuscript Author Manuscript Author Manuscript Author Manuscript

Axial adhesion strength, one of the simplest methods to test the adhesion of the material, defines the maximum load that an adhesive can tolerate under tensile loading.[119] In this case, the axial detachment of the adherents determines the failure point. Peeling tests reflect the normal adhesion of the materials, which can be carried out in 90° or 180° configurations.[119] Another method is the burst pressure test, which simulates the seals on tissue incisions while subject to liquid pressure. Here, the stability of the sealant under increasing liquid/air pressure is measured. This test determines the origin of failure, which can be related to cohesion, adhesion, or a combination of both. The lap shear test evaluates the adhesion under shear deformations. The wound-closure test consists of filling the gap between two separate pieces of tissues or filling an incision on an integral tissue piece with an adhesive material. In this test, the tensile load applied to the tissue ends is transferred to bioadhesive in both shear (adhesive) and tensile (cohesive) modes.[120]

The sealing capacity of the sealants can be evaluated *ex vivo* by polymerizing the prepolymer on punctured tissue while flowing biological fluids at the tissue/adhesive interface to mimic the real-time sealing performance under heavy bleeding conditions.[121] Given the dynamic loading applied to the tissue adhesives, looking at the cyclic decays in the above-mentioned testing platforms can be of importance. However, the cyclic response of bioadhesives has not been as thoroughly investigated as the static tests in the literature.

Synthetic bioadhesives

Synthetic polymers are synthesized using organic compounds to develop bioadhesives with the desired functionality.[122] Synthetic hydrogels provide a versatile platform for introducing functional bioadhesives with thermo-responsive, electrical conductivity, and stimuli-responsive properties. For example, a thermo-responsive sealant was engineered based on the copolymerization of physically crosslinked PNIPAM and butylacrylate molecules for occluding open globe injuries of the eyewall.[123] Being liquid at room temperature, the resulting copolymer enabled facile injection, which then transitioned to a solidified occlusion at (higher) body temperature. This sealant showed reversible sealing with adhesive strength comparable to cyanoacrylate glue, with no neurotoxicity nor significant inflammatory responses. Thermosensitive coacervate complex formation for bioadhesion was also demonstrated in a PNIPAM-based hydrogel containing charged polyelectrolyte moieties.[124] The precursor solution was in the liquid state at room temperature and could form a nonflowing adhesive coacervate complex at temperatures above the lower critical solution temperature (LCST) (with lap shear strength on the order of ~7 kPa). Another example of temperature-driven coacervate formation with LCST was proposed by Narayanan *et al.*[125] A protein-like polyester statistical copolymer composed of a tropoelastin-mimicking unit responsible for coacervate formation (*i.e.*, bis(2-methoxyethyl)succinimide pendant), a catechol containing unit for adhesion, and a light-activatable mechanical strengthener was incorporated into a hydrogel for underwater adhesion over a wide pH range, 3–12. The highest adhesion strength was measured to be ~100 kPa for the optimal conditions in lap shear tests.

Synthetic approaches have leveraged bioadhesive electronics for monitoring chemical and physical signals.[126–128] Implantable sensors and wireless devices[129] should be adhered

Author Manuscript Author Manuscript Author Manuscript Author Manuscript

firmly to their target tissue to be able to function for long periods to monitor diseases.[130–132] Several bioadhesive materials have been proposed for the attachment of bioelectronic devices to tissue. Zhao and coworkers fabricated a stretchable adhesive dry patch based on PAA[133] that adheres to wet tissue surfaces. Here, hydrogels were formed by absorbing tissue moisture,[133] as a result of which the reactive functionalities in the designed materials could interact readily with the biological surfaces to form covalent and noncovalent linkages. The PAA was functionalized with *N*-hydroxysuccinimide (NHS) to stabilize long-term adhesion through covalent attachment to the amine groups present on the tissue.[133] A similar patch was used as a platform to develop graphene nanocomposite-based conducting adhesive patches with high electrical stability.[134] These dry patches were fabricated based on origami architectures to enable their application in minimally invasive surgical tissue sealing.[135] Another example involves an adhesive supercapacitor based on polyaniline (PANI), rGO, and MXenes embedded in a hybrid hydrogel based on PVA and NHS functionalized PAA.[136] Here, hydrogel electrodes can bind efficiently to the biological surfaces for bio-integration of electronic systems. Synthetic patches were also designed with stimuli-responsive functionality to fabricate on-demand detachable bioadhesives.[132,137–139]

Many synthetic adhesives demonstrated in the literature require the use of cytotoxic procedures and hence, may not be used in biomedical applications;[140] however, studies of these materials can lead to insight into the design of biocompatible medical adhesives. For instance, a creeper sucker-inspired adhesive was synthesized utilizing poly(hydroxyethyl methacrylate) (PHEMA) containing crystallizable 1-ethyl-3-methylimidazolium bromide ([EMIM]Br) solvents.[141] This study highlighted that hydrogen åbonding has tremendous potential to transmit adhesion stress robustly, to enable high adhesive strengths of ~10 MPa (in lap shear test using glass substrates). Strong hydrogen-bonding-driven bioadhesives were demonstrated *via* coacervate formation[142] as well as the incorporation of triple hydrogen-bonding clusters (THBC) in other examples.[143] For the latter, a copolymer composed of *N*-(3-aminopropyl)methacrylamide hydrochloride (APMA) decorated with *N*-[tris(hydroxymethyl)methyl]acrylamide (THMA) (a branched hydroxyl-capped component) was synthesized. A so-called “load shearing” effect in the high-density hydrogen-bonding network explained the high maximum adhesion strength of ~120 kPa in a lap shear test using glass slides.

Other synthetic copolymers were developed for bioadhesion with specific functionality for a wide variety of tissues. In a recent study, a copolymer composed of AAm (for network cohesion), methyl acrylate (for hydrophobicity), AA (for mucoadhesion), and MBAA (for crosslinking) was synthesized.[144] This hydrogel system was obtained through a photocrosslinking process either as an *ex situ* patch or *in situ* glue for the prevention of intestinal anastomotic leakage. Adhesion strength (lap shear test) for *ex situ* (~7 kPa) was significantly lower than *in situ* application (~12 kPa). The study found that AA plays a major role in adhesion force as increasing the AA acid content from 0 to 25 wt.% led to increases in adhesion force by over ~700%. Further increases in acrylic acid content, however, deteriorated mechanical properties. Bioadhesive powders[145] were introduced for rapid hemostasis *e.g.*, using a synthetic/natural combination of PEI, PAA, and quaternized chitosan (QCS).[146] The powders were characterized by self-gelling properties (gelation in 4 s) upon contact with and absorption of blood plasma. Due to

Author Manuscript Author Manuscript Author Manuscript Author Manuscript

the strong adhesion (burst pressure ~ 240 mmHg), bleeding could be arrested in 10 s. Thermoplastic biomaterials such as polycaprolactone (PCL) have also shown potential for use as bioadhesives.[147] These materials could be applied topically at elevated temperatures (40–50 °C, depending on the PCL molecular weight) using a glue gun.[148] The star-PCL structures with carboxyl end groups were activated using amine-reactive NHS ester for bioadhesion. The proposed bioadhesive achieved ~50% of the Dermabond®'s adhesion strength (a commercial cyanoacrylate-based glue). Elastomeric bioadhesives are emerging as promising backbones due to their intrinsic toughness and stretchability. Poly(glycerol sebacate) (PGS) is one example of a degradable elastomer synthesized through condensation reactions between sebacic acid and glycerol.[149] A modified PGS involving PEG chain expanders and dihydrocaffeic acid additives for adhesion was demonstrated in combination with a secondary gelatin-based network.[150] Here, gelatin was modified with UPy to endow self-assembly and self-healing properties to the biomaterial. Significant improvements in adhesive strength were achieved by increasing the gelatin-UPy content (by over ~10×).

Synthetic bioadhesives, in many cases, are designed to mimic the structures of adhesive materials found in natural organisms.[151] The strong hydrogen-bonding interactions in DNA molecules inspired the design of a nucleobase-modified polyphosphoester hydrogel adhesive (Figure 8A–C).[152] This monomer consists of purine rings and pyrimidine functionality that introduce hydrophobic reactions as well as hydrogen bonding to the hydrogel. The resulting hydrogel is degradable under alkaline conditions; therefore, these adhesive hydrogels (maximum lap shear ~40 kPa) can be removed on demand with exposure to high pH, without leaving behind any glue residues on the tissue surface. In another study, barnacle-inspired adhesive pads were synthesized using a copolymer consisting of hydrophobic aromatic 2-phenoxyethyl acrylate and positively charged 2-(acryloyloxy)ethyl trimethylammonium chloride (ATAC).[153] Mechanical toughness was achieved due to the dynamic **π**–**π** and cation–**π** interactions, leading to stretchability of over ~700%. The high maximum adhesion strength of 180 kPa was obtained in the axial adhesion tests for samples with hydrophobic monomer (*i.e.*, 2-phenoxyethyl acrylate) molar fractions of 0.85, which was ~7× larger than those with 0.7 aromatic content ratio. In general, synthetic adhesives result in higher adhesion strength (in the MPa range) compared to most natural bioadhesives. In a recent study, a waterborne, synthetic yet biocompatible, and strong (~6 MPa adhesive strength) bioadhesive was proposed for dental tissues.[154] Here, inspired by insect sclerotization, a cost-effective procedure based on phenol-polyamine reaction served to seal skin wounds within a few seconds.

Combinations of synthetic networks with natural hydrogels are used frequently to enable biodegradation and to improve bioadhesion performance in tough hydrogel platforms.[155,138] Recently, a mixture of PAM and alginate macromolecules was used to design tough hydrogel materials, which were applied to the tissue surfaces in the presence of 1-ethyl-3-(3-dimethylaminopropyl)carbodiimide (EDC) and NHS coupling reagents. *Ex vivo* adhesion energy for these materials was in the range of 300–700 J/m^2.[156] In another report, an adhesive hydrogel patch was developed using a covalent network containing energy dissipative alginate (tough IPN matrix) as shown in Figure 8D–F.[157] This patch was treated with coupling chemicals that diffused through the hydrogel matrix and acted as a bridging layer. The bridging polymer, comprised of amine-rich macromolecules,

Author Manuscript Author Manuscript Author Manuscript Author Manuscript

enabled the covalent bonding between hydrogel and tissue surface through substitution reactions. Active functional groups present on the tissues favored covalent adhesion and responded spontaneously upon the application of gentle pressure on the hydrogel patch. The materials synthesized with polyallylamine and chitosan (bridging polymers) possessed the strongest adhesion when compared to PEI, collagen, and gelatin with adhesion energy on the order of 10^3 J/m^2. This adhesion energy was significantly higher for tough PAM-alginate-based double network hydrogels when compared to the corresponding adhesion energy of individual constitutive components, indicating the substantial roles of cohesion in bioadhesion.

Topological adhesion has recently emerged as a potential mechanism for bioadhesion. In this process, polymer chains of two hydrogel networks are stitched together at their interfaces through a stitching polymer chain that can entangle within the hydrogel networks through diffusion. The diffused and entangled chains of stitching polymer are then associated together *via* an external trigger such as pH.[113] This concept was demonstrated using a variety of synthetic hydrogels and different stitching polymers (*i.e.*, chitosan, alginate, and cellulose) that can associate strongly and crystallize at higher pH than their pK_a at the adhesion interface. Stitching (gluing) polymers can also be used to attach *ex situ* crosslinked hydrogels to tissues. An example of a gluing polymer developed by Gao *et al.* involves a PAA modified with catechol groups where entanglement and crosslinking with the backing hydrogel are triggered by $NaIO_4$ solution.[158] This bioadhesive system was able to adhere PAM hydrogels to tissue surfaces robustly (with peel-off adhesive energies of ~150–200 J/m^2). Overall, synthetic approaches provide more versatility when it comes to designing multifunctional and stimuli-responsive bioadhesives.

Cyanoacrylates

Since the 1960s, cyanoacrylate-based polymers were used extensively as surgical sealants due to their high adhesion strength to wet surfaces. However, the heat generated during polymerization and the resulting toxic degradation byproducts have limited their use for internal tissues.[159] Moreover, complications associated with exothermic reaction-induced tissue damage, granulomatous keratitis, glaucoma, and cataract formation have further caused concerns for the application of such biomaterials in clinical settings.[160] These complications have motivated researchers to design biosafe alternatives with similar adhesive strengths. One common example of such materials includes the chemical synthesis of cyanoacrylate adhesives that express minimal toxicity. For instance, a PEG biscyanoacrylate-based bioadhesive hydrogel was used as a crosslinker in an octyl cyanoacrylate adhesive polymer.[161] Here, anthracenyl cyanoacrylic acid was esterified while anthracene protected the vinyl groups. This copolymerization resulted in a cytocompatible strong and adhesive (over 200 kPa peel-off strength) material. Polymerization of allyl 2-cyanoacrylate (ACA) in mixture with poly(L-3,4-dihydroxyphenylalanine) P(L-DOPA) demonstrated biocompatible adhesives for medical applications.[162] Recently, ACA was polymerized in the presence of hydroxyapatite and bisphenol-A glycidyl methacrylate (bis-GMA) to improve the biocompatibility and physical properties of the adhesive material.[163] Moreover, an adhesive based on the mixture of poly(L-lactic acid) (PLLA) and pre-polymerized ACA molecules promoted wound healing and showed better

Author Manuscript Author Manuscript Author Manuscript Author Manuscript

biocompatibility.[164] The healed tissues treated with this adhesive exhibited better tensile tearing strength compared to control samples treated with commercially available adhesives.

Polyurethanes

Polyurethane (PU) is a tough polymer, with inherent flexibility, making it a suitable candidate for sealing wounds.[165] The PU macromolecules are synthesized through the formation of covalent carbamate linkage between the isocyanate functionalized molecules and a polyol (with two or more hydroxyl groups) in the presence of a catalyst or upon UV light activation.[166] The flexibility and elasticity of the polymer depend on the long-chain monomers. Polyurethane and acrylate-modified PU can be designed for *in vivo* biodegradation.[167] For this purpose, a two-step reaction, catalyzed with dibutyltin dilaurate, was designed using isophoronediisocyanate (IPDI), polycaprolactonediol (PCLD), and hydroxyethyl acrylate (HEA), where a faster biodegradation rate was attained by incorporating PCLD molecules into the PU acrylate backbone.[168] The adhesion strength and gel fraction for the biodegradable polyurethane adhesive were reported to be 9 MPa and 93%, respectively. In a further study, IPDI was also polymerized with castor oil and PEG at 70 °C for synthesizing a PU-based bioadhesive material.[169] The monomer ratio (-NCO/-OH) was optimized to attain strong chemical bonding interactions between the material and tissue by tailoring the distribution of -NCO groups. These groups could later couple with the amine groups of the tissue surface for covalent adhesion. Here, the curing time at room temperature was ~7–25 min and *in vitro* degradation of the hydrogel occurred over 7 weeks. In this study, a maximum lap shear strength of ~40 kPa and burst strength of ~30 kPa were reported for samples containing 12 v/v% castor oil. These figures dropped to ~30 and ~15 kPa when the castor oil content was reduced to 3 v/v%. Recently, hydroxyl-rich xylose monosaccharide molecules were mixed with diisocyanate molecules, 4,4′-methylenebis(cyclohexyl isocyanate) (MCI), in combination with PEG and triethylamine as a catalyst to synthesize muscle tissue adhesive (Figure 8G).[170] The bioadhesive was left for 1 to 24 h in the air before the adhesion tests. Hydrogel materials had maximum lap shear strengths of 94 kPa and showed biodegradation of 20% upon incubation for 8 weeks. Inspired by mussel adhesion, catechol groups have also been introduced into urethane-based chains for improved adhesion. In a recent study, dopamine was incorporated into a polyurethane backbone.[171] As a result, mechanical strength was improved from <0.05 MPa (no dopamine addition) to ~1.9 MPa. The improved cohesion also favored adhesion strength: lap shear strength was increased to ~70 kPa compared to ~30 kPa in the absence of dopamine.

Poly(ethylene glycol)

Poly(ethylene glycol) adhesives are well-established and already commercialized for use as tissue sealants (*e.g.*, CoSeal™ and DuraSeal™). Apart from biocompatibility, PEG hydrogels are nonimmunogenic and bioresorbable. However, PEG by itself is a poor adhesive,[17] and further chemical modifications are required to improve its adhesion.[172] Hence, PEG polymers are processed in composite form with other components or modified chemically to tailor their physical properties for bioadhesive applications. For instance, a covalent network of polymerized PEGDA was formed in the presence of giant PEG chain networks

Author Manuscript Author Manuscript Author Manuscript Author Manuscript

to develop bioadhesives that could entangle spontaneously and penetrate within the substrate tissues.[173] The hydrogels also promoted wound healing and reduced the immune response. Lap shear tests indicated that the use of high molecular weight PEG as a secondary network leads to adhesion strength and toughness close to those of cyanoacrylate glues. In terms of stretchability, the double network PEGDA hydrogels with high molecular weight PEG molecules exhibited a *ca.* two-fold increase as compared to the low molecular weight PEG.

To reduce the high swelling of PEG for bioadhesion, hyperbranched PEG-polyester polymers demonstrated robust adhesion with low swelling and improved biodegradability.[37] Multi-arm PEG molecules can also improve adhesion and be used as crosslinkers in bioadhesives. For instance, cyclic succinyl ester functionalized tetra-PEG was reported to be highly reactive to amine functional groups and established covalent adhesion to the underlying tissue in a mixture with amine-capped tetra-PEG.[174] Gelation in this material system occurred within 5 min compared to fibrin glue, which took over 20 min to form a gel.[174] The synthesized hydrogels showed cohesive strength of ~20 kPa and burst pressure strength of up to 300 mmHg. In another study, the end group modification of an 8-arm PEG molecule with amine and aldehyde functionalities enabled an adhesive PEG polymer. Schiff base formation between the active chemical sites facilitated both crosslinking of the material and its adhesion to the tissue surface through reactions with nucleophilic amine groups (Figure 8H,I). While the gelation time was measured to be in the range of 30–75 s, the adhesion strength in the lap shear test was ~0.2× of the cyanoacrylate adhesive (Figure 8J,K). Recently, a 4-arm methacrylate capped pentaerythritol molecule was polymerized in presence of dopamine and PEGDA using Michael addition (in a dimethyl sulfoxide, DMSO, medium).[175] This procedure resulted in branched hydrophobic polymers with abundant catechol end groups. Upon contact with water, these polymers form coacervates and thereby trigger adhesion to the surface (lap shear adhesion strengths of ~100–200 kPa, depending on the substrate material). This bioadhesive was effective for application in bone fracture and bleeding prevention from deep wounds.

Hybrid PEG hydrogels containing poly(lactic-*co*-glycolic acid) (PLGA) have shown potential for use as bioadhesives. A mixture of PEG, PLGA, and silica particles in acetone was solution blow spun onto the tissue surface (Figure 8L). The resulting sealant showed strong tissue adhesion, comparable to that of cyanoacrylate adhesives (160 mmHg burst pressure strength), as shown in Figure 8M.[176] Increasing the silica particle size (from 20 to 620 nm) led to a 2-fold increase in the burst strength. Here, the larger silica particles (620 nm) suppressed crack formation and propagation, which led to improved stretchability and adhesive strength. In addition, lower swelling of hydrogel compared to CoSeal™ was reported. In another study, a mixture of PEG and PLGA polymers (both at 5 wt.%) dissolved in acetone was solution blow spun to form temperature-responsive fiber mats (~0.5–2.5 μm diameter).[5] The fibers retained their fibrous form at temperatures below 31 °C. Once applied to the tissue using an airbrush, the fiber mats transitioned to an adhesive film layer, which could conform to the shape of tissues at body temperature. The pull-off tests demonstrated increased adhesion strength with the PEG concentration at body temperature, with a maximum of ~120 kPa.

Author Manuscript Author Manuscript Author Manuscript Author Manuscript

Natural bioadhesives

One of the main advantages of using natural polymers for the synthesis of adhesive sealants is their innate biocompatibility and biodegradability. Hence, a surge of interest has been directed at the addition of selective chemical functionalities to natural polymeric backbones to enhance their adhesion. Although inflammatory responses induced by natural backbones such as chitosan and gelatin have raised concerns over their internal use, current research is striving to mitigate those effects while enabling their widespread as biodegradable tough bioadhesives. Below, we discuss different classes of natural polymeric backbones used for the development of adhesive hydrogel materials.

Polysaccharide-based bioadhesives

Polysaccharides are formed from monosaccharide repeating units connected through glycosidic linkages.[177] Various types of natural polysaccharide-based backbones are used in bioadhesive materials, including chitosan,[178] alginate,[179] HA,[180] carboxymethyl cellulose,[181] *etc.* Active functional groups present in the polysaccharide backbones enable different chemistries leading to adhesive characteristics through intra- or intermolecular interactions. One of the common procedures both to functionalize with chemical moieties and to establish adhesion with tissues is to oxidize the vicinal diol groups present in their monosaccharide units that enable Schiff base formation with tissue surfaces.[121] Other nucleophiles present in some polysaccharides can also be employed to graft adhesive functionalities. Below, examples of approaches undertaken to modify polysaccharide-based biomaterials for tissue adhesion are reviewed.

Hyaluronic acid

Hyaluronic acid is an immunoneutral polysaccharide that exists in the human body comprised of repeating β−1,4-D-glucuronic acid and β−1,3-N-acetyl-D-glucosamine disaccharide units.[182] Many biological functions and cellular activities rely on HA in tissues such as the eye and cartilage. Hyaluronic acid has served as a critical building block to develop biomaterials with tissue regenerative properties.[182] Modification of HA for bioadhesion through its abundant carboxyl conjugation sites has frequently been demonstrated.[183] For instance, serotonin is a neurotransmitter released from platelets; it can activate platelets to enable secretion of blood-clotting factors such as platelet factor IV, factor V, von Willebrand factor, and fibrinogen. Serotonin can react with the functional groups present on the tissue surfaces and also act as a crosslinking component for gel formation.[184] Serotonin conjugated to HA was shown to promote adhesion during gelation due to the free radicals generated that promote reaction with the underlying tissue substrate.[184] This adhesion, however, is terminated upon completion of gelation (after 10 min) probably due to the full consumption of the oxidative intermediates. The adhesion-terminating character of the hydrogel after crosslinking was assigned to its anti-biofouling properties, which prevent unwanted and abnormal adhesion to the neighboring tissues. Catechol modification of HA is another approach to achieve bioadhesion. A two-component HA hydrogel involving HA-catechol mixed with HA modified with thiourea groups (HA-NCSN) was developed for healing gastric wounds.[185] The pre-polymer solution

Author Manuscript Author Manuscript Author Manuscript Author Manuscript

was crosslinked using a $NaIO_4$ spray. The thiourea groups in this formulation prevented auto-oxidation of catechol groups that cause adhesion loss. As opposed to HA-catechol bioadhesives, the HA-catechol/HA-NCSN composition led to stable adhesion in an acidic environment (pH ~2) making the gel a suitable candidate for sealing gastric wounds. In other examples,[121,186] glycosaminoglycan HA was functionalized with a photoreactive functional group *N*-(2-aminoethyl)−4-(4-(hydroxymethyl)−2-methoxy-5-nitrosophenoxy) butanamide (NB), which generated aldehyde groups upon UV light irradiation. Aldehyde groups were able to form Schiff bases with the primary amine groups on the tissue surface for adhesion (Figure 9A). The NB-modified HA was reinforced with GelMA. High cohesion and adhesion led to burst pressure of up to 290 mmHg, higher than most commercial bioadhesives. The sealant rapidly stopped heavy bleeding from incisions in carotid arteries and the heart *in vivo* in a pig model (Figure 9B,C) due to its strong adhesion.

Chitosan

Chitosan is obtained from one of the most abundant polysaccharides in nature (*i.e.*, chitin from marine organisms such as shrimp, crab, *etc.*)[187] and consists of β-(1→4)-linked *N*-acetyl-D-glucosamine homopolymers.[188] Primary amine groups present on the chitosan backbone provide positive charges leading to its antimicrobial[189] and hemostatic[190] properties. Positive charges can be further enhanced by the quaternization of chitosan (QCS).[191] The mixture of QCS with Fe^{3+}-associated protocatechualdehydes, in a recent example, produced a strong antibacterial, photothermal, and bioadhesive hydrogel for the treatment of infected wounds.[192] Note that both humoral and cell-mediated immune responses are associated with chitosan.[193] Nevertheless, chitosan has shown promise in bioadhesives and has been used to treat bleeding and diabetic wounds.[194,195]

Amine groups on the chitosan backbone can be used to modify chitosan for improving adhesion *via* substitution reactions.[196–198] For instance, the NB functional groups were grafted on chitosan backbones to enable photo-triggerable injectable bioadhesives in a mixture with unmodified chitosan.[199] The optimized composition achieved a maximum adhesion strength of ~100 kPa (~5× larger than fibrin glue). Inspired by trichrome in tunicates, pyrogallol groups were grafted chemically onto the chitosan backbone to improve both its solubility under physiological conditions and wet adhesion beyond that of commercial adhesive fibrin glue.[200] Recently, a gallic acid-modified chitosan hydrogel was electrospun to form microfiber structures mimicking the natural tunicate's body armor.[201] Chitin derivatives have also shown promising adhesion strength. Water-soluble 2-hydroxy-3-methacryloyloxypropylated carboxymethyl chitin (HMA-CM-chitin) was polymerized using hydrogen peroxide.[202] The addition of chitin nanofibers (CNFs) and surface-deacetylated chitin nanofibers (S-DACNFs) significantly enhanced adhesive strength, comparable to the cyanoacrylate adhesives. The lap shear strength of the material was close to 3 kPa, and the burst pressure was measured to be ~170 kPa. Schiff base formation in the chitosan hydrogel system using PEG-dialdehyde in the presence of reductive agents was investigated.[203] Here, chitosan was functionalized initially with PEG molecules to enhance their water solubility. Further, the chain length of the PEG molecules was engineered to lower the gelation time down to ~1 min. *Ex vivo* lap shear tests on porcine skin showed a two-fold increase compared to the low molecular weight PEG chains (750 versus 2000 g/mol).

Author Manuscript Author Manuscript Author Manuscript Author Manuscript

Alginate

Alginate is a major component of algae and is composed of alternative units of 1→4 linked β-D-mannuronic acid and α-l-guluronic acid monosaccharides.[204] Abundant carboxyl groups result in negative charges and enable ionic crosslinking with multivalent cations (such as Ca^{2+}) as well as functionalization through coupling reactions. In one example, to develop alginate-based bioadhesives, methacrylated alginate molecules were oxidized to introduce aldehyde functionality for bioadhesion.[205] The hydrogels made of non-oxidized methacrylated alginate molecules exhibited larger burst strength values compared to the oxidized methacrylated alginate-based hydrogels. While non-oxidized molecules resulted in delamination failure, material failure was observed for the oxidized methacrylated alginate molecule in burst pressure tests. Even though the oxidation of alginate molecules introduced aldehyde groups to improve the adhesion of the hydrogel material, it lowered mechanical cohesion somewhat. The higher degree of methacrylation in this study was associated with larger adhesive strength, which is attributed to both improved cohesion (due to increased crosslink density) as well as covalent adhesive bonds (through Michael addition between acrylate groups and primary amines on the tissue). Modification of alginate with boronic acid is another method to improve the adhesion strength of alginate.[179] Boronic acid conjugates enable pH-triggerable crosslinking at slightly alkaline conditions. They play similar roles to catechol groups in terms of bioadhesion mechanism. Peel-off tests using mouse intestine adherents suggested adhesive strength of ~22 kPa for the crosslinked samples while no significant adhesion force was recorded for unmodified alginate.

Cellulose

Cellulose nanocrystals (CNCs) are being investigated as additives to promote adhesion in hydrogels. To promote adhesive and mechanical properties in PAA-based hydrogels, CNCs were coated with tannic acid (TA).[206] In this approach, the abundant catechol groups on TA were utilized to create mussel-inspired adhesives. The TA-coated cellulose nanocrystals were embedded in the PAA network, which was further crosslinked ionically with Fe^{3+} ions through the catechol functionalities. The fabricated hydrogels showed self-healing properties and tensile adhesive strength of 5–15 kPa to various substrates (*e.g.*, aluminum and hog skin), and the stretchability was enhanced by 5× (strain at rupture ~3000%) compared to pristine PAA.

Polypeptide-based bioadhesives

Protein and polypeptides such as silk fibroin (SF),[207] albumin,[208] and decellularized tissues[209] have become attractive candidates to design adhesive backbones mainly due to their excellent biodegradation, biocompatibility, and abundance in nature.[210,211] Many proteins are inherently glutinous. One of the promising examples of such materials is the recombinant human protein tropoelastin, which was shown to provide an extensible matrix upon crosslinking.[212] Methacryloyl-substituted tropoelastin molecules (MeTro) showed excellent sealing when applied on lung and artery leakages (Figure 9D–H).[213] When the pre-polymer was synthesized *in situ*, the hydrophobic interactions led the macromolecules to coacervate at body temperature and to form physical crosslinks. This process can aid in

Author Manuscript Author Manuscript Author Manuscript Author Manuscript

initial conformation to tissue shape. Later, the hydrogel was attached covalently to the tissue surface by UV curing. The mechanical properties were readily tunable with the degree of methacryloyl-modification as well as the prepolymer composition. In terms of adhesion, the lap shear, burst pressure, and wound-closure tests all suggested that the adhesion strength increased with the degree of methacryloyl-modification and MeTro concentration. Here, the maximum values related to these experiments were 172.1 kPa, 11.9 kPa, and 75.9 kPa, respectively, which were significantly higher than commercial Evicel® and CoSeal™ counterparts (Figure 9E). An extracellular matrix (ECM) mimicking glycopolypeptide, *i.e.*, poly(L-lysine) (PLL) was functionalized with catechol groups[214] and glucose[215] to develop bioadhesives for hemostasis and wound-healing applications. This study[215] revealed that metal ion coordination crosslinking using Fe^{3+} resulted in stronger adhesion force compared to those of crosslinked enzymatically using horseradish peroxidase (HRP)/H_2O_2 systems. Another study revealed the adhesion of a double network PLL modified with 4-hydroxyphenylacetic acid in mixture with agarose (enzymatically crosslinked *via* HRP/H_2O_2).[216] The hydrogels were characterized by self-healing properties. Schiff base formation between oxidized phenols and amine groups on the tissue led to adhesion strength of ~34.5 kPa in burst pressure tests, which is larger than arterial blood pressure (16 kPa). Lysozyme protein, derived from eggs, with excellent antibacterial properties, has also been used to design adhesive sealants.[17,217] *In situ* crosslinking between the amine groups present in lysozyme molecules and reactive NHS capped 4-arm-PEG (4-arm-PEG-NHS) crosslinker was recently proposed as a bioadhesive.[140] Covalent adhesion through bonding with the tissue amine groups led to stable covalent adhesion (with burst pressure strengths up to 250 mmHg) and sealing incisions (such as blood vessel lacerations, repairing the tracheal trauma, and heart wall defects) effectively. In another recent example, injectable bioadhesives were made from *Bacillus subtilis* biofilms, containing catechol-functionalized amyloid and hydrophobin-like proteins.[218] Metal ion solutions (*i.e.*, $CaCl_2$, $MgCl_2$, and $FeCl_3$) were applied to crosslink the hydrogel precursors, among which $FeCl_3$ led to the strongest adhesion strength (*i.e.*, ~250 kPa). Among the polypeptide-based bioadhesives, gelatin and fibrin have received particular attention due to their superior biocompatibility and biodegradability. Next, the latest advances in gelatin and fibrin-based bioadhesives are discussed.

Gelatin

Gelatin is an ECM-mimicking protein obtained by hydrolysis of collagen from animals. Along with its excellent biocompatibility and biodegradability, gelatin-based hydrogels have shown intrinsic adhesion that promotes their application as sealing materials.[219] For instance, gelatin forms crosslinked hydrogels in mixtures with oxidized chondroitin sulfate for thermosensitive bioadhesion.[220] Thermosensitive gelation of gelatin at low temperature (20 °C) results in lower adhesion when compared to higher temperature (37 °C). Hence, bioadhesive patches with body temperature-triggered adhesion were achieved where on-demand removal of the bioadhesive is possible by treating the adhesion site with cold water.

Various chemical modifications are implemented to improve bioadhesive strength and durability of gelatin for bioadhesion. Catechol functionalization of gelatin followed by crosslinking through metal ion (Fe^{3+}) coordination is an example of injectable bioadhesives

Author Manuscript Author Manuscript Author Manuscript Author Manuscript

developed for sealing internal leaks.[221] In another study, gelatin-catechol conjugates were crosslinked through Michael addition reactions, *i.e.*, crosslinking reactions through thiol and amine groups of keratin, as well as biaryl formation (coupling the catechol groups).[222] Mixtures of keratin and gelatin-catechol led to gelation times as low as 20 s. These bioadhesives led to ~30–40% improvement in wound breaking strength, compared to cyanoacrylate and fibrin glue. In a recent study, gelatin was functionalized with 3,4-hydroxyphenylpropionic acid (HPA) (Gtn-HPA) where crosslinking was achieved *via* HPA groups upon irradiation of visible-light in the presence of sodium persulfate and $[RuII(bpy)_3]^{2+}$ within ~30 s.[223] A second component, *i.e.*, carboxymethyl cellulose-tyramine (CMC-Tyr) conjugates, was added to the bioadhesive material formulation to introduce porous structures within the hydrogel network. The hydrogels had tensile adhesive strengths of ~57 kPa and ~87 kPa for the Gtn-HPA and Gtn-HPA/CMC-Tyr hydrogels, respectively, which were significantly higher than that of fibrin glue (~7 kPa). The bioadhesive was tailored for *in situ* 3D printing of adhesive sealants.

Methacryloyl-modification of gelatin enables both crosslinking and *in situ* adhesion on wet tissues.[224–227] For example, injectable GelMA pre-polymers (containing 20 wt.% GelMA) crosslinked on corneal tissue using a visible light exhibited significant improvements in terms of adhesion (*e.g.*, up to more than 15× burst pressure compared to commercial sealants).[228] Bioadhesion of *in situ* crosslinked GelMA is attributed to the free radical polymerization of methacryloyl groups *via* Michael addition reaction, coupling pre-polymer backbone to the tissue surface nucleophiles (*e.g.*, primary amines).[229] Composites of GelMA with ECM protein derivatives such as MeTro have also shown promise for the treatment of chronic non-healing wounds (Figure 9I,J).[230] In this case, the GelMA/MeTro hydrogel was crosslinked using a visible light source. In addition, antimicrobial peptide (AMP) Tet213 (KRWWKWWRRC) peptide was conjugated to gelatin to endow the hydrogels with antimicrobial properties. The mechanical properties of the hydrogel were tunable by changing the concentrations of the constitutive components (*e.g.*, increasing the MeTro content resulted in a lower elastic modulus and higher stretchability). Adhesion strength measured with lap shear, burst pressure, and wound-closure tests suggested that increasing the GelMA:MeTro ratio as well as the total hydrogel concentration results in better adhesive strength. Gelatin methacryloyl could also be functionalized with dopamine and dual-crosslinked through Fenton reaction.[231] Fenton chemistry generates hydroxyl radicals from ferrous salts (Fe^{2+}) and H_2O_2, both of which promote the rapid polymerization of the vinyl-containing macromers. The normal adhesive strength obtained by applying the bioadhesive between the tissue layers was on the order of ~15 kPa, which was 2- and 4-fold higher than fibrin glue and GelMA, respectively. In addition, a wide range of mechanical strengths (100–5000 kPa) was obtained by controlling the initiator components in the Fenton reaction. Other catechol-integrated GelMA polymers are developed for bioadhesion. *In situ* polymerization of dopamine in the presence of GelMA enabled growth of PDA moieties at the methacryloyl sites.[42] Photocrosslinking of the resulting pre-polymer introduced stickiness to the GelMA patches (up to ~7× increase in adhesion force), and improved stretchability of GelMA hydrogels by ~6×. In another study, GelMA chains were complexed *via* oxidized gallic acid species and polymerized in the presence of PEGDA using APS/TEMED radical polymerization system.[232] The hydrogels adhered reversibly to fragile skin

Author Manuscript Author Manuscript Author Manuscript Author Manuscript

tissues of infants as well as diabetic patients *via* body temperature trigger and could be detached painlessly by cooling the adhesive using an ice bag.

Fibrin

Fibrin is a protein formed from fibrinogen that plays important roles in hemostasis, thrombosis, wound healing, and several other major pathological conditions. The enzymatic cleavage of fibrinogen by thrombin leads to the formation of fibrin monomers and thereby its polymerization by factor XIII in the presence of calcium ions.[233] Fibrin facilitates enzymatic self-crosslinks as well as bonding with tissue.[176] Fibrin-based materials are commercialized for tissue adhesive applications (such as Evicel®); they offer biodegradability, but they pose the risk of disease transmission and have short life spans (~2 weeks).[233] Fibrin composites with other types of bioadhesives have been used to improve the physical properties of hydrogel materials. For example, fibrin microparticles were integrated into NHS-capped multi-arm PEG matrices for the synthesis of an injectable hydrogel. The results showed improved adhesion to wet tissue.[234] Further improvement in adhesion was observed when nitric oxide (NO), a wound-healing reagent, was added to the material. The lap shear strength was ~3.5 kPa compared to control PEG-NO with 1 kPa strength. In general, fibrin bioadhesives lead to weak bioadhesive strength.

Mussel-inspired bioadhesives

Various living organisms in nature, such as mussels[235] and ivies,[236] establish strong adhesion under wet conditions. The physical and chemical mechanisms behind their adhesion have inspired researchers to develop bioadhesives with similar strong wet adhesion. Mussels produce abundant catechol-containing proteins involving L-DOPA amino acids that are responsible for their adhesive functionality, acting alongside positively charged[237,238] and hydrophobic amino acid residues present on the protein backbone to establish adhesion in wet environments.[239] Hence, catechol groups play important roles in adhesion. Catechol-based adhesives were first found in the byssal threads of mussels,[240] and obtained through purification of precursors produced from *Escherichia coli*.[241] The catechol group in L-DOPA undergoes an oxidation process and produces reactive quinone species. These reactive quinones couple with the functional groups present on the wet surfaces of the tissues (*i.e.*, amines, thiols, *etc.*) through a variety of chemical mechanisms, resulting in covalent attachment.[242,243] Underwater adhesives are mostly supported by the synergistic contribution of catechol-induced reactions, hydrophobic, electrostatic, and hydrogen-bonding interactions.[244] Similar phenolic hydroxyl functional groups are seen in nature, such as TA[245] and lignin[246–249] that are extracted from plants and used for the synthesis of different adhesive hydrogels.

During the past decade, over 100,000 articles have been published on mussel-inspired hydrogels.[250] Although several attempts were made to mimic the strong underwater adhesion of marine living organisms, current research remains unable to replicate and to explain the chemical mechanisms leading to such strong adhesion. The adhesion mechanisms of mussels do not rely solely on the catechol groups present in their secreted proteins; rather, it is a complex process that involves the synergistic contribution of L-DOPA,

Author Manuscript Author Manuscript Author Manuscript Author Manuscript

lysine, and oppositely charged amino acid resides (such as those comprising of phosphates and amines).[251,252] Lysine aids in removing the hydrated cations from the surfaces and thereby facilitates the adhesion of catechol to the oxide groups present on the substrate.[253] It has been discovered that before mussel feet are engaged with the substrate surface underwater, the local pH of the protein is maintained under acidic conditions, at pH below ~2. By this means, catechol groups are protected from oxidation. Once the mussel adhesive proteins (MAPs) are secreted into the alkaline pH of seawater (pH~8), *in situ* oxidation of catechol moieties enables their reaction with the substrate underneath as they turn into their reactive quinone form.[254] The MAPs secreted by the underwater living organisms are insoluble in the ocean (due to electrostatic coacervate formation of oppositely charged proteins), and their curing is timed accurately to avoid clogging the adhesive ducts (*e.g.*, in the case of sandcastle worms, this protection is ensured by the low pH in their secretory granules).[252] In addition, liquid–liquid phase separation of MAPs driven by L-DOPA enables mussel fiber formation.[255] Inspired by natural adhesion mechanisms, ongoing research strives to engineer catechol-functionalized polymers for the development of biomedical adhesives.[256] Next, chemistries and examples of mussel-inspired bioadhesives are reviewed and the latest methods to incorporate mussel-inspired adhesive functionality into polymer backbones are discussed.

Crosslinking mechanisms *via* catechol groups

In addition to adhesion, catechol moieties enable polymerization of hydrogel networks.[257] Catechol groups also introduce dynamic intra/intermolecular interactions to covalent networks to enhance their toughness.[257] Catechol-catechol and catechol-nucleophilic covalent bonding form through oxidative crosslinking under certain chemical conditions. These conditions include (i) basic pH (pH > 8), (ii) oxidants such as persulfates, periodates, and HRP/H_2O_2, (iii) enzymes such as tyrosinase or laccase, and (iv) catalysts such as hematic.[257,258] All these chemical mechanisms trigger the transformation of catechol functionality to highly reactive quinone intermediates.

Catechol groups can generate crosslinked networks in hydrogels through various chemistries. The Michael addition reaction between catechol and thiol groups can lightly crosslink the hydrogel networks at neutral pH.[33] Recently, chitosan[259] and HA[260] were functionalized with catechol-carrying dopamine molecules to crosslink their hydrogels using thiol-capped Pluronic F127 (Figure 10A).[260] The catechol-functionalized HA showed excellent tissue adhesion and reversible thermo-sensitivity, enabling its injection as a liquid solution at room temperature *in vivo*, and solidification at body temperature.

Reversible dynamic interactions, enabled by catechol groups, are introduced through hydrogen-bonding, π-π stacking, π-cation interactions, and metal-ion coordination.[261] Catechol groups can form pH-sensitive metal ion coordination complexes *via* their hydroxyl sites, in the presence of multivalent metal cations such as Fe^{3+}, V^{3+}, Cu^{2+}, *etc*. The number of catechol groups chelated per multivalent cation increases with pH.[262] Note that catechol oxidation through metal ion coordination, however, turns the reversible attractions into covalent bonds. To avoid this oxidation, which consumes catechol groups that promote adhesion, electron-withdrawing substituents such as -CN, -NO_2, and -Cl can

Author Manuscript Author Manuscript Author Manuscript Author Manuscript

be introduced.[263] Recently, a 3-hydroxy-4-pyridinone polymer was designed to avoid fast catechol oxidation in mussel-inspired polymers by lowering pK_a of the phenolic ring.[264]

Metal-ligand chemistry can produce free radicals that can drive gelation in the polymer network.[264] The low [vanadium]/[catechol] molar ratio led to the generation of organic radicals in catechol-modified chitosan, where the addition of excess vanadium ions inhibited the gelation process (Figure 10B–D).[265] The polymerization of dopamine molecules is accompanied by generation of stable free radicals.[266] Dopamine-initiated polymerization with the acrylate monomers on solid surfaces with high molecular weight was demonstrated for anti-fouling coating applications.[266] Oxidization of dopamine is accelerated in the presence of oxygen.[267] Irradiation with UV light promoted polymerization of dopamine due to the generation of reactive oxygen species (ROS, *i.e.*, hydrogel radicals, superoxide radicals, and singlet oxygen).[267]

Catechol groups can form hydrogen-bonding-driven hydrogels. Tough hydrogels based on composites of SF and TA were developed, as shown in Figure 10E–G.[268] Tannic acid has abundant hydroxylated benzyne rings that can form strong hydrogen bonds with proteins and peptides, leading to their instant gelation. An optimal concentration of 0.3 g/ml TA enabled the gelation process. Moreover, the addition of TA to the SF backbone resulted in SF conformational changes from coil to β-sheet structures, leading to the formation of nanofibrillar structures that provided high toughness (123 kJ/m^3) and strong binding affinity to wet tissue surfaces (lap shear strength of 134 kPa). A similar SF-based hydrogel system with hydroxyapatite and TA additives was developed for the fixation of bone fractures.[269] Hydroxyapatite additives introduced additional coordination bonds with TA. As a result, significant improvements in both toughness (from below 50 kJ/m^3 to ~450 kJ/m^3) and adhesion strength (from below 20 kPa to above 600 kPa in the presence of blood) were achieved. Fractured rat femur bones treated with the developed bioadhesives were tested after two weeks of healing *in vivo*. The treated bone was reported to be approximately twice as strong as those of non-treated groups.

Chemistry of catechol adhesion

Catechol groups can generate non-covalent (*e.g.*, hydrogen-bonding) and covalent interactions with the nucleophilic functional groups on tissue surfaces. These covalent interactions involve: (i) Schiff base formation, wherein amine groups from the polymeric macromolecule react with the oxidized catechol (*i.e.*, quinone), (ii) Michael-type addition, where amine groups couple to the benzyl, as a result of which a secondary amine is formed to bridge the polymer chains, and (iii) di-catechol formation, in which C-C bonds form between two quinone moieties.[243] Theoretical analyses have indicated that catecholic moieties can repel water molecules aside to facilitate their direct bonding to the underlying surfaces.[270] Note that the structure of the polymer backbone plays key roles in its binding affinity.[271] For instance, hydrophobic backbones are repelled from hydrophilic surfaces. Therefore, the catechol-modified hydrophobic backbones may fail to bind to the hydrophilic surfaces effectively. On the other hand, there should be a trade-off between hydrophilicity and solubility. High solubility in water is associated with lower underwater adhesion strength mainly due to the compromised cohesion when exposed to aqueous media.[26]

Author Manuscript Author Manuscript Author Manuscript Author Manuscript

The adhesion of catechol-conjugated polymers is highly sensitive to parameters such as processing factors and whether the hydrogel is used as an injectable bioadhesive or in the form of a patch. The adhesion environment is another limiting factor.[271] For example, catechol-containing polyoxetane-based polymer that is crosslinked with $FeCl_3$ exhibited a strong adhesive strength to dry surfaces (5.6 MPa lap shear strength on a stainless steel surface); however, adhesion strength was much lower when placed on wet surfaces (0.41 MPa on a porcine skin).[272]

The charged units and hydrophobic residues in the secreted proteins of mussels have motivated researchers to study their synergistic effects on adhesion.[273] A mussel-inspired bioadhesive consisting of zwitterionic surfactant molecules (having charged quaternary amine and phosphate groups) and hydrophobic alkyl tails was developed, as shown in Figure 11, to study the roles of different interactions in wet adhesion.[274] In this study, similar composition ratios of charged residues, hydrophobic moieties, and catechol content as in the mussel foot proteins (mfp) were used to mimic mfp structures in synthetic polymers. Strong wet adhesion (~20 mJ/m^2) was attributed to the hydrophobic interactions between the alkyl tails as well as the electrostatic interaction through the phosphate and amine functionalities. In a similar approach, to mimic the catechol content and hydrophobic resides of mpf, copolymerization of styrene and 3,4-dimethoxystyrene followed by deprotection of methoxy groups (using BBr_3) led to an adhesive polymer (*i.e.*, poly[(3,4-dihydroxystyrene)-*co*-styrene]) that had a maximum lap shear adhesion strength of 11 MPa on dry aluminum plate surfaces. Although the developed material could not be used as a bioadhesive due to the presence of organic solvents,[275] the results demonstrated the importance of hydrophobic residues in adhesion strength. Similarly, a copolymer with an additional component containing positive charges was synthesized, which had lap shear adhesion strengths of 2.8 MPa (dry) and 0.4 MPa (wet), suggesting the role of positive charges in catechol adhesion.[276]

Catechol functionalization of biomolecules for bioadhesion

A wide variety of methodologies has been implemented to graft catechol groups on different polymer backbones. These approaches are primarily based on the conjugation of catechol-carrying small molecules that possess nucleophile functional groups, and hence, can be coupled to biopolymer backbones. Some reagents carrying catechol groups used for polymer conjugation involve dopamine (conjugation through amine groups),[258,277] 3,4-dihydroxyhydrocinnamic acid,[278] caffeic acid (conjugation through carboxylic groups),[279] and 3,4-dihydroxybenzaldehyde (conjugation through aldehyde groups).[280]

Various coupling chemistries are used to introduce catechol functionality to biopolymers. For instance, a catechol-coupled poly(vinyl pyrrolidone) (PVP) was synthesized *via* click chemistry.[271] The catechol-grafted polymer solution was later crosslinked with Fe^{3+}. Interestingly, a high wet adhesion lap shear strength (1.13 MPa) was obtained (using glass slides), which was twice as high as the dry adhesion strength (0.56 MPa). The higher adhesion strength under wet conditions was explained by (i) easier Fe^{3+} ion diffusion compared to the dry condition, and (ii) the lower water solubility of the polymer as a result of catechol conjugation. In another study, low-cost and scalable synthesis of catechol-

Author Manuscript Author Manuscript Author Manuscript Author Manuscript

containing PVA-based dry adhesive materials was demonstrated *via* an acid-catalyzed acetal formation reaction. In that case, 3,4-dihydroxybenzaldehyde (DBA) molecules were linked chemically to the PVA molecules (in DMSO using *p*-toluenesulfonic acid (TsOH) as catalysts).[281] This mixture was applied to the adherent surfaces and cured *via* solvent evaporation. The excellent lap shear adhesion strengths (as high as 17.5 MPa) obtained here were far higher than those of commercially available adhesives (*e.g.*, Krazy glue, 7.25 MPa).

A common approach to add catechol functionalities is to infuse catechol-carrying molecules within pre-crosslinked hydrogels (primarily for wound-closure patches). For example, a mixture of quaternary ammonium-modified chitosan and PEGDA was photocrosslinked and soaked in a TA solution to allow infusion within the hydrogel material.[282] This process resulted in increased stretchability of the chitosan-based hydrogel from less than 200% to ~700% in addition to the significant improvement in adhesion (*i.e.*, with burst pressure up to ~60 mmHg). A similar TA infusion process for GelMA hydrogels was demonstrated by Liu *et al.*[227] Tannic acid acted as a secondary network to toughen GelMA, leading to a 4-fold increase in tensile strength. In addition, the swelling ratio was reduced by 1/3 and the adhesion strength in lap shear tests improved by more than 10× compared to GelMA (maximum adhesive strength was measured ~80 kPa).

Copolymerization with catechol-containing monomers

Copolymerization of monomers carrying catechol moieties is one of the most popular and the easiest approach to incorporate catechol groups within the hydrogel networks.[283] As an example, methacrylated dopamine (DMA) molecules were oligomerized in an alkaline Tris-HCl solution (pH ~8).[284] The DMA oligomers were copolymerized within the GelMA polymer to reduce the physical chain entanglement between GelMA macromolecules, which thereby enhanced the mechanical deformability and strain recoverability of the hydrogel. A temperature-responsive bioadhesive was obtained using a host-guest macromolecular configuration using slide-ring chemistry.[285] A guest chain was synthesized by copolymerization of DMA molecules (responsible for adhesion) with adamantane motifs (acting as host receivers) and methoxyethyl acrylate (enabling hydrophobic interactions). The host molecule was based on PNIPAM copolymerized with β-cyclodextrin (hosting adamantane in the guest chain). Here, at temperatures lower than LCST (*i.e.*, 25 °C), water molecules easily infuse within the polymer chains, reducing adhesive strength; whereas, at higher temperatures, the hydrogen bonding between water molecules and PNIPAM breaks down, resulting in collapsed chain conformations and thereby exposing the catechol groups to adhere freely to the substrate. Underwater adhesion strength changed reversibly with temperature so that a 20-fold larger adhesive strength was measured at 40 °C compared to 25 °C. In another study, adhesion in a shear-thinning, injectable, and fit-to-shape sealant was demonstrated *via* copolymerization of DMA with maleic-modified chitosan (MCS), dibenzaldehyde-terminated poly(ethylene glycol) (PEGDF), and PEGDA monomers (Figure 12A).[18] The shear-thinning properties were observed due to the reversible Schiff base formation between dibenzaldehyde-terminated poly(ethylene glycol) (PEGDF) and the chitosan backbone. The adhesion stability of the designed hydrogels even at pH~1 demonstrated the applicability of the material in acidic environments (such as the stomach).

Author Manuscript Author Manuscript Author Manuscript Author Manuscript

The lap shear test results indicated improved adhesive strength of 46 kPa, which was almost 8× greater than that of commercially available fibrin glue.

Copolymerization of catechol-functionalized PEG has also gained interest in creating mussel-inspired bioadhesives. Catechol-modified PEG chains were copolymerized in a solvent and initiator-free setup with polymer units that (i) promoted hydrophobic interactions and reduced the glass transition temperature, and (ii) enhanced cohesive strength through a UV light-sensitive side chain for crosslinking (Figure 12B,C).[286] In this study, by tuning the polymerization feeding ratio, a variety of pre-gel solutions with different viscosity levels were obtained. The adhesion increased for low viscosity polymers. Hydrophobic groups play key roles in achieving high levels of adhesive strength. The ester bonds present in the polymer backbone provided rapid biodegradation and biocompatibility. In a further study, a set of branched PEG-catechol was polymerized with strong cohesion and a thermo-responsive negative swelling.[287] Introducing the catechol moieties significantly improved the adhesive strength of the PEG-based polymers (with maximum lap shear strength of 209 kPa).

Carbodiimide coupling

Carbodiimide EDC/NHS chemistry is a standard coupling reaction between carboxyl and primary amines, implemented extensively to conjugate catechol-carrying moieties to large biomacromolecules. The catechol loading capacity in this approach is limited by the available conjugation sites and depends on the reaction yield. For successful reaction and to achieve a maximum yield, it is important to control the pH of the conjugation process (pH~5.5–6). Dopamine molecules, containing amine groups, were conjugated to the carboxylic-rich HA at pH 5, resulting in 47% substitution.[260] The synthesized catechol-functionalized HA polymer was then crosslinked chemically through covalent interactions between catechol and thiol-capped Pluronic crosslinkers. The adhesion strength for the modified HA-Pluronic hydrogels was improved by 150% compared to each of the constitutive components.[288]

A wide variety of natural biomolecules, including protein/peptides and polysaccharides, have been functionalized with catechol groups using EDC/NHS coupling. For instance, gelatin was coupled with caffeic acid and crosslinked using oxidative agents (*i.e.*, sodium meta-periodate) to form catechol-catechol crosslinks (Figure 12D).[289] The synthesized hydrogel demonstrated enhanced wound healing, radical scavenging, antimicrobial, and antioxidant properties as compared to unmodified gelatin. In another study, dopamine was grafted to gelatin using EDC/NHS, followed by double-crosslinked with Fe^{3+} (catechol coordination), and genipin (a covalent crosslinker for gelatin) as illustrated in Figure 12E,F.[219] The adhesion of the material characterized by the lap shear test using porcine skin, showed an adhesive strength of 24.7 kPa (Figure 12G,H). Here, the bioadhesion was attributed to the infusion of the macromer solution into the skin.

Author Manuscript Author Manuscript Author Manuscript Author Manuscript

Reductive amination

Different reductive agents such as $NaBH_4$ and $NaCNBH_3$ can be used to couple aldehyde-containing catechol derivatives, such as 3,4-dihydroxybenzaldehyde, to amine groups on the monomer backbone.[290] This approach leads to high and controllable synthetic yield (substitution of 18–80% in less than 5 h).[239] One example is the reaction between amine-functionalized star PEG and dextran aldehyde, wherein imine bonds between aldehyde and amine groups) drive the crosslinking process.[291] To circumvent the detrimental effect of swelling on adhesion, Shazly *et al.* conjugated L-DOPA to a PEG-dextran network through a reductive amination process and optimized the biomaterial to minimize swelling of the hydrogel by tuning the concentration and thereby improved the durability of the wet adhesion.[292] The *ex vivo* burst pressure tests with the L-DOPA-conjugated polymers on the intestinal puncture wounds did not reduce the adhesion strength, whereas 1 h soaking of neat (control) samples led to a 39% decrease in the burst strength.

Enzymatic coupling

With the aid of enzymes such as tyrosinase or laccase, one can catalyze the oxidization of catechol groups that are later reacted with nucleophiles. Amine groups bind chemically to the carbonyl groups of the quinones through the Schiff-base reaction and thereby form stable conjugates.[257] Recently, a tyrosine-containing mfp-3S mimetic peptide with a similar protein composition was engineered with the aim of recapitulating natural mfp. Here, positive charges were introduced to enable coacervate formation due to electrostatic interactions as they occurred in natural mfp.[293] Further, tyrosine was hydroxylated enzymatically to L-DOPA using mushroom tyrosinase to enhance adhesion by replacing surface-bound water molecules. Using a similar approach, the tyrosine residues of gelatin derived from the human adipose tissue were converted to L-DOPA to develop tissue-adhesive hydrogels.[294] Complexation crosslinks were formed by the addition of Fe^{3+} ions within seconds after mixing. The hydrogels were adhesive and stable at body temperature.

Catechol-based nanoparticles

Catechol-coated nanoparticles can improve adhesive and toughness in hydrogels simultaneously.[295,296] Tough nanocomposite PAM-based hydrogels enabled by mesoporous silica nanoparticles (MSNs) and PDA additives were proposed as an example of bioadhesive patches for transdermal drug delivery.[297] This study revealed the critical roles of MSNs in leveraging hydrogel toughness and adhesion strength. Typically, the synthesis of catechol-coated nanoparticles (*e.g.*, coating with PDA) is carried out by dispersing nanoparticles in an alkaline solution in the presence of catechol-containing molecules (mostly dopamine).[298] Clay particles release ions in water and hence provide the alkaline conditions required for catechol polymerization.[299] In this case, polymerization occurs in the nanoscale space between the nanoclay sheets. In one study, dopamine molecules were intercalated into Hectorite nanoclay sheets and polymerized along with the clay particles.[299] Then, the AAm monomers were added to the solution and polymerized along with the PDA-coated clay sheets. The hydrogels produced were tough and adhesive, with a maximum adhesion strength of over 30 kPa and toughness over 6000 J/m^2, which is significantly higher than

Author Manuscript Author Manuscript Author Manuscript Author Manuscript

that of the human skin (2000 J/m^2). However, adhesion was reduced when the hydrogel was applied under wet conditions.

Catechol groups can be loaded onto different chemical moieties before being coated on the nanoparticle surface. For instance, dopamine-modified PEG interacts with Laponite® nanoclays through a combination of dynamic (dopamine-Laponite® reversible bonding *via* the hydroxyl groups) and covalent bonding (dopamine-dopamine covalent crosslinking), as shown in Figure 13A,B.[300] Increasing the Laponite® content leads to higher hydrogel toughness. Further, PEG branching was associated with stronger burst pressure. Hydrogels were stretchable and adhesive, as shown in Figure 13C–E.

Carbon-based nanoparticles can also be coated with PDA to promote adhesion. In addition, such chemical modifications enhance the dispersibility of the carbon-based nanoparticles in the pre-gel solution by altering their surface properties/energy. Coating with PDA also deactivates the van der Waals interactions between the carbon nanomaterials, which are responsible for their agglomeration.[15] Recently, PDA-coated carbon nanotubes (CNTs) were embedded within the PAM-PAA hybrid hydrogels (Figure 13F). Polymerization was carried out in a binary solvent mixture containing water and glycerol to maintain hydrogel moisture in the long term. The synthesized hydrogels were introduced as highly adhesive materials with a tensile adhesive strength of up to 57 kPa and characterized with long-lasting stable physical properties even at extremely cold and hot temperature ranges (−20 to 60 °C).[15] The high adhesion of the hydrogel is attributed to the chemical linkages with the tissue substrates through catechol moieties. Moreover, improved cohesion was related to the additional strong hydrogen bonds introduced by glycerol. In another approach, a pre-polymerized dopamine solution was used to reduce GO nanoparticles partially[301] during the polymerization of AAm monomers. Apart from strong adhesion (~25 kPa tensile adhesive strength), the hydrogels exhibited electrical conductivity, self-healing properties, and high stretchability (up to ~37×). Similar properties were also reported for PDA-functionalized single-wall carbon nanotube (SWCNT)/PVA hydrogels.[302] Apart from electrical conductivity and high self-healing efficiency of 99%, tensile adhesion strength of ~4.5 kPa was reported for the porcine skin substrates. Huang *et al.* incorporated PDA-coated rGO nanoparticles in a polymer matrix composed of poly(*N*,*N*-dimethylacrylmide-stat-3-acrylamidophenylboronic acid) (PDMA-stat-PAPBA), and poly(glycerol monomethacrylate) (PGMA).[303] The PDA-modified rGO played important roles in both the crosslinker and the reinforcing filler. The addition of nanoparticle fillers showed significant improvements in the mechanical properties and adhesion to different substrates. Despite the improvements seen in the adhesion of hydrogels containing catechol-coated core/shell nanoparticles, some studies have reported conflicting trends of adhesion performance with these additives. For instance, PDA-coated silica particles embedded within a blend of PLGA and PEG failed to improve the burst pressure strength on the material, whereas the noncoated particles were associated with significant enhancements in adhesion.[176] Chemical mechanisms and hydrogel system types are important factors that should be considered for design of nanocomposite bioadhesives.

Metal nanoparticles are other candidates for modification with catecholic components. In one study, lignin-coated Ag nanoparticles were synthesized through the reduction of

Author Manuscript Author Manuscript Author Manuscript Author Manuscript

silver ions (Ag^+) by the phenolic and methoxy groups present on lignin molecules.[304] The resulting core-shell nanoparticles were incorporated within a PAA hydrogel, where quinone functionalities enabled durable adhesion. Pectin molecules were introduced to this hydrogel to promote the mechanical properties and toughness (stretchability over 2500%) through the formation of the hydrogen bonds between the carboxyl and hydroxyl groups. The Ag-lignin hydrogels showed a tensile adhesive strength of 27 kPa, which was higher than that of the native PAA (17 kPa). The adhesion of the material was attributed hydrogen-bonding, metal complexation, hydrophobic interactions, and covalent-bonding interactions between catechol and tissue surfaces.

Nature-inspired mechanical bioadhesives

Adhesion in hydrogels based on chemical and physical molecular attractions suffers from poor durability in wet environments, especially when subjected to various harsh conditions due to the effects of pH and many other factors related to the media and chemical constituents. In addition, it is difficult to avoid toxic chemicals during synthesis of most bioadhesives. There are many examples of mechanical adhesion systems in nature that have inspired adhesive patches with engineered surface micro- nanostructure for on-demand application on wet tissues. Surface features of such adhesives mimic living organisms including octopus, gecko, tree frogs, clingfish,[305] and mayfly larvae.[306] Micro- and nanoscale surface features in these examples promote mechanically driven adhesion through physical mechanisms such as suction, capillary forces, mechanical interlocking, van der Waals attractions, and friction.[307] Below, we discuss adhesive patches developed to mimic adhesion in biological systems.

Octopus-inspired suction cup arrays

A cluster of suction cups present on the tentacles[308] of octopi enables adhesion to a variety of rough surfaces.[309] The suction cups (a few-centimeters thick) contain an orifice (or acetabulum) and a dome-shaped protuberance that contracts to produce negative pressure at the tissue-surface interface. These architectures can be reproduced by filling an array of micro-holes partially on a silicon mold with a PU acrylate pre-polymer, as shown in Figure 14.[310] During the casting process, the trapped bubbles inside the holes along with the circumferential capillary effects mimic the dome-shaped protuberance. An adhesive patch was developed where the backpressure activates the adhesion of the material to wet/dry surfaces with adhesion strengths proportional to the applied pressure. Peeling tests indicate adhesion forces as high as 170 kPa. Adhesion in these materials arise from a set of capillary actions, moving the trapped liquids inside the chamber. The cohesive attractions between the liquid molecules in the internal chambers originate from the compressive elastic deformation of the pad. Following a similar concept, octopus-like micro tips were fabricated in micropillars by manipulating the meniscus of the pre-polymer in mold features. The results indicated the same order of magnitude peel-off adhesion strength (110 kPa) as reported in the previous study.[311] Octopus-inspired adhesives have leveraged the application of smart artificial skins and flexible electronics. Adhesive patches are designed to monitor body temperature, activity, tremor, respiration, electrocardiogram (ECG), *etc.* continuously.[312] The octopus-inspired adhesive pads exhibited durable conformations to

Author Manuscript Author Manuscript Author Manuscript Author Manuscript

match moving human joints during finger bending, as opposed to flat polydimethylsiloxane (PDMS) and “scotch tape.”[313] Adhesion in the adhesive pads stems from the capillary interactions with the wet substrate due to the bottom wrinkles. These adhesive pads enable efficient sealing of heart and liver lacerations (Figure 15). Temperature-responsive adhesive pads were also developed by placing a PNIPAM hydrogel layer on the top of an elastomeric PDMS pad comprising an array of microcavities.[314] Due to the thermal expansion of PDMS, adhesion was switched reversibly by changing the temperature between 22 and 61 °C. The highest normal adhesion strength was reported to be 94 kPa. In another work, pads with nanosuction cups were templated by monolayer non-close-packed silica colloidal crystals (250 nm diameter).[315] The pads effectively adhered to wet tissues such as myocardium as well as microrough surfaces.

Tree-frog-inspired polygonal patterns

The ‘soft’ hexagonal arrays of the epithelial cells on the toe pads of tree frogs are surrounded by oriented ‘hard’ keratin nanofibrils. Due to this microstructural design, tree frogs adhere to dry/wet surfaces regardless of surface roughness. Such adhesion stems from the synergistic contributions of the capillary forces (enabled by secreted mucus), mechanical interlocking (friction), and van der Waals forces.[316] This mechanism of adhesion has motivated the development of fabrication processes by incorporating hard/soft microphases on the adhesive surfaces. A micropatterned surface consisting of PDMS (soft) micropillars was prepared recently in which polystyrene (PS) nanopillars (hard) were templated using anodic aluminum oxides.[317] Embedded PS pillar arrays enabled adhesion and friction to different surfaces. In another study, toe-like hexagonal micropatterns were inscribed inside the octopus-inspired convex suction cups using photolithography.[318] The rGO nanoparticles were coated on the microstructured surface to enable their application in flexible electronics. The adhesive pads had peeling strength on the order of ~0.8 N (maximum peeling energy was ~45 J/m^2). The application of these pads as stretchable electrodes for long-term vital sign monitoring and real-time recording of the electrophysiologic patterns of heart motion was demonstrated for wearable devices. A comprehensive parametric study on the design factors was conducted to maximize the adhesion strength.[319] It was found that elongated hexagonal patterns improve the anisotropic friction force due to the large pillar deformability as well as the edge density in the direction of sliding.

Gecko-inspired nanopillars

Gecko toes are decorated with millions of epidermally derived adhesive ~200 nm setae. This architecture enables fast switching of adhesion (within 15 ms) by rotating the setal shafts by 30°.[320] Adhesion in gecko toes is driven mainly by van der Waals interactions.[321] However, recent studies revealed the contributions of capillarity to adhesion due to the effects of humidity.[322] A number of studies have been conducted on gecko-inspired adhesives for developing graspers in soft robotics applications.[323,324] The fabrication of gecko-mimetic high-aspect-ratio structures is difficult and requires complicated engineering designs. In one study, a sacrificial template-mediated nanoimprinting approach was employed to develop gecko-inspired hierarchical arrays on flexible polycarbonate sheets with the aid of micropillar and anodic aluminum oxide sacrificial templates.[325] The shear strength of

Author Manuscript Author Manuscript Author Manuscript Author Manuscript

the adhesives was measured to be ~119 kPa, which decayed by 20% when subjected to a cyclic adhesion test over 200 cycles. In a later study, a microfabrication approach was implemented to fabricate 20 μm circular pillars on a PDMS surface.[326] This study showed that surface roughness can significantly alter the adhesion strength due to changes in the contact area due to mechanical interlocking. A similar fabrication process was demonstrated to develop asymmetric-pillared architectures.[327] In this approach, gripping-direction switchable adhesive pads resulted in an adhesive force of 12.5 kPa (when actuated), which decreased to 3.4 kPa when deactivated. Patterned silicon nanowires were also used as a template to fabricate swellable nanofibrillar surfaces where the friction coefficient was augmented with the water uptake content for wet bioadhesion.[328] In another study, a simplified one-step fabrication scheme was introduced resulting in a chitosan film covered with nanofibril structures of 100–600 nm diameter and 70 nm height.[329] The adhesive pad was laser-bonded to the tissue to establish full adhesion through van der Waals and electrostatic interactions, with a wet tissue adhesion strength of ~8 kPa. Recently, high-resolution 3D printing using two-photon polymerization was used to fabricate flexible springtail-gecko-inspired adhesive patches from acrylated urethanes.[330] The patches consisted of pillar microstructures that repel liquids from the sides to establish wet adhesion. It was further demonstrated that modifying the pillars by adding octopus-inspired suction cups on the micropillars can significantly improve adhesion compared to those of patches with simple pillar architectures. A similar design concept was reported by Wang and Hensel in a recent study on PU-based patches architected with cupped micropillars.[331] The patches were fabricated by two-photon lithography and demonstrated maximum peel-off adhesive strengths of ~200 kPa, which was almost 7× larger than that of micropillars without cups.

Needle-interlocking adhesives

Mechanical adhesives rely primarily on interlocking surface features patterned on the adhesive materials with the roughness of adherents. Animal parts such as the quills of North American porcupines (*Erethizon dorsatum*), where their backward-facing barbs result in strong adhesion of their stingers, have inspired microneedle array designs for efficient bioadhesion of patches to the tissues.[332] To fabricate microneedle arrays with backward-curved barbs, a 4D printing approach was undertaken using digital light processing (DLP). A graded through-thickness crosslinking density was obtained in the synthetic barb structure *via* directional UV irradiation, which enabled backward bending after dissolving the uncured polymers in solvents. Pull-out tests demonstrated ~3.5× increases in adhesion force for the barbed microneedles compared to barbless microneedle patches.

Integration of interpenetrating interlocks and their swelling upon exposure to biofluids can be used to strengthen adhesion. Using a photolithographic approach, an array of swellable microhooks was patterned on a PEGDA hydrogel surface.[333] The interlocking microhooks resulted in maximum adhesion strengths of 799 kPa after a 20 h swelling period, which was significantly (730%) greater than in dry conditions. In another study, microneedle patches with swellable needle tips (for interlocking adhesion) inspired by the adhesion mechanism in endoparasites were reported.[116] One way to create these surfaces is to copolymerize a layer of soft swellable PS-*b*-PAA block copolymers on top of a non-swellable stiff PS

Author Manuscript Author Manuscript Author Manuscript Author Manuscript

microneedle platform (Figure 16).[334] Normal adhesion tests on the mucosal surfaces of intestinal tissue measured 45.3 kPa adhesion strength (compared to 9.3 kPa for dry skin), which is attributed to the strong chemical interactions between the material and mucin. This strong adhesion is attributed to swelling, which promotes interlocking with the tissue. In addition, the flexible backing material facilitated adhesion to mucosal surfaces. In a further study, double-layered microneedles with similar working mechanisms were designed with the soft swellable mussel-inspired protein phase integrated with a non-swellable SF on a microneedle core.[116] The *ex vivo* wound sealing of the microneedle in wet environments (18.6 kPa) was found to be comparable to sutured tissue controls (20.1 kPa).

Conclusions and Prospects

The fast-paced progress made towards designing bioadhesives has paved the way for advancing sutureless wound-closure techniques. Hydrogels have demonstrated enormous potential in this regard; however, the state of research identifies the need for highly elastic and tough bioadhesives before they can be brought to the market on larger scales. Tough bioadhesion is a result of synergistic contributions of cohesion and adhesion. While the lack of sufficient cohesion entails poor tissue adhesion, strong cohesion is necessary but not sufficient for tough bioadhesion. Hence, a rational bioadhesive design begins with engineering cohesive forces followed by integration of adhesive functionality in a closed-loop optimization process. These interrelations between adhesion and cohesion have largely been ignored and need further attention. For instance, introducing adhesion *via* catechol functionality (which acts as a radical scavenger) in photocrosslinkable injectable bioadhesives can counteract polymerization reactions, thereby impairing cohesion. Bioadhesive requirements differ from tissue to tissue, most studies thus far have focused on designing bioadhesives for soft tissues (such as liver, heart, lung, and skin). Other tissues such as bone and nerves require further attention.

In terms of intrinsic mechanical properties, improvements in elasticity and toughness are necessary. Such properties have been explored primarily by introducing dynamic interactions to covalent hydrogel networks. Stretchability in hydrogels is achieved mainly by synthetic hydrogels that express intrinsic stretchability such as PAM and PAA. More efforts towards natural polymers such as gelatin derivatives, which are more common in biological settings, are in demand. Characterization of toughness and stretchability in hydrogels is measured by tensile tests, whereas other mechanical aspects, such as fatigue and impact performance, are neglected largely. Given the dynamic loading required, gaining a deeper understanding of the cyclic response of such hydrogels is essential for evaluating their use as biomedical sealants. The lack of standardized methods used for measuring adhesion presents further obstacles in comparing observations reported in different studies.

Wet adhesion in hydrogels is a primary challenge. The main approaches undertaken to attain adhesion include mechanical interlocks with the uneven surface of tissues and covalent and noncovalent bonds. One goal of the ongoing research is to move the adhesive strength of the natural hydrogels to levels comparable to strong synthetic hydrogels to circumvent the biocompatibility and biodegradability issues. Despite the advances made thus far, there are major aspects of bioadhesive performance that need to be understood. First, understanding

Author Manuscript Author Manuscript Author Manuscript Author Manuscript

the time-dependent evolution of adhesion is necessary. Water content in the hydrogels varies over time, with significant consequences in terms of dry *versus* wet conditions and at different humidity levels. Environmental conditions such as local pH differ in organs (such as the stomach or lungs) and therefore need to be addressed in testing processes. In addition, due to the dynamic deformations in most organs inside the body, more attention needs to be paid to the characterization of adhesion under cyclic loads.

Future work is also encouraged in adding electrical conductivity to bioadhesives to enable applications as nerve glues and heart sealants. We imagine embedded sensing elements that can report the properties of the bioadhesive materials in action, both for scientific understanding and also as diagnostics of the state of the tissue repair. Stimuli-responsive and smart adhesives (such as those of thermoresponsive hydrogels having LSCT temperature between room and body temperature) are attractive candidates for the development of injectable sealants that solidify at body temperature. A large number of studies have revealed the potential brought to the field by the mussel-inspired bioadhesives introducing catechol groups into different hydrogel systems. However, their adhesion still fails to mimic the strong adhesion in mussels, since multiple complex aspects are yet to be recapitulated in synthetic and hybrid materials designs. To address the high sensitivity of adhesion to environmental and testing parameters, more robust and controllable testing protocols need to be developed for better consistency in the analyses of these materials and comparisons of results between laboratories.

ACKNOWLEDGMENTS

This work was supported financially by funding from the National Institutes of Health (1R01EB023052-01A1, 1R01HL140618-01).

Biographies

Hossein Montazerian

Hossein Montazerian is a PhD candidate in the Department of Bioengineering at the University of California, Los Angeles (UCLA). He works jointly at Terasaki Institute for Biomedical Innovation. He received his BSc in Mechanical Engineering at Shahid Rajaee University, Tehran, Iran, and continued his MASc studies at the School of Engineering, University of British Columbia, Canada. His research focus involves development of hydrogel biomaterials for bioadhesives and hemostatic sealants.

Author Manuscript Author Manuscript Author Manuscript Author Manuscript

Elham Davoodi

Elham Davoodi is a Postdoctoral Fellow at the California Institute of Technology. She received her PhD from the Mechanical and Mechatronics Department of the University of Waterloo in 2021. She completed her MSc in Mechanical Engineering at Texas Tech University. Her research interests include additive manufacturing technologies, bioprinting, and flexible electronics for health monitoring wearable devices.

Nasim Annabi

Nasim Annabi is an Assistant Professor in the Department of Chemical and Biomolecular Engineering at UCLA. Her multidisciplinary research program at UCLA aims to integrate novel chemistries with microscale technologies to develop the next generation of biomaterials for medical applications. In addition, her group has devised innovative strategies for the development of surgical sealants for the repair and sealing of elastic tissues. Her interdisciplinary research has been recognized by several awards such as the 2020 NSEF Young Investigator Award of American Institute of Chemical Engineers (AIChE), the 2021 Young Investigator Award from the Society for Biomaterials (SFB), and the 2021 Biomaterials Science Lectureship Award from the Royal Society of Chemistry (RSC).

Ali Khademhosseini

Ali Khademhosseini is currently the CEO and Founding Director at the Terasaki Institute for Biomedical Innovation. Previously, he was a Professor of Bioengineering, Chemical Engineering, and Radiology at UCLA. He joined UCLA as the Levi Knight Chair in November 2017 from Harvard University, where he was a Professor at Harvard Medical School and faculty member at Harvard-MIT's Division of Health Sciences and Technology and Brigham and Women's Hospital, and associate faculty at the Wyss Institute. At Harvard

Author Manuscript Author Manuscript Author Manuscript Author Manuscript

University, he directed the Biomaterials Innovation Research Center, a leading initiative in making engineered biomedical materials.

Paul S. Weiss

Paul S. Weiss is a nanoscientist, UC Presidential Chair, and distinguished professor of chemistry, bioengineering, and materials science and engineering at UCLA. He explores the ultimate limits of miniaturization, developing new tools and methods for spectroscopic imaging and chemical patterning. He applies these advances in quantum information, neuroscience, microbiome studies, tissue engineering, and high-throughput cellular therapies. He has won awards in science, engineering, teaching, publishing, and communications. He is a fellow of the American Academy of Arts & Sciences, AAAS, ACS, AIMBE, APS, AVS, Canadian Academy of Engineering, IEEE, and MRS. He was the founding editor-in-chief of *ACS Nano*.

List of Abbreviations

[EMIm][DCA]	1-Ethyl-3-methylimidazolium dicyanamide
[EMIM]Br	1-Ethyl-3-methylimidazolium bromide
AA	Acrylic acid
AAcNa	Sodium acrylic acid
AAm	Acrylamide
ACA	Allyl 2-cyanoacrylate
AMP	Antimicrobial peptide
AMPS	2-Acrylamide-2-methylpropane sulfonic acid
APMA	*N*-(3-aminopropyl)methacrylamide hydrochloride
APS	Ammonium persulfate
ATAC	2-(Acryloyloxy)ethyl trimethylammonium chloride
BAC	*N,N*-bis(acryloyl)cystamine
BIS	*N,N*′-methylene-bis(acrylamide)
bis-GMA	Bisphenol-A glycidyl methacrylate
CBG	Caffeic acid bioconjugated gel

Author Manuscript Author Manuscript Author Manuscript Author Manuscript

CHI-C	Catechol functionalized chitosan
CMC-Tyr	Carboxymethyl cellulose-tyramine hydrogels
CNC	Cellulose nanocrystals
CNFs	Chitin nanofibers
CNS	Calcium hydroxide nano-spherulites
CNT	Carbon nanotubes
DBA	3,4-Dihydroxybenzaldehyde
DLH	Double-layer hydroxide
DLP	Digital light processing
DMA	Methacrylated dopamine
DMAPS	Methacryloyloxyethyl ammonium propane sulfonate
DMSO	Dimethyl sulfoxide
ECG	Electrocardiogram
EDC	1-Dthyl-3-(3-dimethylaminopropyl)carbodiimide
F127DA	Pluronic F127
FDA	U.S. Food and Drug Administration
GelMA	Gelatin methacryloyl
GO	Graphene oxide
HA	Hyaluronic acid
HA-NCSN	Hyaluronic acid modified with thiourea groups
HEA	2-Hydroxyethyl acrylate
HEA	Hydroxyethyl acrylate
HFP	Hexafluoropropylene
HMA-CM-chitin	2-Hydroxy-3-methacryloyloxypropylated carboxymethyl chitin
HPA	3,4-Hydroxyphenylpropionic acid
HPR	Hydroxypropylated Polyrotaxane
HPR	Hydroxypropylated polyrotaxane
HPR-C	Hydroxypropylated polyrotaxane crosslinker

Author Manuscript Author Manuscript Author Manuscript Author Manuscript

HRP	Horseradish peroxidase
I2959	Irgacure 2959
IPDI	Isophoronediisocyanate
IPN	Interpenetrating polymer networks
KPS	Potassium persulfate
LCST	Lower critical solution temperature
LZM	Lysozyme
MAP	Mussel adhesive proteins
MBAA	*N,N*′-methylene-bis(acrylamide)
MCI 4	4′-methylenebis(cyclohexyl isocyanate)
MCS	Maleic-modified chitosan
MeTro	Methacryloyl-substituted tropoelastin molecules
MMT	Montmorillonite
MSN	Mesoporous silica nanoparticles
NB	*N*-(2-aminoethyl)−4-(4-(hydroxymethyl)−2-methoxy-5-nitrosophenoxy) butanamide
NC	Nanocomposite
NHS	*N*-hydroxysuccinimide
NIPA	*N*-isopropyl(acrylamide)
P(L-DOPA)	Poly(L-3,4-dihydroxyphenylalanine)
PAA	Poly(acrylic acid)
PAM	Poly(acrylamide)
PANI	Polyaniline
PCE	Polycarboxylate-ether superplasticizer
PCL	Polycaprolactone
PCLD	Polycaprolactonediol
PDA	Polydopamine
PDDA	Poly(diallyldimethylammonium chloride)
PDMAPS	Poly(3-dimethyl(methacryloyloxyethyl) ammonium propane sulfonate)

Author Manuscript Author Manuscript Author Manuscript Author Manuscript

PDMA-stat-PAPBA	Poly(*N,N*-dimethylacrylmide-stat-3-acrylamidophenylboronic acid)
PDMS	Polydimethylsiloxane
PEA	Polymeric network containing polyetheramine
PEG	Poly(ethylene glycol)
PEGDA	Poly(ethylene glycol)diacrylate
PEGDF	Dibenzaldehyde-terminated polyethylene glycol
PEI	Poly(ethylenimine)
PEO	Poly(ethylene oxide)
PGMA	Poly(glycerol monomethacrylate)
PGS	Poly(glycerol sebacate)
PHEMA	Poly(hydroxyethyl methacrylate)
PIA	Protuberance-inspired architectures
PLGA	Poly(lactic-*co*-glycolic acid)
PLL	Poly(L-lysine)
PLLA	Poly(L-lactic acid)
Plu-SH	Thiolated Pluronic F127
PNIPAM	Poly(*N*-Isopropyl acrylamide)
PR	Polyrotaxane
PS	Polystyrene
PS-b-PAA	Polystyrene-*b*-poly(acrylic acid)
PSS	Poly(sodium 4-styrenesulfonate)
PU	Polyurethane
PVA	Poly(vinyl alcohol)
PVDF	Poly(vinylidene fluoride-co-hexafluoropropylene)
PVP	Poly(vinyl pyrrolidone)
QCS	Quaternized chitosan
rGO	Reduced graphene oxide
ROS	Reactive oxygen species

Author Manuscript Author Manuscript Author Manuscript Author Manuscript

S-DACNFs	Surface-deacetylated chitin nanofibers
SDBS	Sodium dodecyl benzene sulfonate
SDS	Sodium dodecyl sulfate
SF	Silk fibroin
SFT	Silk fibroin hydrogel sealant
SMA	Stearyl methacrylate
SWCNT	Single-wall carbon nanotube
TA	Tannic acid
TEM	Transmission electron microscopy
TEMED	*N,N,N',N'*-tetramethylethylenediamine
THBC	Triple hydrogen-bonding clusters
THMA	*N*-[tris(hydroxymethyl)methyl]acrylamide
TPO	2,4,6-Trimethylbenzoyl-diphenylphosphine oxide
TsOH	*p*-Toluenesulfonic acid
UPy	2-Ureido-4-pyrimidone
UPyHCBA	Alkyl spacer connected by carbamate, and a 2-ureido-4-pyrimidone tail
VSNPs	Vinyl-functionalized hybrid silica nanoparticles
VTES	Vinyltriethoxysilane
α-CD	*α*-cyclodextrin

REFERENCES

1. US Outpatient Surgical Procedures Market by Surgical Procedure Type, Patient Care Setting - US Forecast to 2023; United States, January 2019; p 59.
2. Cuddy LC Wound Closure, Tension-Relieving Techniques, and Local Flaps. 2017; Vol. 47, p 1221–35.
3. Wallen TJ; Habertheuer A; Gottret JP; Kramer M; Abbas Z; Siki M; Hobbs R; Vasquez C; Molina M; Kanchwala S; Low D; Acker M; Vallabhajosyula P.Sternal Wound Complications in Patients Undergoing Orthotopic Heart Transplantation. J. Card. Surg 2019, 34, 186–189. [PubMed: 30803021]
4. Haghniaz R; Rabbani A; Vajhadin F; Khan T; Kousar R; Khan AR; Montazerian H; Iqbal J; Libanori A; Kim H-J; Wahid F.Anti-Bacterial and Wound Healing-Promoting Effects of Zinc Ferrite Nanoparticles. J. Nanobiotechnol 2021, 19, 38.
5. Kazemzadeh-Narbat M; Annabi N; Khademhosseini A.Surgical Sealants and High Strength Adhesives. Mater. Today 2015, 18, 176–177.
6. Li M; Pan G; Zhang H; Guo B.Hydrogel Adhesives for Generalized Wound Treatment: Design and Applications. J. Polym Sci 2022, 60, 1328–1359.

Author Manuscript Author Manuscript Author Manuscript Author Manuscript

7. Liang Y; He J; Guo B.Functional Hydrogels as Wound Dressing to Enhance Wound Healing. ACS Nano 2021, 15, 12687–12722. [PubMed: 34374515]
8. Li M; Zhang Z; Liang Y; He J; Guo B.Multifunctional Tissue-Adhesive Cryogel Wound Dressing for Rapid Nonpressing Surface Hemorrhage and Wound Repair. ACS Appl. Mater. Interfaces 2020, 12, 35856–35872. [PubMed: 32805786]
9. Jiang Y; Trotsyuk AA; Niu S; Henn D; Chen K; Shih C-C; Larson MR; Mermin-Bunnell AM; Mittal S; Lai J-C; Saberi A; Beard E; Jing S; Zhong D; Steele SR; Sun K; Jain T; Zhao E; Neimeth CR; Viana WG; Tang J; Sivaraj D; Padmanabhan J; Rodrigues M; Perrault DP; Chattopadhyay A; Maan ZN; Leeolou MC; Bonham CA; Kwon SH; Kussie HC; Fischer KS; Gurusankar G; Liang K; Zhang K; Nag R; Snyder MP; Januszyk M; Gurtner GC; Bao Z.Wireless Closed-Loop Smart Bandage for Chronic Wound Management and Accelerated Tissue Regeneration. bioRxiv 2022, 2022.01.16.476432.
10. Mostafalu P; Tamayol A; Rahimi R; Ochoa M; Khalilpour A; Kiaee G; Yazdi IK; Bagherifard S; Dokmeci MR; Ziaie B; Sonkusale SR; Khademhosseini A.Smart Bandage for Monitoring and Treatment of Chronic Wounds. Small 2018, 14, 1703509.
11. Derakhshandeh H; Aghabaglou F; Mccarthy A; Mostafavi A; Wiseman C; Bonick Z; Ghanavati I; Harris S; Kreikemeier-Bower C; Moosavi Basri SM; Rosenbohm J; Yang R; Mostafalu P; Orgill D; Tamayol A.A Wirelessly Controlled Smart Bandage with 3D-Printed Miniaturized Needle Arrays. Adv. Funct. Mater 2020, 30, 1905544.
12. Mclister A; Mchugh J; Cundell J; Davis J.New Developments in Smart Bandage Technologies for Wound Diagnostics. Adv. Mater 2016, 28, 5732–5737. [PubMed: 26821765]
13. Kassal P; Kim J; Kumar R; De Araujo WR; Steinberg IM; Steinberg MD; Wang J.Smart Bandage with Wireless Connectivity for Uric Acid Biosensing as an Indicator of Wound Status. Electrochem. Commun 2015, 56, 6–10.
14. Umar M; Ullah A; Nawaz H; Areeb T; Hashmi M; Kharaghani D; Kim KO; Kim IS Wet-Spun Bi-Component Alginate Based Hydrogel Fibers: Development and in-Vitro Evaluation as a Potential Moist Wound Care Dressing. Int. J. Biol. Macromol 2021, 168, 601–610. [PubMed: 33338524]
15. Han L; Liu K; Wang M; Wang K; Fang L; Chen H; Zhou J; Lu X.Mussel-Inspired Adhesive and Conductive Hydrogel with Long-Lasting Moisture and Extreme Temperature Tolerance. Adv. Funct. Mater 2018, 28, 1704195.
16. Blacklow SO; Li J; Freedman BR; Zeidi M; Chen C; Mooney DJ Bioinspired Mechanically Active Adhesive Dressings to Accelerate Wound Closure. Sci. Adv 2019, 5, eaaw3963.
17. Tan H; Jin D; Qu X; Liu H; Chen X; Yin M; Liu C.A PEG-Lysozyme Hydrogel Harvests Multiple Functions as a Fit-to-Shape Tissue Sealant for Internal-Use of Body. Biomaterials 2019, 192, 392–404. [PubMed: 30497024]
18. Bian S; Zheng Z; Liu Y; Ruan C; Pan H; Zhao X.A Shear-Thinning Adhesive Hydrogel Reinforced by Photo-Initiated Crosslinking as a Fit-to-Shape Tissue Sealant. J. Mater. Chem. B 2019, 7, 6488–6499. [PubMed: 31576899]
19. Montazerian H; Davoodi E; Baidya A; Baghdasarian S; Sarikhani E; Meyer CE; Haghniaz R; Badv M; Annabi N; Khademhosseini A; Weiss PS Engineered Hemostatic Biomaterials for Sealing Wounds. Chem. Rev 2022, 122, 12864–12903. [PubMed: 35731958]
20. Spotnitz WD Fibrin Sealant: The Only Approved Hemostat, Sealant, and Adhesive—A Laboratory and Clinical Perspective. ISRN Surgery 2014, 2014, 203943.
21. Carvalho MV; Marchi E; Fruchi AJ; Dias BV; Pinto CL; Dos Santos GR; Acencio MM Local and Systemic Effects of Fibrin and Cyanoacrylate Adhesives on Lung Lesions in Rabbits. Clinics 2017, 72, 624–628. [PubMed: 29160425]
22. Primus FE; Young DM; Grenert JP; Harris HW Silver Microparticles Plus Fibrin Tissue Sealant Prevents Incisional Hernias in Rats. J. Surg. Res 2018, 227, 130–136. [PubMed: 29804844]
23. Carr BD; Grant CN; Overman RE; Gadepalli SK; Geiger JD Retroperitoneal Exploration with Vicryl Mesh and Fibrin Tissue Sealant for Refractory Chylous Ascites. J. Pediatr. Surg 2019, 54, 604–607. [PubMed: 30340876]
24. Grunzweig KA; Ascha M; Kumar AR Fibrin Tissue Sealant and Minor Skin Grafts in Burn Surgery: A Systematic Review and Meta-Analysis. J. Plast. Reconstr. Aesthet. Surg 2019, 72, 871–883. [PubMed: 30642795]

Author Manuscript Author Manuscript Author Manuscript Author Manuscript

25. Saffarzadeh M; Mulpuri A; Arneja JS Recalcitrant Anaphylaxis Associated with Fibrin Sealant: Treatment with “TISSEEL-ectomy”. Plast. Reconstr. Surg 2021, 9, e3382.
26. Taboada GM; Yang KS; Pereira MJN; Liu SHS; Hu YS; Karp JM; Artzi N; Lee YH Overcoming the Translational Barriers of Tissue Adhesives. Nat. Rev. Mater 2020, 5, 310–329.
27. Qu X; Wang S; Zhao Y; Huang H; Wang Q; Shao J; Wang W; Dong X.Skin-Inspired Highly Stretchable, Tough and Adhesive Hydrogels for Tissue-Attached Sensor. Chem. Eng. J 2021, 425, 131523.
28. Yang W; Sherman VR; Gludovatz B; Schaible E; Stewart P; Ritchie RO; Meyers MA On the Tear Resistance of Skin. Nat. Commun 2015, 6, 1–10.
29. Lu XL; Shi SJ; Li HM; Gerhard E; Lu ZH; Tan XY; Li WL; Rahn KM; Xie DH; Xu GD; Zou F; Bai XC; Guo JS; Yang J.Magnesium Oxide-Crosslinked Low-Swelling Citrate-Based Mussel-Inspired Tissue Adhesives. Biomaterials 2020, 232, 119719.
30. Nam S; Mooney D.Polymeric Tissue Adhesives. Chem. Rev 2021, 121, 11336–11384. [PubMed: 33507740]
31. Yu ZC; Wu PY A Highly Transparent Ionogel with Strength Enhancement Ability for Robust Bonding in an Aquatic Environment. Mater. Horiz 2021, 8, 2057–2064. [PubMed: 34846483]
32. Walker BW; Lara RP; Yu CH; Sani ES; Kimball W; Joyce S; Annabi N.Engineering a Naturally-Derived Adhesive and Conductive Cardiopatch. Biomaterials 2019, 207, 89–101. [PubMed: 30965152]
33. Cui C; Liu W.Recent Advances in Wet Adhesives: Adhesion Mechanism, Design Principle and Applications. Prog. Polym. Sci 2021, 116, 101388.
34. Su X; Luo Y; Tian ZL; Yuan ZY; Han YM; Dong RF; Xu L; Feng YT; Liu XZ; Huang JY Ctenophore-Inspired Hydrogels for Efficient and Repeatable Underwater Specific Adhesion to Biotic Surfaces. Mater. Horiz 2020, 7, 2651–2661.
35. Guo B; Dong R; Liang Y; Li M.Haemostatic Materials for Wound Healing Applications. Nat. Rev. Chem 2021, 5, 773–791.
36. Pourshahrestani S; Zeimaran E; Kadri NA; Mutlu N; Boccaccini AR Polymeric Hydrogel Systems as Emerging Biomaterial Platforms to Enable Hemostasis and Wound Healing. Adv. Healthcare Mater 2020, 9, 2000905.
37. Zhang H; Zhao T; Duffy P; Dong Y; Annaidh AN; O’Cearbhaill E; Wang W.Hydrolytically Degradable Hyperbranched PEG-Polyester Adhesive with Low Swelling and Robust Mechanical Properties. Adv. Healthcare Mater 2015, 4, 2260–2268.
38. Gao Y; Han X; Chen J; Pan Y; Yang M; Lu L; Yang J; Suo Z; Lu T.Hydrogel–Mesh Composite for Wound Closure. Proc. Natl. Acad. Sci. U.S.A 2021, 118, e2103457118.
39. Guo H; Bai W; Ouyang W; Liu Y; Wu C; Xu Y; Weng Y; Zang H; Liu Y; Jacobson L; Hu Z; Wang Y; Arafa HM; Yang Q; Lu D; Li S; Zhang L; Xiao X; Vázquez-Guardado A; Ciatti J; Dempsey E; Ghoreishi-Haack N; Waters EA; Haney CR; Westman AM; Macewan MR; Pet MA; Rogers JA Wireless Implantable Optical Probe for Continuous Monitoring of Oxygen Saturation in Flaps and Organ Grafts. Nat. Commun 2022, 13, 3009. [PubMed: 35637230]
40. Choi YS; Jeong H; Yin RT; Avila R; Pfenniger A; Yoo J; Lee JY; Tzavelis A; Lee YJ; Chen SW; Knight HS; Kim S; Ahn H-Y; Wickerson G; Vázquez-Guardado A; Higbee-Dempsey E; Russo BA; Napolitano MA; Holleran TJ; Razzak LA; Miniovich AN; Lee G; Geist B; Kim B; Han S; Brennan JA; Aras K; Kwak SS; Kim J; Waters EA; Yang X; Burrell A; Chun KS; Liu C; Wu C; Rwei AY; Spann AN; Banks A; Johnson D; Zhang ZJ; Haney CR; Jin SH; Sahakian AV; Huang Y; Trachiotis GD; Knight BP; Arora RK; Efimov IR; Rogers JA A Transient, Closed-Loop Network of Wireless, Body-Integrated Devices for Autonomous Electrotherapy. Science 2022, 376, 1006–1012. [PubMed: 35617386]
41. Qiao Z; Cao M; Michels K; Hoffman L; Ji H-F Design and Fabrication of Highly Stretchable and Tough Hydrogels. Polym. Rev 2020, 60, 420–441.
42. Montazerian H; Baidya A; Haghniaz R; Davoodi E; Ahadian S; Annabi N; Khademhosseini A; Weiss PS Stretchable and Bioadhesive Gelatin Methacryloyl-Based Hydrogels Enabled by *in Situ* Dopamine Polymerization. ACS Appl. Mater. Interfaces 2021, 13, 40290–40301. [PubMed: 34410697]

Author Manuscript Author Manuscript Author Manuscript Author Manuscript

43. Fuchs S; Shariati K; Ma M.Specialty Tough Hydrogels and Their Biomedical Applications. Adv. Healthcare Mater 2020, 9, 1901396.
44. Liu R; Liang S; Tang X-Z; Yan D; Li X; Yu Z-Z Tough and Highly Stretchable Graphene Oxide/Polyacrylamide Nanocomposite Hydrogels. J. Mater. Chem 2012, 22, 14160–14167.
45. Haraguchi K.Synthesis and Properties of Soft Nanocomposite Materials with Novel Organic/Inorganic Network Structures. Polym. J 2011, 43, 223.
46. Simha N; Carlson CS; Lewis JL Evaluation of Fracture Toughness of Cartilage by Micropenetration. J. Mater. Sci.: Mater. Med 2004, 15, 631–639. [PubMed: 15386973]
47. Nonoyama T; Gong JP Tough Double Network Hydrogel and Its Biomedical Applications. Annu. Rev. Chem. Biomol. Eng 2021, 12, 393–410. [PubMed: 33770463]
48. Zhang Q; Liu X; Duan LJ; Gao GH Ultra-Stretchable Wearable Strain Sensors Based on Skin-Inspired Adhesive, Tough and Conductive Hydrogels. Chem. Eng. J 2019, 365, 10–19.
49. Zheng Y; Yu Z; Zhang S; Kong X; Michaels W; Wang W; Chen G; Liu D; Lai J-C; Prine N; Zhang W; Nikzad S; Cooper CB; Zhong D; Mun J; Zhang Z; Kang J; Tok JBH; Mcculloch I; Qin J; Gu X; Bao Z.A Molecular Design Approach towards Elastic and Multifunctional Polymer Electronics. Nat. Commun 2021, 12, 5701. [PubMed: 34588448]
50. Liu Y; Feig VR; Bao Z.Conjugated Polymer for Implantable Electronics toward Clinical Application. Adv. Healthcare Mater 2021, 10, 2001916.
51. Wang C; Chen X; Wang L; Makihata M; Liu H-C; Zhou T; Zhao X.Bioadhesive Ultrasound for Long-term Continuous Imaging of Diverse Organs. Science 2022, 377, 517–523. [PubMed: 35901155]
52. Sun J-Y; Zhao X; Illeperuma WR; Chaudhuri O; Oh KH; Mooney DJ; Vlassak JJ; Suo Z.Highly Stretchable and Tough Hydrogels. Nature 2012, 489, 133. [PubMed: 22955625]
53. Lin S; Yuk H; Zhang T; Parada GA; Koo H; Yu C; Zhao X.Stretchable Hydrogel Electronics and Devices. Adv. Mater 2016, 28, 4497–4505. [PubMed: 26639322]
54. Yuk H; Zhang T; Lin S; Parada GA; Zhao X.Tough Bonding of Hydrogels to Diverse Non-Porous Surfaces. Nat. Mater 2016, 15, 190–196. [PubMed: 26552058]
55. Hong S; Sycks D; Chan HF; Lin S; Lopez GP; Guilak F; Leong KW; Zhao X.3D Printing of Highly Stretchable and Tough Hydrogels into Complex, Cellularized Structures. Adv. Mater 2015, 27, 4035–4040. [PubMed: 26033288]
56. Webber RE; Creton C; Brown HR; Gong JP Large Strain Hysteresis and Mullins Effect of Tough Double-Network Hydrogels. Macromolecules 2007, 40, 2919–2927.
57. Zhang K; Cai L; Chen G.Highly Stretchable Ionic Conducting Hydrogels for Strain/Tactile Sensors. Polymer 2019, 167, 154–158.
58. Liu XJ; Li HQ; Zhang BY; Wang YJ; Ren XY; Guan S; Gao GH Highly Stretchable and Tough pH-Sensitive Hydrogels with Reversible Swelling and Recoverable Deformation. RSC Adv. 2016, 6, 4850–4857.
59. Yuan T; Cui X; Liu X; Qu X; Sun J.Highly Tough, Stretchable, Self-Healing, and Recyclable Hydrogels Reinforced by *in Situ*-Formed Polyelectrolyte Complex Nanoparticles. Macromolecules 2019, 52, 3141–3149.
60. Lalevée G; David L; Montembault A; Blanchard K; Meadows J; Malaise S; Crépet A; Grillo I; Morfin I; Delair T.Highly Stretchable Hydrogels from Complex Coacervation of Natural Polyelectrolytes. Soft Matter 2017, 13, 6594–6605. [PubMed: 28905969]
61. Ying B; Chen RZ; Zuo R; Li J; Liu X.An Anti-Freezing, Ambient-Stable and Highly Stretchable Ionic Skin with Strong Surface Adhesion for Wearable Sensing and Soft Robotics. Adv. Funct. Mater 2021, 31, 2104665.
62. Yuan Z; Hou L; Bariya M; Nyein HYY; Tai L-C; Ji W; Li L; Javey A.A Multi-Modal Sweat Sensing Patch for Cross-Verification of Sweat Rate, Total Ionic Charge, and Na+ Concentration. Lab Chip 2019, 19, 3179–3189. [PubMed: 31433434]
63. Mackanic DG; Yan X; Zhang Q; Matsuhisa N; Yu Z; Jiang Y; Manika T; Lopez J; Yan H; Liu K; Chen X; Cui Y; Bao Z.Decoupling of Mechanical Properties and Ionic Conductivity in Supramolecular Lithium Ion Conductors. Nat. Commun 2019, 10, 5384. [PubMed: 31772158]
64. Cao Y; Morrissey TG; Acome E; Allec SI; Wong BM; Keplinger C; Wang C.A Transparent, Self-Healing, Highly Stretchable Ionic Conductor. Adv. Mater 2017, 29, 1605099.

Author Manuscript Author Manuscript Author Manuscript Author Manuscript

65. Zhou Y; Wan C; Yang Y; Yang H; Wang S; Dai Z; Ji K; Jiang H; Chen X; Long Y.Highly Stretchable, Elastic, and Ionic Conductive Hydrogel for Artificial Soft Electronics. Adv. Funct. Mater 2019, 29, 1806220.

66. Lai J; Zhou H; Jin Z; Li S; Liu H; Jin X; Luo C; Ma A; Chen W.Highly Stretchable, Fatigue Resistant, Electrically Conductive and Temperature Tolerant Ionogels for High-Performance Flexible Sensors. ACS Appl. Mater. Interfaces 2019, 11, 26412–26420. [PubMed: 31257857]

67. Sun L; Chen S; Guo Y; Song J; Zhang L; Xiao L; Guan Q; You Z.Ionogel-Based, Highly Stretchable, Transparent, Durable Triboelectric Nanogenerators for Energy Harvesting and Motion Sensing over a Wide Temperature Range. Nano Energy 2019, 63, 103847.

68. Dai LX; Zhang W; Sun L; Wang XH; Jiang W; Zhu ZW; Zhang HB; Yang CC; Tang J.Highly Stretchable and Compressible Self-Healing P(AA-*co*-AAM)/CoCl2 Hydrogel Electrolyte for Flexible Supercapacitors. Chemelectrochem 2019, 6, 467–472.

69. Lei Z; Wu P.A Highly Transparent and Ultra-Stretchable Conductor with Stable Conductivity During Large Deformation. Nat. Commun 2019, 10, 3429. [PubMed: 31366932]

70. Guo Y; Zheng K; Wan P.A Flexible Stretchable Hydrogel Electrolyte for Healable All-in-One Configured Supercapacitors. Small 2018, 14, 1704497.

71. Cai G; Wang J; Qian K; Chen J; Li S; Lee PS Extremely Stretchable Strain Sensors Based on Conductive Self-Healing Dynamic Cross-Links Hydrogels for Human-Motion Detection. Adv. Sci 2017, 4, 1600190.

72. Chang Q; Darabi MA; Liu Y; He Y; Zhong W; Mequanin K; Li B; Lu F; Xing MMQ Hydrogels from Natural Egg White with Extraordinary Stretchability, Direct-Writing 3D Printability and Self-Healing for Fabrication of Electronic Sensors and Actuators. J. Mater. Chem. A 2019, 7, 24626–24640.

73. Tong R,; Chen G,; Pan D,; Qi H,; Li R. a.,; Tian J,; Lu F,; He M, Highly Stretchable and Compressible Cellulose Ionic Hydrogels for Flexible Strain Sensors. Biomacromolecules 2019, 20, 2096–2104. [PubMed: 30995834]

74. Abe K; Ifuku S; Kawata M; Yano H.Preparation of Tough Hydrogels Based on β-Chitin Nanofibers via NaOH Treatment. Cellulose 2014, 21, 535–540.

75. Zhang S; Shi Z; Xu H; Ma X; Yin J; Tian M.Revisiting the Mechanism of Redox-Polymerization to Build the Hydrogel with Excellent Properties Using a Novel Initiator. Soft Matter 2016, 12, 2575–2582. [PubMed: 26906449]

76. Xu Y; Rothe R; Voigt D; Hauser S; Cui MY; Miyagawa T; Gaillez MP; Kurth T; Bornhauser M; Pietzsch J; Zhang YX Convergent Synthesis of Diversified Reversible Network Leads to Liquid Metal-Containing Conductive Hydrogel Adhesives. Nat. Commun 2021, 12, 2407. [PubMed: 33893308]

77. Hu Y; Zhuo H; Zhang Y; Lai H; Yi J; Chen Z; Peng X; Wang X; Liu C; Sun R; Zhong L.Graphene Oxide Encapsulating Liquid Metal to Toughen Hydrogel. Adv. Funct. Mater 2021, 31, 2106761.

78. Kalantar-Zadeh K; Tang J; Daeneke T; O'mullane AP; Stewart LA; Liu J; Majidi C; Ruoff RS; Weiss PS; Dickey MD Emergence of Liquid Metals in Nanotechnology. ACS Nano 2019, 13, 7388–7395. [PubMed: 31245995]

79. Peng H; Xin Y; Xu J; Liu H; Zhang J.Ultra-Stretchable Hydrogels with Reactive Liquid Metals as Asymmetric Force-Sensors. Mater. Horiz 2019, 6, 618–625.

80. Du R; Xu Z; Zhu C; Jiang Y; Yan H; Wu H-C; Vardoulis O; Cai Y; Zhu X; Bao Z; Zhang Q; Jia X.A Highly Stretchable and Self-Healing Supramolecular Elastomer Based on Sliding Crosslinks and Hydrogen Bonds. Adv. Funct. Mater 2020, 30, 1907139.

81. Imran AB; Esaki K; Gotoh H; Seki T; Ito K; Sakai Y; Takeoka Y.Extremely Stretchable Thermosensitive Hydrogels by Introducing Slide-Ring Polyrotaxane Cross-Linkers and Ionic Groups into the Polymer Network. Nat. Commun 2014, 5, 5124. [PubMed: 25296246]

82. Jiang L; Liu C; Mayumi K; Kato K; Yokoyama H; Ito K.Highly Stretchable and Instantly Recoverable Slide-Ring Gels Consisting of Enzymatically Synthesized Polyrotaxane with Low Host Coverage. Chem. Mater 2018, 30, 5013–5019.

83. Huang G-B; Wang S-H; Ke H; Yang L-P; Jiang W.Selective Recognition of Highly Hydrophilic Molecules in Water by Endo-Functionalized Molecular Tubes. J. Am. Chem. Soc 2016, 138, 14550–14553. [PubMed: 27792319]

Author Manuscript Author Manuscript Author Manuscript Author Manuscript

84. Ke H; Yang L-P; Xie M; Chen Z; Yao H; Jiang W.Shear-Induced Assembly of a Transient yet Highly Stretchable Hydrogel Based on Pseudopolyrotaxanes. Nat. Chem 2019, 11, 470. [PubMed: 30936522]

85. Zhang R; Fu Q; Zhou K; Yao Y; Zhu X.Ultra Stretchable, Tough and Self-Healable Poly(acrylic acid) Hydrogels Cross-Linked by Self-Enhanced High-Density Hydrogen Bonds. Polymer 2020, 199, 122603.

86. Qin Z; Yu X; Wu H; Li J; Lv H; Yang X.Nonswellable and Tough Supramolecular Hydrogel Based on Strong Micelle Cross-Linkings. Biomacromolecules 2019, 20, 3399–3407. [PubMed: 31339699]

87. Jeon I; Cui J; Illeperuma WR; Aizenberg J; Vlassak JJ Extremely Stretchable and Fast Self-Healing Hydrogels. Adv. Mater 2016, 28, 4678–4683. [PubMed: 27061799]

88. Cui W; Ji J; Cai Y-F; Li H; Ran R.Robust, Anti-Fatigue, and Self-Healing Graphene Oxide/Hydrophobically Associated Composite Hydrogels and Their Use as Recyclable Adsorbents for Dye Wastewater Treatment. J. Mater. Chem. A 2015, 3, 17445–17458.

89. Zhang Y; Song M; Diao Y; Li B; Shi L; Ran R.Preparation and Properties of Polyacrylamide/Polyvinyl Alcohol Physical Double Network Hydrogel. RSC Adv. 2016, 6, 112468–112476.

90. Huangágoh W; Hoseinásakhaei A.Highly Stretchable Hydrogels for UV Curing Based High-Resolution Multimaterial 3D Printing. J. Mater. Chem. B 2018, 6, 3246–3253. [PubMed: 32254382]

91. Seaberg J; Montazerian H; Hossen MN; Bhattacharya R; Khademhosseini A; Mukherjee P.Hybrid Nanosystems for Biomedical Applications. ACS Nano 2021, 15, 2099–2142. [PubMed: 33497197]

92. Cheng F-M; Chen H-X; Li H-D Recent Advances in Tough and Self-Healing Nanocomposite Hydrogels for Shape Morphing and Soft Actuators. Eur. Polym. J 2020, 124, 109448.

93. Jing X; Mi H-Y; Peng X-F; Turng L-S Biocompatible, Self-Healing, Highly Stretchable Polyacrylic Acid/Reduced Graphene Oxide Nanocomposite Hydrogel Sensors via Mussel-Inspired Chemistry. Carbon 2018, 136, 63–72.

94. Ma J; Lee J; Han SS; Oh KH; Nam KT; Sun J-Y Highly Stretchable and Notch-Insensitive Hydrogel Based on Polyacrylamide and Milk Protein. ACS Appl. Mater. Interfaces 2016, 8, 29220–29226. [PubMed: 27749026]

95. Xu J; Wang G; Wu Y; Ren X; Gao G.Ultra-Stretchable Wearable Strain and Pressure Sensors Base on Adhesive, Tough and Self-Healing Hydrogels for Human Motion Monitoring. ACS Appl. Mater. Interfaces 2019, 11, 25613–25623. [PubMed: 31273992]

96. Sun G; Li Z; Liang R; Weng L-T; Zhang L.Super Stretchable Hydrogel Achieved by Non-Aggregated Spherulites with Diameters< 5 nm. Nat. Commun 2016, 7, 12095. [PubMed: 27352822]

97. Liang R; Li Z; Weng L-T; Zhang L; Sun G.Recoverable Hydrogel with High Stretchability and Toughness Achieved by Low-Temperature Hydration of Portland Cement. Mater. Chem. Front 2018, 2, 2076–2080.

98. Jiang H; Zhang G; Li F; Zhang Y; Lei Y; Xia Y; Jin X; Feng X; Li H.A Self-Healable and Tough Nanocomposite Hydrogel Crosslinked by Novel Ultrasmall Aluminum Hydroxide Nanoparticles. Nanoscale 2017, 9, 15470–15476. [PubMed: 28976516]

99. Gao G; Du G; Sun Y; Fu J.Self-Healable, Tough, and Ultrastretchable Nanocomposite Hydrogels Based on Reversible Polyacrylamide/Montmorillonite Adsorption. ACS Appl. Mater. Interfaces 2015, 7, 5029–5037. [PubMed: 25668063]

100. Su X; Mahalingam S; Edirisinghe M; Chen B.Highly Stretchable and Highly Resilient Polymer–Clay Nanocomposite Hydrogels with Low Hysteresis. ACS Appl. Mater. Interfaces 2017, 9, 22223–22234. [PubMed: 28609609]

101. Xiong L; Hu X; Liu X; Tong Z.Network Chain Density and Relaxation of *in Situ* Synthesized Polyacrylamide/Hectorite Clay Nanocomposite Hydrogels with Ultrahigh Tensibility. Polymer 2008, 49, 5064–5071.

102. Hu Z; Chen G.Novel Nanocomposite Hydrogels Consisting of Layered Double Hydroxide with Ultrahigh Tensibility and Hierarchical Porous Structure at Low Inorganic Content. Adv. Mater 2014, 26, 5950–5956. [PubMed: 24923256]

Author Manuscript Author Manuscript Author Manuscript Author Manuscript

103. Jing X; Mi H-Y; Lin Y-J; Enriquez E; Peng X-F; Turng L-S Highly Stretchable and Biocompatible Strain Sensors Based on Mussel-Inspired Super-Adhesive Self-Healing Hydrogels for Human Motion Monitoring. ACS Appl. Mater. Interfaces 2018, 10, 20897–20909. [PubMed: 29863322]
104. Huang Y; Zhong M; Shi F; Liu X; Tang Z; Wang Y; Huang Y; Hou H; Xie X; Zhi C.An Intrinsically Stretchable and Compressible Supercapacitor Containing a Polyacrylamide Hydrogel Electrolyte. Angew. Chem. Int. Ed 2017, 56, 9141–9145.
105. Shi F-K; Wang X-P; Guo R-H; Zhong M; Xie X-M Highly Stretchable and Super Tough Nanocomposite Physical Hydrogels Facilitated by the Coupling of Intermolecular Hydrogen Bonds and Analogous Chemical Crosslinking of Nanoparticles. J. Mater. Chem. B 2015, 3, 1187–1192. [PubMed: 32264469]
106. Zhong M; Liu X-Y; Shi F-K; Zhang L-Q; Wang X-P; Cheetham AG; Cui H; Xie X-M Self-Healable, Tough and Highly Stretchable Ionic Nanocomposite Physical Hydrogels. Soft Matter 2015, 11, 4235–4241. [PubMed: 25892460]
107. Huang Y; Zhong M; Huang Y; Zhu M; Pei Z; Wang Z; Xue Q; Xie X; Zhi C.A Self-Healable and Highly Stretchable Supercapacitor Based on a Dual Crosslinked Polyelectrolyte. Nat. Commun 2015, 6, 10310. [PubMed: 26691661]
108. Chen CR; Qin H; Cong HP; Yu SH A Highly Stretchable and Real-Time Healable Supercapacitor. Adv. Mater 2019, 31, 1900573.
109. Xie L; Gong L; Zhang JW; Han LB; Xiang L; Chen JS; Liu JF; Yan B; Zeng HB A Wet Adhesion Strategy *via* Synergistic Cation-π and Hydrogen Bonding Interactions of Antifouling Zwitterions and Mussel-Inspired Binding Moieties. J. Mater. Chem. A 2019, 7, 21944–21952.
110. Bal-Ozturk A; Cecen B; Avci-Adali M; Topkaya SN; Alarcin E; Yasayan G; Li Y-CE; Bulkurcuoglu B; Akpek A; Avci H.Tissue Adhesives: From Research to Clinical Translation. Nano Today 2021, 36, 101049.
111. Kim S; Yoo HY; Huang J; Lee Y; Park S; Park Y; Jin S; Jung YM; Zeng HB; Hwang DS; Jho Y.Salt Triggers the Simple Coacervation of an Underwater Adhesive When Cations Meet Aromatic π Electrons in Seawater. ACS Nano 2017, 11, 6764–6772. [PubMed: 28614666]
112. Gebbie MA; Wei W; Schrader AM; Cristiani TR; Dobbs HA; Idso M; Chmelka BF; Waite JH; Israelachvili JN Tuning Underwater Adhesion with Cation-π Interactions. Nat. Chem 2017, 9, 473–479. [PubMed: 28430190]
113. Yang JW; Bai RB; Suo ZG Topological Adhesion of Wet Materials. Adv. Mater 2018, 30, 1800671.
114. Ghobril C; Grinstaff M.The Chemistry and Engineering of Polymeric Hydrogel Adhesives for Wound Closure: A Tutorial. Chem. Soc. Rev 2015, 44, 1820–1835. [PubMed: 25649260]
115. Yang J; Bai R; Chen B; Suo Z.Hydrogel Adhesion: A Supramolecular Synergy of Chemistry, Topology, and Mechanics. Adv. Funct. Mater 2019, 30, 1901693.
116. Jeon EY; Lee J; Kim BJ; Joo KI; Kim KH; Lim G; Cha HJ Bio-Inspired Swellable Hydrogel-Forming Double-Layered Adhesive Microneedle Protein Patch for Regenerative Internal/External Surgical Closure. Biomaterials 2019, 222, 119439.
117. Ma Z; Bourquard C; Gao Q; Jiang S; De Iure-Grimmel T; Huo R; Li X; He Z; Yang Z; Yang G; Wang Y; Lam E; Gao Z.-h.; Supponen O; Li J.Controlled Tough Bioadhesion Mediated by Ultrasound. Science 2022, 377, 751–755. [PubMed: 35951702]
118. Assmann A; Vegh A; Ghasemi-Rad M; Bagherifard S; Cheng G; Sani ES; Ruiz-Esparza GU; Noshadi I; Lassaletta AD; Gangadharan S; Tamayol A; Khademhosseini A; Annabi N.A Highly Adhesive and Naturally Derived Sealant. Biomaterials 2017, 140, 115–127. [PubMed: 28646685]
119. Ma Z; Bao G; Li J.Multifaceted Design and Emerging Applications of Tissue Adhesives. Adv. Mater 2021, 33, 2007663.
120. Tavafoghi M; Sheikhi A; Tutar R; Jahangiry J; Baidya A; Haghniaz R; Khademhosseini A.Engineering Tough, Injectable, Naturally Derived, Bioadhesive Composite Hydrogels. Adv. Healthcare Mater 2020, 9, 1901722.
121. Hong Y; Zhou F; Hua Y; Zhang X; Ni C; Pan D; Zhang Y; Jiang D; Yang L; Lin Q.A Strongly Adhesive Hemostatic Hydrogel for the Repair of Arterial and Heart Bleeds. Nat. Commun 2019, 10, 2060. [PubMed: 31089131]

Author Manuscript Author Manuscript Author Manuscript Author Manuscript

122. Han L; Wang MH; Prieto-Lopez LO; Deng X; Cui JX Self-Hydrophobization in a Dynamic Hydrogel for Creating Nonspecific Repeatable Underwater Adhesion. Adv. Funct. Mater 2020, 30, 1907064.

123. Bayat N; Zhang Y; Falabella P; Menefee R; Whalen JJ; Humayun MS; Thompson ME A Reversible Thermoresponsive Sealant for Temporary Closure of Ocular Trauma. Sci. Transl. Med 2017, 9, eaan3879.

124. Dompe M; Cedano-Serrano FJ; Heckert O; Van Den Heuvel N; Van Der Gucht J; Tran Y; Hourdet D; Creton C; Kamperman M.Thermoresponsive Complex Coacervate-Based Underwater Adhesive. Adv. Mater 2019, 31, 1808179.

125. Narayanan A; Menefee JR; Liu QH; Dhinojwala A; Joy A.Lower Critical Solution Temperature-Driven Self-Coacervation of Nonionic Polyester Underwater Adhesives. ACS Nano 2020, 14, 8359–8367. [PubMed: 32538616]

126. Xie CM; Wang X; He H; Ding YH; Lu X.Mussel-Inspired Hydrogels for Self-Adhesive Bioelectronics. Adv. Funct. Mater 2020, 30, 1909954.

127. Yang Q; Wei T; Yin RT; Wu M; Xu Y; Koo J; Choi YS; Xie Z; Chen SW; Kandela I; Yao S; Deng Y; Avila R; Liu T-L; Bai W; Yang Y; Han M; Zhang Q; Haney CR; Benjamin Lee K; Aras K; Wang T; Seo M-H; Luan H; Lee SM; Brikha A; Ghoreishi-Haack N; Tran L; Stepien I; Aird F; Waters EA; Yu X; Banks A; Trachiotis GD; Torkelson JM; Huang Y; Kozorovitskiy Y; Efimov IR; Rogers JA Photocurable Bioresorbable Adhesives as Functional Interfaces between Flexible Bioelectronic Devices and Soft Biological Tissues. Nat. Mater 2021, 20, 1559–1570. [PubMed: 34326506]

128. Ko H; Javey A.Smart Actuators and Adhesives for Reconfigurable Matter. Acc. Chem. Res 2017, 50, 691–702. [PubMed: 28263544]

129. Yamagishi K; Kirino I; Takahashi I; Amano H; Takeoka S; Morimoto Y; Fujie T.Tissue-Adhesive Wirelessly Powered Optoelectronic Device for Metronomic Photodynamic Cancer Therapy. Nat. Biomed. Eng 2019, 3, 27–36. [PubMed: 30932063]

130. Park H; Song C; Jin SW; Lee H; Keum K; Lee YH; Lee G; Jeong YR; Ha JS High Performance Flexible Micro-Supercapacitor for Powering a Vertically Integrated Skin-Attachable Strain Sensor on a Bio-Inspired Adhesive. Nano Energy 2021, 83, 105837.

131. Yamagishi K; Zhou WS; Ching T; Huang SY; Hashimoto M.Ultra-Deformable and Tissue-Adhesive Liquid Metal Antennas with High Wireless Powering Efficiency. Adv. Mater 2021, 33, 2008062.

132. Xue Y; Zhang J; Chen X; Zhang J; Chen G; Zhang K; Lin J; Guo C; Liu J.Trigger-Detachable Hydrogel Adhesives for Bioelectronic Interfaces. Adv. Funct. Mater 2021, 31, 2106446.

133. Yuk H; Varela CE; Nabzdyk CS; Mao XY; Padera RF; Roche ET; Zhao XH Dry Double-Sided Tape for Adhesion of Wet Tissues and Devices. Nature 2019, 575, 169–174. [PubMed: 31666696]

134. Deng J; Yuk H; Wu JJ; Varela CE; Chen XY; Roche ET; Guo CF; Zhao XH Electrical Bioadhesive Interface for Bioelectronics. Nat. Mater 2021, 20, 229–236. [PubMed: 32989277]

135. Wu SJ; Yuk H; Wu JJ; Nabzdyk CS; Zhao XH A Multifunctional Origami Patch for Minimally Invasive Tissue Sealing. Adv. Mater 2021, 33, 2007667.

136. Liu Y; Zhou H; Zhou W; Meng S; Qi C; Liu Z; Kong T.Biocompatible, High-Performance, Wet-Adhesive, Stretchable All-Hydrogel Supercapacitor Implant Based on PANI@rGO/Mxenes Electrode and Hydrogel Electrolyte. Adv. Energy Mater 2021, 11, 2101329.

137. Huang J; Liu Y; Yang Y; Zhou Z; Mao J; Wu T; Liu J; Cai Q; Peng C; Xu Y.Electrically Programmable Adhesive Hydrogels for Climbing Robots. Sci. Rob 2021, 6, eabe1858.

138. Shi X; Wu P.A Smart Patch with on-Demand Detachable Adhesion for Bioelectronics. Small 2021, 17, 2101220.

139. Chen XY; Yuk H; Wu JJ; Nabzdyk CS; Zhao XH Instant Tough Bioadhesive with Triggerable Benign Detachment. Proc. Natl. Acad. Sci. U.S.A 2020, 117, 15497–15503. [PubMed: 32576692]

140. Luo J; Luo J; Bai Y; Gao Q; Li J.A High Performance Soy Protein-Based Bio-Adhesive Enhanced with a Melamine/Epichlorohydrin Prepolymer and Its Application on Plywood. RSC Adv. 2016, 6, 67669–67676.

Author Manuscript Author Manuscript Author Manuscript Author Manuscript

141. Xi S; Tian F; Wei G; He X; Shang Y; Ju Y; Li W; Lu Q; Wang Q.Reversible Dendritic-Crystal-Reinforced Polymer Gel for Bioinspired Adaptable Adhesive. Adv. Mater 2021, 33, 2103174.
142. Peng QY; Chen JS; Zeng ZC; Wang T; Xiang L; Peng XW; Liu JF; Zeng HB Adhesive Coacervates Driven by Hydrogen-Bonding Interaction. Small 2020, 16, 2004132.
143. Chen J; Wang D; Wang LH; Liu WJ; Chiu A; Shariati K; Liu QS; Wang X; Zhong Z; Webb J; Schwartz RE; Bouklas N; Ma ML An Adhesive Hydrogel with "Load-Sharing" Effect as Tissue Bandages for Drug and Cell Delivery. Adv. Mater 2020, 32, 2001628.
144. Anthis AHC; Hu XQ; Matter MT; Neuer AL; Wei KC; Schlegel AA; Starsich FHL; Herrmann IK Chemically Stable, Strongly Adhesive Sealant Patch for Intestinal Anastomotic Leakage Prevention. Adv. Funct. Mater 2021, 31, 2007099.
145. Peng X; Xia XF; Xu XY; Yang XF; Yang BG; Zhao PC; Yuan WH; Chiu PWY; Bian LM Ultrafast Self-Gelling Powder Mediates Robust Wet Adhesion to Promote Healing of Gastrointestinal Perforations. Sci. Adv 2021, 7, eabe8739.
146. Peng X; Xu X; Deng Y; Xie X; Xu L; Xu X; Yuan W; Yang B; Yang X; Xia X.Ultrafast Self-Gelling and Wet Adhesive Powder for Acute Hemostasis and Wound Healing. Adv. Funct. Mater 2021, 31, 2102583.
147. Li X; Deng Y; Lai JL; Zhao G; Dong SY Tough, Long-Term, Water-Resistant, and Underwater Adhesion of Low-Molecular-Weight Supramolecular Adhesives. J. Am. Chem. Soc 2020, 142, 5371–5379. [PubMed: 32092262]
148. Shagan A; Zhang W; Mehta M; Levi S; Kohane DS; Mizrahi B.Hot Glue Gun Releasing Biocompatible Tissue Adhesive. Adv. Funct. Mater 2020, 30, 1900998.
149. Zanjanizadeh Ezazi N; Ajdary R; Correia A; Mäkilä E; Salonen J; Kemell M; Hirvonen J; Rojas OJ; Ruskoaho HJ; Santos HA Fabrication and Characterization of Drug-Loaded Conductive Poly(glycerol sebacate)/Nanoparticle-Based Composite Patch for Myocardial Infarction Applications. ACS Appl. Mater. Interfaces 2020, 12, 6899–6909. [PubMed: 31967771]
150. Zhao X; Liang YP; Huang Y; He JH; Han Y; Guo BL Physical Double-Network Hydrogel Adhesives with Rapid Shape Adaptability, Fast Self-Healing, Antioxidant and NIR/pH Stimulus-Responsiveness for Multidrug-Resistant Bacterial Infection and Removable Wound Dressing. Adv. Funct. Mater 2020, 30, 1910748.
151. Zhang J; Chen Z; Zhang Y; Dong S; Chen Y; Zhang S.Poly(ionic liquid)s Containing Alkoxy Chains and Bis(trifluoromethanesulfonyl) Imide Anions as Highly Adhesive Materials. Adv. Mater 2021, 33, 2100962.
152. Wang W; Liu S; Chen B; Yan X; Li S; Ma X; Yu X.DNA-Inspired Adhesive Hydrogels Based on the Biodegradable Polyphosphoesters Tackified by a Nucleobase. Biomacromolecules 2019, 20, 3672–3683. [PubMed: 31513395]
153. Fan HL; Wang JH; Gong JP Barnacle Cement Proteins-Inspired Tough Hydrogels with Robust, Long-Lasting, and Repeatable Underwater Adhesion. Adv. Funct. Mater 2021, 31, 2009334.
154. Wang Y; Jeon EJ; Lee J; Hwang H; Cho SW; Lee H.A Phenol-Amine Superglue Inspired by Insect Sclerotization Process. Adv. Mater 2020, 32, 2002118.
155. Niu Y; Liu H; He RY; Luo MQ; Shu MG; Xu F.Environmentally Compatible Wearable Electronics Based on Ionically Conductive Organohydrogels for Health Monitoring with Thermal Compatibility, Anti-Dehydration, and Underwater Adhesion. Small 2021, 17, 2101151.
156. Yang H; Li C; Tang J; Suo Z.Strong and Degradable Adhesion of Hydrogels. ACS Appl. Bio Mater 2019, 2, 1781–1786.
157. Li J; Celiz A; Yang J; Yang Q; Wamala I; Whyte W; Seo B; Vasilyev N; Vlassak J; Suo Z.Tough Adhesives for Diverse Wet Surfaces. Science 2017, 357, 378–381. [PubMed: 28751604]
158. Gao Y; Chen JJ; Han XY; Pan YD; Wang PY; Wang TJ; Lu TQ A Universal Strategy for Tough Adhesion of Wet Soft Material. Adv. Funct. Mater 2020, 30, 2003207.
159. Kumar A; Domb AJ Polymerization Enhancers for Cyanoacrylate Skin Adhesive. Macromol. Biosci 2021, 21, 2100143.
160. Sagar P; Prasad K; Lalitha RM; Ranganath K.Cyanoacrylate for Intraoral Wound Closure: A Possibility? Int. J. Biomater 2015, 2015, 165428.

Author Manuscript Author Manuscript Author Manuscript Author Manuscript

161. Basu A; Veprinsky-Zuzulia I; Levinman M; Barkan Y; Golenser J; Domb AJ PEG-Biscyanoacrylate Crosslinker for Octyl Cyanoacrylate Bioadhesive. Macromol. Rapid Commun 2016, 37, 251–256. [PubMed: 26572088]
162. Lee YJ; Jung GB; Choi S; Lee G; Kim JH; Son HS; Bae H; Park H-K Biocompatibility of a Novel Cyanoacrylate Based Tissue Adhesive: Cytotoxicity and Biochemical Property Evaluation. PLoS One 2013, 8, e79761.
163. Lim JI; Hyeon SJ; Lee W-K Enhanced Chemophysical Properties by bis-GMA-Modified Allyl 2-Cyanoacrylate-Based Bioadhesives for Hard Tissue. J. Adhes. Sci. Technol 2017, 31, 149–158.
164. Lee YJ; Son HS; Jung GB; Kim JH; Choi S; Lee G-J; Park H-K Enhanced Biocompatibility and Wound Healing Properties of Biodegradable Polymer-Modified Allyl 2-Cyanoacrylate Tissue Adhesive. Mater. Sci. Eng., C 2015, 51, 43–50.
165. Liu X; Shi LX; Wan XZ; Dai B; Yang M; Gu Z; Shi XH; Jiang L; Wang ST A Spider-Silk-Inspired Wet Adhesive with Supercold Tolerance. Adv. Mater 2021, 33, 2007301.
166. Huang Y-J; Chou Y-N; Lin Y-J; Chen W-Y; Chen C-Y; Lin H-R Polyurethane Modified by Oxetane Grafted Chitosan as Bioadhesive. Int. J. Polym. Mater. Polym. Biomater 2021, 70, 1100–1114.
167. Feng Y; Xiao K; He Y; Du B; Hong J; Yin H; Lu D; Luo F; Li Z; Li J; Tan H; Fu Q.Tough and Biodegradable Polyurethane-Curcumin Composited Hydrogel with Antioxidant, Antibacterial and Antitumor Properties. Mater. Sci. Eng., C 2021, 121, 111820.
168. Huang J; Sun J; Zhang R; Zou R; Liu X; Yang Z; Yuan T.Improvement of Biodegradability of UV-Curable Adhesives Modified by a Novel Polyurethane Acrylate. Prog. Org. Coat 2016, 95, 20–25.
169. Su Q; Wei D; Dai W; Zhang Y; Xia Z.Designing a Castor Oil-Based Polyurethane as Bioadhesive. Colloids Surf., B 2019, 181, 740–748.
170. Balcioglu S; Parlakpinar H; Vardi N; Denkbas EB; Karaaslan MG; Gulgen S; Taslidere E; Koytepe S; Ates B.Design of Xylose-Based Semisynthetic Polyurethane Tissue Adhesives with Enhanced Bioactivity Properties. ACS Appl. Mater. Interfaces 2016, 8, 4456–4466. [PubMed: 26824739]
171. Xu ZC; Chen LT; Lu LL; Du RC; Ma WC; Cai YF; An XM; Wu HM; Luo Q; Xu Q; Zhang QH; Jia XD A Highly-Adhesive and Self-Healing Elastomer for Bio-Interfacial Electrode. Adv. Funct. Mater 2021, 31, 2006432.
172. Ghosh S; Cabral JD; Hanton LR; Moratti SC Strong Poly(ethylene oxide) Based Gel Adhesives *via* Oxime Cross-Linking. Acta Biomater. 2016, 29, 206–214. [PubMed: 26476342]
173. Chen K; Feng Y; Zhang Y; Yu L; Hao X; Shao F; Dou Z; An C; Zhuang Z; Luo Y.Entanglement-Driven Adhesion, Self-Healing, and High Stretchability of Double-Network PEG-Based Hydrogels. ACS Appl. Mater. Interfaces 2019, 11, 36458–36468. [PubMed: 31509371]
174. Bu Y; Zhang L; Sun G; Sun F; Liu J; Yang F; Tang P; Wu D.Tetra-PEG Based Hydrogel Sealants for *in Vivo* Visceral Hemostasis. Adv. Mater 2019, 31, 1901580.
175. Cui CY; Fan CC; Wu YH; Xiao M; Wu TL; Zhang DF; Chen XY; Liu B; Xu ZY; Qu B; Liu WG Water-Triggered Hyperbranched Polymer Universal Adhesives: From Strong Underwater Adhesion to Rapid Sealing Hemostasis. Adv. Mater 2019, 31, 1905761.
176. Daristotle JL; Zaki ST; Lau LW; Torres L Jr; Zografos A; Srinivasan P; Ayyub OB; Sandler AD; Kofinas P.Improving the Adhesion, Flexibility, and Hemostatic Efficacy of a Sprayable Polymer Blend Surgical Sealant by Incorporating Silica Particles. Acta Biomater. 2019, 90, 205–216. [PubMed: 30954624]
177. Tchobanian A; Van Oosterwyck H; Fardim P.Polysaccharides for Tissue Engineering: Current Landscape and Future Prospects. Carbohydr. Polym 2019, 205, 601–625. [PubMed: 30446147]
178. Sun C; Zeng X; Zheng S; Wang Y; Li Z; Zhang H; Nie L; Zhang Y; Zhao Y; Yang X.Bio-Adhesive Catechol-Modified Chitosan Wound Healing Hydrogel Dressings through Glow Discharge Plasma Technique. Chem. Eng. J 2022, 427, 130843.
179. Hong SH; Shin M; Park E; Ryu JH; Burdick JA; Lee H.Alginate-Boronic Acid: pH-Triggered Bioinspired Glue for Hydrogel Assembly. Adv. Funct. Mater 2020, 30, 1908497.
180. Yang Y; Xu T; Zhang Q; Piao Y; Bei HP; Zhao X.Biomimetic, Stiff, and Adhesive Periosteum with Osteogenic-Angiogenic Coupling Effect for Bone Regeneration. Small 2021, 17, 2006598.

Author Manuscript Author Manuscript Author Manuscript Author Manuscript

181. Suneetha M; Moo OS; Choi SM; Zo S; Rao KM; Han SS Tissue-Adhesive, Stretchable, and Self-Healable Hydrogels Based on Carboxymethyl Cellulose-Dopamine/PEDOT:PSS *via* Mussel-Inspired Chemistry for Bioelectronic Applications. Chem. Eng. J 2021, 426, 130847.

182. Burdick JA; Prestwich GD Hyaluronic Acid Hydrogels for Biomedical Applications. Adv. Mater 2011, 23, H41–H56. [PubMed: 21394792]

183. Kim SH; Kim K; Kim BS; An YH; Lee UJ; Lee SH; Kim SL; Kim BG; Hwang NS Fabrication of Polyphenol-Incorporated Anti-Inflammatory Hydrogel *via* High-Affinity Enzymatic Crosslinking for Wet Tissue Adhesion. Biomaterials 2020, 242, 119905.

184. An S; Jeon EJ; Jeon J; Cho S-W A Serotonin-Modified Hyaluronic Acid Hydrogel for Multifunctional Hemostatic Adhesives Inspired by a Platelet Coagulation Mediator. Mater. Horiz 2019, 6, 1169–1178.

185. Xu XY; Xia XF; Zhang KY; Rai A; Li Z; Zhao PC; Wei KC; Zou L; Yang BG; Wong WK; Chiu PWY; Bian LM Bioadhesive Hydrogels Demonstrating pH-Independent and Ultrafast Gelation Promote Gastric Ulcer Healing in Pigs. Sci. Transl. Med 2020, 12, eaba8014.

186. Hua Y; Xia H; Jia L; Zhao J; Zhao D; Yan X; Zhang Y; Tang S; Zhou G; Zhu L.Ultrafast, Tough, and Adhesive Hydrogel Based on Hybrid Photocrosslinking for Articular Cartilage Repair in Water-Filled Arthroscopy. Sci. Adv 2021, 7, eabg0628.

187. Bai L; Liu L; Esquivel M; Tardy BL; Huan S; Niu X; Liu S; Yang G; Fan Y; Rojas OJ Nanochitin: Chemistry, Structure, Assembly, and Applications. Chem. Rev 2022, 122, 11604–11674. [PubMed: 35653785]

188. Bakshi PS; Selvakumar D; Kadirvelu K; Kumar NS Chitosan as an Environment Friendly Biomaterial – A Review on Recent Modifications and Applications. Int. J. Biol. Macromol 2020, 150, 1072–1083. [PubMed: 31739057]

189. Sahariah P; Másson M.Antimicrobial Chitosan and Chitosan Derivatives: A Review of the Structure–Activity Relationship. Biomacromolecules 2017, 18, 3846–3868. [PubMed: 28933147]

190. Khan MA; Mujahid M.A Review on Recent Advances in Chitosan Based Composite for Hemostatic Dressings. Int. J. Biol. Macromol 2019, 124, 138–147. [PubMed: 30447365]

191. Yu R; Li M; Li Z; Pan G; Liang Y; Guo B.Supramolecular Thermo-Contracting Adhesive Hydrogel with Self-Removability Simultaneously Enhancing Noninvasive Wound Closure and MRSA-Infected Wound Healing. Adv. Healthcare Mater 2022, 11, 2102749.

192. Liang Y; Li Z; Huang Y; Yu R; Guo B.Dual-Dynamic-Bond Cross-Linked Antibacterial Adhesive Hydrogel Sealants with on-Demand Removability for Post-Wound-Closure and Infected Wound Healing. ACS Nano 2021, 15, 7078–7093. [PubMed: 33764740]

193. Zaharoff DA; Rogers CJ; Hance KW; Schlom J; Greiner JW Chitosan Solution Enhances Both Humoral and Cell-Mediated Immune Responses to Subcutaneous Vaccination. Vaccine 2007, 25, 2085–2094. [PubMed: 17258843]

194. Liang Y; Li M; Yang Y; Qiao L; Xu H; Guo B.pH/Glucose Dual Responsive Metformin Release Hydrogel Dressings with Adhesion and Self-Healing via Dual-Dynamic Bonding for Athletic Diabetic Foot Wound Healing. ACS Nano 2022, 16, 3194–3207. [PubMed: 35099927]

195. Chen J; He J; Yang Y; Qiao L; Hu J; Zhang J; Guo B.Antibacterial Adhesive Self-Healing Hydrogels to Promote Diabetic Wound Healing. Acta Biomater. 2022, 146, 119–130. [PubMed: 35483628]

196. Huang WJ; Cheng S; Wang XL; Zhang Y; Chen LY; Zhang LN Noncompressible Hemostasis and Bone Regeneration Induced by an Absorbable Bioadhesive Self-Healing Hydrogel. Adv. Funct. Mater 2021, 31, 2009189.

197. Wang L; Zhang XH; Yang K; Fu YV; Xu TS; Li SL; Zhang DW; Wang LN; Lee CS A Novel Double-Crosslinking-Double-Network Design for Injectable Hydrogels with Enhanced Tissue Adhesion and Antibacterial Capability for Wound Treatment. Adv. Funct. Mater 2020, 30, 1904156.

198. Han W; Zhou B; Yang K; Xiong X; Luan SF; Wang Y; Xu Z; Lei P; Luo ZS; Gao J; Zhan YJ; Chen GP; Liang L; Wang R; Li S; Xu H.Biofilm-Inspired Adhesive and Antibacterial Hydrogel with Tough Tissue Integration Performance for Sealing Hemostasis and Wound Healing. Bioact. Mater 2020, 5, 768–778. [PubMed: 32637741]

Author Manuscript Author Manuscript Author Manuscript Author Manuscript

199. Ma YF; Yao JX; Liu Q; Han T; Zhao JP; Ma XH; Tong YM; Jin GR; Qu K; Li BQ; Xu F.Liquid Bandage Harvests Robust Adhesive, Hemostatic, and Antibacterial Performances as a First-Aid Tissue Adhesive. Adv. Funct. Mater 2020, 30, 2001820.

200. Sanandiya ND; Lee S; Rho S; Lee H; Kim IS; Hwang DS Tunichrome-Inspired Pyrogallol Functionalized Chitosan for Tissue Adhesion and Hemostasis. Carbohydr. Polym 2019, 208, 77–85. [PubMed: 30658834]

201. Oh DX; Kim S; Lee D; Hwang DS Tunicate-Mimetic Nanofibrous Hydrogel Adhesive with Improved Wet Adhesion. Acta Biomater. 2015, 20, 104–112. [PubMed: 25841348]

202. Azuma K; Nishihara M; Shimizu H; Itoh Y; Takashima O; Osaki T; Itoh N; Imagawa T; Murahata Y; Tsuka T.Biological Adhesive Based on Carboxymethyl Chitin Derivatives and Chitin Nanofibers. Biomaterials 2015, 42, 20–29. [PubMed: 25542790]

203. Kim M; Ahn Y; Lee K; Jung W; Cha C.*In Situ* Facile-Forming Chitosan Hydrogels with Tunable Physicomechanical and Tissue Adhesive Properties by Polymer Graft Architecture. Carbohydr. Polym 2019, 229, 115538.

204. Pawar SN; Edgar KJ Alginate Derivatization: A Review of Chemistry, Properties and Applications. Biomaterials 2012, 33, 3279–3305. [PubMed: 22281421]

205. Charron PN; Fenn SL; Poniz A; Oldinski RA Mechanical Properties and Failure Analysis of Visible Light Crosslinked Alginate-Based Tissue Sealants. J. Mech. Behav. Biomed. Mater 2016, 59, 314–321. [PubMed: 26897093]

206. Shao C; Wang M; Meng L; Chang H; Wang B; Xu F; Yang J; Wan P.Mussel-Inspired Cellulose Nanocomposite Tough Hydrogels with Synergistic Self-Healing, Adhesive, and Strain-Sensitive Properties. Chem. Mater 2018, 30, 3110–3121.

207. Urie R; Guo CC; Ghosh D; Thelakkaden M; Wong V; Lee JK; Kilbourne J; Yarger J; Rege K.Rapid Soft Tissue Approximation and Repair Using Laser-Activated Silk Nanosealants. Adv. Funct. Mater 2018, 28, 1802874.

208. Zhu WZ; Peck Y; Iqbal J; Wang DA A Novel DOPA-Albumin Based Tissue Adhesive for Internal Medical Applications. Biomaterials 2017, 147, 99–115. [PubMed: 28938165]

209. Lee JS; Choi YS; Lee JS; Jeon EJ; An S; Lee MS; Yang HS; Cho S-W Mechanically-Reinforced and Highly Adhesive Decellularized Tissue-Derived Hydrogel for Efficient Tissue Repair. Chem. Eng. J 2022, 427, 130926.

210. Deng J; Tang YY; Zhang Q; Wang C; Liao M; Ji P; Song JL; Luo GX; Chen L; Ran XH; Wei ZM; Zheng LW; Dang RY; Liu X; Zhang HM; Zhang YS; Zhang XM; Tan H.A Bioinspired Medical Adhesive Derived from Skin Secretion of Andrias Davidianus for Wound Healing. Adv. Funct. Mater 2019, 29, 1809110.

211. Sun J; Su JJ; Ma C; Gostl R; Herrmann A; Liu K; Zhang HJ Fabrication and Mechanical Properties of Engineered Protein-Based Adhesives and Fibers. Adv. Mater 2020, 32, 1906360.

212. Brennan MJ; Kilbride BF; Wilker JJ; Liu JC A Bioinspired Elastin-Based Protein for a Cytocompatible Underwater Adhesive. Biomaterials 2017, 124, 116–125. [PubMed: 28192773]

213. Annabi N; Zhang Y-N; Assmann A; Sani ES; Cheng G; Lassaletta AD; Vegh A; Dehghani B; Ruiz-Esparza GU; Wang X.Engineering a Highly Elastic Human Protein–Based Sealant for Surgical Applications. Sci. Transl. Med 2017, 9, eaai7466.

214. Li SD; Chen N; Li XP; Li Y; Xie ZP; Ma ZY; Zhao J; Hou X; Yuan XB Bioinspired Double-Dynamic-Bond Crosslinked Bioadhesive Enables Post-Wound Closure Care. Adv. Funct. Mater 2020, 30, 2000130.

215. Teng L; Shao Z; Bai Q; Zhang X; He YS; Lu J; Zou D; Feng C; Dong CM Biomimetic Glycopolypeptide Hydrogels with Tunable Adhesion and Microporous Structure for Fast Hemostasis and Highly Efficient Wound Healing. Adv. Funct. Mater 2021, 31, 2105628.

216. Lei K; Wang KQ; Sun YL; Zheng Z; Wang XL Rapid-Fabricated and Recoverable Dual-Network Hydrogel with Inherently Anti-Bacterial Abilities for Potential Adhesive Dressings. Adv. Funct. Mater 2021, 31, 2008010.

217. Tan HQ; Jin DW; Sun JJ; Song JL; Lu Y; Yin M; Chen X; Qu X; Liu CS Enlisting a Traditional Chinese Medicine to Tune the Gelation Kinetics of a Bioactive Tissue Adhesive for Fast Hemostasis or Minimally Invasive Therapy. Bioact. Mater 2021, 6, 905–917.

Author Manuscript Author Manuscript Author Manuscript Author Manuscript

218. Zhang C; Huang JF; Zhang JC; Liu SY; Cui MK; An BL; Wang XY; Pu JH; Zhao TX; Fan CH; Lu TK; Zhong C.Engineered Bacillus Subtilis Biofilms as Living Glues. Mater. Today 2019, 28, 40–48.
219. Fan C; Fu J; Zhu W; Wang D-A A Mussel-Inspired Double-Crosslinked Tissue Adhesive Intended for Internal Medical Use. Acta Biomater. 2016, 33, 51–63. [PubMed: 26850148]
220. Zhou L; Dai C; Fan L; Jiang Y; Liu C; Zhou Z; Guan P; Tian Y; Xing J; Li X; Luo Y; Yu P; Ning C; Tan G.Injectable Self-Healing Natural Biopolymer-Based Hydrogel Adhesive with Thermoresponsive Reversible Adhesion for Minimally Invasive Surgery. Adv. Funct. Mater 2021, 31, 2007457.
221. Hong S; Pirovich D; Kilcoyne A; Huang CH; Lee H; Weissleder R.Supramolecular Metallo-Bioadhesive for Minimally Invasive Use. Adv. Mater 2016, 28, 8675–8680. [PubMed: 27515068]
222. Raja STK; Thiruselvi T; Sailakshmi G; Ganesh S; Gnanamani A.Rejoining of Cut Wounds by Engineered Gelatin–Keratin Glue. Biochim. Biophys. Acta 2013, 1830, 4030–4039. [PubMed: 23583368]
223. Al-Abboodi A; Zhang S; Al-Saady M; Ong JW; Chan PP; Fu J.Printing *in Situ* Tissue Sealant with Visible-Light-Crosslinked Porous Hydrogel. Biomed. Mater 2019, 14, 045010.
224. Zhao X; Li S; Du X; Li W; Wang Q; He D; Yuan J.Natural Polymer-Derived Photocurable Bioadhesive Hydrogels for Sutureless Keratoplasty. Bioact. Mater 2021, 8, 196–209. [PubMed: 34541396]
225. Sharifi S; Islam MM; Sharifi H; Islam R; Koza D; Reyes-Ortega F; Alba-Molina D; Nilsson PH; Dohlman CH; Mollnes TE Tuning Gelatin-Based Hydrogel Towards Bioadhesive Ocular Tissue Engineering Applications. Bioact. Mater 2021, 6, 3947–3961. [PubMed: 33937594]
226. Xuan CK; Hao LJ; Liu XM; Zhu Y; Yang HS; Ren YP; Wang L; Fujie T; Wu HK; Chen YH; Shi XT; Mao CB Wet-Adhesive, Haemostatic and Antimicrobial Bilayered Composite Nanosheets for Sealing and Healing Soft-Tissue Bleeding Wounds. Biomaterials 2020, 252, 120018.
227. Liu BC; Wang Y; Miao Y; Zhang XY; Fan ZX; Singh G; Zhang XY; Xu KG; Li BY; Hu ZQ; Xing M.Hydrogen Bonds Autonomously Powered Gelatin Methacrylate Hydrogels with Super-Elasticity, Self-Heal and Underwater Self-Adhesion for Sutureless Skin and Stomach Surgery and E-Skin. Biomaterials 2018, 171, 83–96. [PubMed: 29684678]
228. Sani ES; Kheirkhah A; Rana D; Sun Z; Foulsham W; Sheikhi A; Khademhosseini A; Dana R; Annabi N.Sutureless Repair of Corneal Injuries Using Naturally Derived Bioadhesive Hydrogels. Sci. Adv 2019, 5, eaav1281.
229. Gu Y; Zhou S; Yang J.Aza-Michael Addition Chemistry for Tuning the Phase Separation of PDMS/PEG Blend Coatings and Their Anti-Fouling Potentials. Macromol. Chem. Phys 2020, 221, 1900477.
230. Annabi N; Rana D; Sani ES; Portillo-Lara R; Gifford JL; Fares MM; Mithieux SM; Weiss AS Engineering a Sprayable and Elastic Hydrogel Adhesive with Antimicrobial Properties for Wound Healing. Biomaterials 2017, 139, 229–243. [PubMed: 28579065]
231. Kim JY; Ryu SB; Park KD Preparation and Characterization of Dual-Crosslinked Gelatin Hydrogel via DOPA-Fe^{3+} Complexation and Fenton Reaction. J. Ind. Eng. Chem 2018, 58, 105–112.
232. Jiang Y; Zhang X; Zhang W; Wang M; Yan L; Wang K; Han L; Lu X.Infant Skin Friendly Adhesive Hydrogel Patch Activated at Body Temperature for Bioelectronics Securing and Diabetic Wound Healing. ACS Nano 2022, 16, 8662–8676. [PubMed: 35549213]
233. Oelker AM; Grinstaff MW Ophthalmic Adhesives: A Materials Chemistry Perspective. J. Mater. Chem 2008, 18, 2521–2536.
234. Joseph CA; Mccarthy CW; Tyo AG; Hubbard KR; Fisher HC; Altscheffel JA; He W; Pinnaratip R; Liu Y; Lee BP Development of an Injectable Nitric Oxide Releasing Poly(ethylene)glycol-Fibrin Adhesive Hydrogel. ACS Biomater. Sci. Eng 2018, 5, 959–969. [PubMed: 31650030]
235. Yang Y; Liang Y; Chen J; Duan X; Guo B.Mussel-Inspired Adhesive Antioxidant Antibacterial Hemostatic Composite Hydrogel Wound Dressing *via* Photo-Polymerization for Infected Skin Wound Healing. Bioact. Mater 2021, 8, 341–354. [PubMed: 34541405]
236. Lee C; Choi SE; Kim JW; Lee SY Boston Ivy Disk-Inspired Pressure-Mediated Adhesive Film Patches. Small 2020, 16, 1904282.

Author Manuscript Author Manuscript Author Manuscript Author Manuscript

237. Rapp MV; Maier GP; Dobbs HA; Higdon NJ; Waite JH; Butler A; Israelachvili JN Defining the Catechol-Cation Synergy for Enhanced Wet Adhesion to Mineral Surfaces. J. Am. Chem. Soc 2016, 138, 9013–9016. [PubMed: 27415839]

238. Degen GD; Stow PR; Lewis RB; Eguiluz RCA; Valois E; Kristiansen K; Butler A; Israelachvili JN Impact of Molecular Architecture and Adsorption Density on Adhesion of Mussel-Inspired Surface Primers with Catechol-Cation Synergy. J. Am. Chem. Soc 2019, 141, 18673–18681. [PubMed: 31771333]

239. Ryu JH; Hong S; Lee H.Bio-Inspired Adhesive Catechol-Conjugated Chitosan for Biomedical Applications: A Mini Review. Acta Biomater. 2015, 27, 101–115. [PubMed: 26318801]

240. Waite JH; Tanzer ML Polyphenolic Substance of Mytilus Edulis: Novel Adhesive Containing L-DOPA and Hydroxyproline. Science 1981, 212, 1038–1040. [PubMed: 17779975]

241. Choi YS; Kang DG; Lim S; Yang YJ; Kim CS; Cha HJ Recombinant Mussel Adhesive Protein Fp-5 (MAP Fp-5) as a Bulk Bioadhesive and Surface Coating Material. Biofouling 2011, 27, 729–737. [PubMed: 21770718]

242. Li YR; Cheng J; Delparastan P; Wang HQ; Sigg SJ; Defrates KG; Cao Y; Messersmith PB Molecular Design Principles of Lysine-DOPA Wet Adhesion. Nat. Commun 2020, 11, 3895. [PubMed: 32753588]

243. Yang J; Stuart MAC; Kamperman M.Jack of All Trades: Versatile Catechol Crosslinking Mechanisms. Chem. Soc. Rev 2014, 43, 8271–8298. [PubMed: 25231624]

244. Saiz-Poseu J; Mancebo-Aracil J; Nador F; Busque F; Ruiz-Molina D.The Chemistry Behind Catechol-Based Adhesion. Angew. Chem. Int. Ed 2019, 58, 696–714.

245. Wang Z; Zhang SF; Zhao SJ; Kang HJ; Wang ZK; Xia CL; Yu YL; Li JZ Facile Biomimetic Self-Coacervation of Tannic Acid and Polycation: Tough and Wide pH Range of Underwater Adhesives. Chem. Eng. J 2021, 404, 127069.

246. Wang QH; Pan XF; Guo JJ; Huang LL; Chen LH; Ma XJ; Cao SL; Ni YH Lignin and Cellulose Derivatives-Induced Hydrogel with Asymmetrical Adhesion, Strength, and Electriferous Properties for Wearable Bioelectrodes and Self-Powered Sensors. Chem. Eng. J 2021, 414, 128903.

247. Cao J; Zhao Y; Jin S; Li J; Wu P; Luo Z.Flexible Lignin-Based Hydrogels with Self-Healing and Adhesive Ability Driven by Noncovalent Interactions. Chem. Eng. J 2021, 429, 132252.

248. Zou T; Sipponen MH; Henn A; ÖSterberg M. Solvent-Resistant Lignin-Epoxy Hybrid Nanoparticles for Covalent Surface Modification and High-Strength Particulate Adhesives. ACS Nano 2021, 15, 4811–4823. [PubMed: 33593063]

249. Qian Y; Zhou Y; Lu M; Guo X; Yang D; Lou H; Qiu X; Guo CF Direct Construction of Catechol Lignin for Engineering Long-Acting Conductive, Adhesive, and UV-Blocking Hydrogel Bioelectronics. Small Methods 2021, 5, 2001311.

250. Ahn BK Perspectives on Mussel-Inspired Wet Adhesion. J. Am. Chem. Soc 2017, 139, 10166–10171. [PubMed: 28657746]

251. Tiu BDB; Delparastan P; Ney MR; Gerst M; Messersmith PB Cooperativity of Catechols and Amines in High-Performance Dry/Wet Adhesives. Angew. Chem. Int. Ed 2020, 59, 16616–16624.

252. Shao H; Stewart RJ Biomimetic Underwater Adhesives with Environmentally Triggered Setting Mechanisms. Adv. Mater 2010, 22, 729–733. [PubMed: 20217779]

253. Maier GP; Rapp MV; Waite JH; Israelachvili JN; Butler A.Adaptive Synergy between Catechol and Lysine Promotes Wet Adhesion by Surface Salt Displacement. Science 2015, 349, 628–632. [PubMed: 26250681]

254. Martinez Rodriguez NR; Das S; Kaufman Y; Israelachvili JN; Waite JH Interfacial pH During Mussel Adhesive Plaque Formation. Biofouling 2015, 31, 221–227. [PubMed: 25875963]

255. Deepankumar K; Guo Q; Mohanram H; Lim J; Mu Y; Pervushin K; Yu J; Miserez A.Liquid–Liquid Phase Separation of the Green Mussel Adhesive Protein Pvfp-5 is Regulated by the Post-Translated Dopa Amino Acid. Adv. Mater 2022, 34, 2103828.

256. Barros NR; Chen Y; Hosseini V; Wang W; Nasiri R; Mahmoodi M; Yalcintas EP; Haghniaz R; Mecwan MM; Karamikamkar S; Dai W; Sarabi SA; Falcone N; Young P; Zhu Y; Sun W; Zhang S; Lee J; Lee K; Ahadian S; Dokmeci MR; Khademhosseini A; Kim H-J Recent Developments

Author Manuscript Author Manuscript Author Manuscript Author Manuscript

in Mussel-Inspired Materials for Biomedical Applications. Biomater. Sci 2021, 9, 6653–6672. [PubMed: 34550125]

257. Zhang W; Wang RX; Sun ZM; Zhu XW; Zhao Q; Zhang TF; Cholewinski A; Yang F; Zhao BX; Pinnaratip R; Forooshani PK; Lee BP Catechol-Functionalized Hydrogels: Biomimetic Design, Adhesion Mechanism, and Biomedical Applications. Chem. Soc. Rev 2020, 49, 433–464. [PubMed: 31939475]
258. Nakatsuka N; Hasani-Sadrabadi MM; Cheung KM; Young TD; Bahlakeh G; Moshaverinia A; Weiss PS; Andrews AM Polyserotonin Nanoparticles as Multifunctional Materials for Biomedical Applications. ACS Nano 2018, 12, 4761–4774. [PubMed: 29664607]
259. Ryu JH; Lee Y; Kong WH; Kim TG; Park TG; Lee H.Catechol-Functionalized Chitosan/Pluronic Hydrogels for Tissue Adhesives and Hemostatic Materials. Biomacromolecules 2011, 12, 2653–2659. [PubMed: 21599012]
260. Lee Y; Chung HJ; Yeo S; Ahn C-H; Lee H; Messersmith PB; Park TG Thermo-Sensitive, Injectable, and Tissue Adhesive Sol–Gel Transition Hyaluronic Acid/Pluronic Composite Hydrogels Prepared from Bio-Inspired Catechol-Thiol Reaction. Soft Matter 2010, 6, 977–983.
261. Lo Presti M; Rizzo G; Farinola GM; Omenetto FG Bioinspired Biomaterial Composite for All-Water-Based High-Performance Adhesives. Adv. Sci 2021, 8, 2004786.
262. Krogsgaard M; Hansen MR; Birkedal H.Metals & Polymers in the Mix: Fine-Tuning the Mechanical Properties & Color of Self-Healing Mussel-Inspired Hydrogels. J. Mater. Chem. B 2014, 2, 8292–8297. [PubMed: 32261997]
263. García-Fernández L; Cui J; Serrano C; Shafiq Z; Gropeanu RA; Miguel VS; Ramos JI; Wang M; Auernhammer GK; Ritz S.Antibacterial Strategies from the Sea: Polymer-Bound Cl-Catechols for Prevention of Biofilm Formation. Adv. Mater 2013, 25, 529–533. [PubMed: 23139083]
264. Menyo MS; Hawker CJ; Waite JH Versatile Tuning of Supramolecular Hydrogels through Metal Complexation of Oxidation-Resistant Catechol-Inspired Ligands. Soft Matter 2013, 9, 10314–10323.
265. Park JP; Song IT; Lee J; Ryu JH; Lee Y; Lee H.Vanadyl–Catecholamine Hydrogels Inspired by Ascidians and Mussels. Chem. Mater 2014, 27, 105–111.
266. Zhang C; Ma M-Q; Chen T-T; Zhang H; Hu D-F; Wu B-H; Ji J; Xu Z-K Dopamine-Triggered One-Step Polymerization and Codeposition of Acrylate Monomers for Functional Coatings. ACS Appl. Mater. Interfaces 2017, 9, 34356–34366. [PubMed: 28893062]
267. Du X; Li L; Li J; Yang C; Frenkel N; Welle A; Heissler S; Nefedov A; Grunze M; Levkin PA UV-Triggered Dopamine Polymerization: Control of Polymerization, Surface Coating, and Photopatterning. Adv. Mater 2014, 26, 8029–8033. [PubMed: 25381870]
268. Bai S; Zhang X; Cai P; Huang X; Huang Y; Liu R; Zhang M; Song J; Chen X; Yang H.A Silk-Based Sealant with Tough Adhesion for Instant Hemostasis of Bleeding Tissues. Nanoscale Horiz. 2019, 4, 1333–1341.
269. Bai SM; Zhang XL; Lv XL; Zhang MY; Huang XW; Shi Y; Lu CH; Song JB; Yang HH Bioinspired Mineral-Organic Bone Adhesives for Stable Fracture Fixation and Accelerated Bone Regeneration. Adv. Funct. Mater 2020, 30, 1908381.
270. Mian SA; Yang L-M; Saha LC; Ahmed E; Ajmal M; Ganz E.A Fundamental Understanding of Catechol and Water Adsorption on a Hydrophilic Silica Surface: Exploring the Underwater Adhesion Mechanism of Mussels on an Atomic Scale. Langmuir 2014, 30, 6906–6914. [PubMed: 24835420]
271. Li A; Mu Y; Jiang W; Wan X.A Mussel-Inspired Adhesive with Stronger Bonding Strength under Underwater Conditions Than under Dry Conditions. Chem. Commun 2015, 51, 9117–9120.
272. Jia M; Li A; Mu Y; Jiang W; Wan X.Synthesis and Adhesive Property Study of Polyoxetanes Grafted with Catechols *via* Cu(I)-Catalyzed Click Chemistry. Polymer 2014, 55, 1160–1166.
273. Pei XJ; Zhang H; Zhou Y; Zhou LJ; Fu J.Stretchable, Self-Healing and Tissue-Adhesive Zwitterionic Hydrogels as Strain Sensors for Wireless Monitoring of Organ Motions. Mater. Horiz 2020, 7, 1872–1882.
274. Ahn BK; Das S; Linstadt R; Kaufman Y; Martinez-Rodriguez NR; Mirshafian R; Kesselman E; Talmon Y; Lipshutz BH; Israelachvili JN High-Performance Mussel-Inspired Adhesives of Reduced Complexity. Nat. Commun 2015, 6, 8663. [PubMed: 26478273]

Author Manuscript Author Manuscript Author Manuscript Author Manuscript

275. Meredith HJ; Jenkins CL; Wilker JJ Enhancing the Adhesion of a Biomimetic Polymer Yields Performance Rivaling Commercial Glues. Adv. Funct. Mater 2014, 24, 3259–3267.

276. White JD; Wilker JJ Underwater Bonding with Charged Polymer Mimics of Marine Mussel Adhesive Proteins. Macromolecules 2011, 44, 5085–5088.

277. Lv C; Li L; Jiao Z; Yan H; Wang Z; Wu Z; Guo M; Wang Y; Zhang P.Improved Hemostatic Effects by Fe^{3+} Modified Biomimetic PLLA Cotton-Like Mat *via* Sodium Alginate Grafted with Dopamine. Bioact. Mater 2021, 6, 2346–2359. [PubMed: 33553820]

278. Roisman S; Dotan AL; Lewitus DY Polycaprolactone-Based Hotmelt Adhesive for Hernia-Mesh Fixation. Polym. Adv. Technol 2020, 31, 3194–3201.

279. Wang LF; Xu JW; Xue PP; Liu JY; Luo LZ; Zhuge DL; Yao Q; Li XK; Zhao YZ; Xu HL Thermo-Sensitive Hydrogel with Mussel-Inspired Adhesion Enhanced the Non-Fibrotic Repair Effect of EGF on Colonic Mucosa Barrier of TNBS-Induced Ulcerative Colitis Rats through Macrophage Polarizing. Chem. Eng. J 2021, 416, 129221.

280. Tan X; Gao P; Li Y; Qi P; Liu J; Shen R; Wang L; Huang N; Xiong K; Tian W; Tu Q.Poly-Dopamine, Poly-Levodopa, and Poly-Norepinephrine Coatings: Comparison of Physico-Chemical and Biological Properties with Focus on the Application for Blood-Contacting Devices. Bioact. Mater 2021, 6, 285–296. [PubMed: 32913935]

281. Mu Y; Wan X.Simple but Strong: A Mussel-Inspired Hot Curing Adhesive Based on Polyvinyl Alcohol Backbone. Macromol. Rapid Commun 2016, 37, 545–550. [PubMed: 26797924]

282. Du X; Wu L; Yan H; Qu L; Wang L; Wang X; Ren S; Kong D; Wang L.Multifunctional Hydrogel Patch with Toughness, Tissue Adhesiveness, and Antibacterial Activity for Sutureless Wound Closure. ACS Biomater. Sci. Eng 2019, 5, 2610–2620. [PubMed: 33405766]

283. Fan XM; Fang Y; Zhou WK; Yan LY; Xu YH; Zhu H; Liu HQ Mussel Foot Protein Inspired Tough Tissue-Selective Underwater Adhesive Hydrogel. Mater. Horiz 2021, 8, 997–1007. [PubMed: 34821330]

284. Gan D; Xu T; Xing W; Wang M; Fang J; Wang K; Ge X; Chan CW; Ren F; Tan H.Mussel-Inspired Dopamine Oligomer Intercalated Tough and Resilient Gelatin Methacryloyl (GelMA) Hydrogels for Cartilage Regeneration. J. Mater. Chem. B 2019, 7, 1716–1725. [PubMed: 32254913]

285. Zhao Y; Wu Y; Wang L; Zhang M; Chen X; Liu M; Fan J; Liu J; Zhou F; Wang Z.Bio-Inspired Reversible Underwater Adhesive. Nat. Commun 2017, 8, 2218. [PubMed: 29263405]

286. Narayanan A; Kaur S; Peng C; Debnath D; Mishra K; Liu Q; Dhinojwala A; Joy A.Viscosity Attunes the Adhesion of Bioinspired Low Modulus Polyester Adhesive Sealants to Wet Tissues. Biomacromolecules 2019, 20, 2577–2586. [PubMed: 31244021]

287. Zhang H; Zhao T; Newland B; Duffy P; Annaidh AN; O'Cearbhaill ED; Wang W.On-Demand and Negative-Thermo-Swelling Tissue Adhesive Based on Highly Branched Ambivalent PEG–Catechol Copolymers. J. Mater. Chem. B 2015, 3, 6420–6428. [PubMed: 32262550]

288. Ghosh K; Shu XZ; Mou R; Lombardi J; Prestwich GD; Rafailovich MH; Clark RA Rheological Characterization of in Situ Cross-Linkable Hyaluronan Hydrogels. Biomacromolecules 2005, 6, 2857–2865. [PubMed: 16153128]

289. Raja STK; Thiruselvi T; Aravindhan R; Mandal AB; Gnanamani A.*In Vitro* and *in Vivo* Assessments of a 3-(3,4-Dihydroxyphenyl)-2-propenoic Acid Bioconjugated Gelatin-Based Injectable Hydrogel for Biomedical Applications. J. Mater. Chem. B 2015, 3, 1230–1244. [PubMed: 32264474]

290. Yan YH; Rong LH; Ge J; Tiu BDB; Cao PF; Advincula RC Mussel-Inspired Hydrogel Composite with Multi-Stimuli Responsive Behavior. Macromol. Mater. Eng 2019, 304, 1800720.

291. Artzi N; Shazly T; Crespo C; Ramos AB; Chenault HK; Edelman ER Characterization of Star Adhesive Sealants Based on PEG/Dextran Hydrogels. Macromol. Biosci 2009, 9, 754–765. [PubMed: 19384975]

292. Shazly TM; Baker AB; Naber JR; Bon A; Van Vliet KJ; Edelman ER Augmentation of Postswelling Surgical Sealant Potential of Adhesive Hydrogels. J. Biomed. Mater. Res Part A 2010, 95, 1159–1169.

Author Manuscript Author Manuscript Author Manuscript Author Manuscript

293. Wei W; Petrone L; Tan Y; Cai H; Israelachvili JN; Miserez A; Waite JH An Underwater Surface-Drying Peptide Inspired by a Mussel Adhesive Protein. Adv. Funct. Mater 2016, 26, 3496–3507. [PubMed: 27840600]

294. Choi YC; Choi JS; Jung YJ; Cho YW Human Gelatin Tissue-Adhesive Hydrogels Prepared by Enzyme-Mediated Biosynthesis of DOPA and Fe^{3+} Ion Crosslinking. J. Mater. Chem. B 2014, 2, 201–209. [PubMed: 32261607]

295. Zhou H; Mayorga-Martinez CC; Pumera M.Microplastic Removal and Degradation by Mussel-Inspired Adhesive Magnetic/Enzymatic Microrobots. Small Methods 2021, 5, 2100230.

296. Yang Z; Huang R; Zheng B; Guo W; Li C; He W; Wei Y; Du Y; Wang H; Wu D.Highly Stretchable, Adhesive, Biocompatible, and Antibacterial Hydrogel Dressings for Wound Healing. Adv. Sci 2021, 8, 2003627.

297. Jung H; Kim MK; Lee JY; Choi SW; Kim J.Adhesive Hydrogel Patch with Enhanced Strength and Adhesiveness to Skin for Transdermal Drug Delivery. Adv. Funct. Mater 2020, 30, 2004407.

298. Jin ZK; Yang L; Shi S; Wang TY; Duan GG; Liu XH; Li YW Flexible Polydopamine Bioelectronics. Adv. Funct. Mater 2021, 31, 2103391.

299. Han L; Lu X; Liu K; Wang K; Fang L; Weng L-T; Zhang H; Tang Y; Ren F; Zhao C.Mussel-Inspired Adhesive and Tough Hydrogel Based on Nanoclay Confined Dopamine Polymerization. ACS Nano 2017, 11, 2561–2574. [PubMed: 28245107]

300. Liu Y; Meng H; Qian Z; Fan N; Choi W; Zhao F; Lee BP A Moldable Nanocomposite Hydrogel Composed of a Mussel-Inspired Polymer and a Nanosilicate as a Fit-to-Shape Tissue Sealant. Angew. Chem. Int. Ed 2017, 56, 4224–4228.

301. Han L; Lu X; Wang M; Gan D; Deng W; Wang K; Fang L; Liu K; Chan CW; Tang Y.A Mussel-Inspired Conductive, Self-Adhesive, and Self-Healable Tough Hydrogel as Cell Stimulators and Implantable Bioelectronics. Small 2017, 13, 1601916.

302. Liao M; Wan P; Wen J; Gong M; Wu X; Wang Y; Shi R; Zhang L.Wearable, Healable, and Adhesive Epidermal Sensors Assembled from Mussel-Inspired Conductive Hybrid Hydrogel Framework. Adv. Funct. Mater 2017, 27, 1703852.

303. Huang W; Qi C; Gao Y.Injectable Self-Healable Nanocomposite Hydrogels with Mussel-Inspired Adhesive Properties for 3D Printing Ink. ACS Appl. Nano Mater 2019, 2, 5000–5008.

304. Gan D; Xing W; Jiang L; Fang J; Zhao C; Ren F; Fang L; Wang K; Lu X.Plant-Inspired Adhesive and Tough Hydrogel Based on Ag-Lignin Nanoparticles-Triggered Dynamic Redox Catechol Chemistry. Nat. Commun 2019, 10, 1487. [PubMed: 30940814]

305. Rao P; Sun TL; Chen L; Takahashi R; Shinohara G; Guo H; King DR; Kurokawa T; Gong JP Tough Hydrogels with Fast, Strong, and Reversible Underwater Adhesion Based on a Multiscale Design. Adv. Mater 2018, 30, 1801884.

306. Baik S; Lee HJ; Kim DW; Kim JW; Lee Y; Pang C.Bioinspired Adhesive Architectures: From Skin Patch to Integrated Bioelectronics. Adv. Mater 2019, 31, 1803309.

307. Chen Y; Meng J; Gu Z; Wan X; Jiang L; Wang S.Bioinspired Multiscale Wet Adhesive Surfaces: Structures and Controlled Adhesion. Adv. Funct. Mater 2019, 30, 1905287.

308. Wang H; Su X; Chai Z; Tian Z; Xie W; Wang Y; Wan Z; Deng M; Yuan Z; Huang J.A Hydra Tentacle-Inspired Hydrogel with Underwater Ultra-Stretchability for Adhering Adipose Surfaces. Chem. Eng. J 2022, 428, 131049.

309. Lee HJ; Baik S; Hwang GW; Song JH; Kim DW; Park B-Y; Min H; Kim JK; Koh J-S; Yang T-H An Electronically Perceptive Bioinspired Soft Wet-Adhesion Actuator with Carbon Nanotube-Based Strain Sensors. ACS Nano 2021, 15, 14137–14148. [PubMed: 34425674]

310. Baik S; Park Y; Lee T-J; Bhang SH; Pang C.A Wet-Tolerant Adhesive Patch Inspired by Protuberances in Suction Cups of Octopi. Nature 2017, 546, 396. [PubMed: 28617467]

311. Baik S; Kim J; Lee HJ; Lee TH; Pang C.Highly Adaptable and Biocompatible Octopus-Like Adhesive Patches with Meniscus-Controlled Unfoldable 3D Microtips for Underwater Surface and Hairy Skin. Adv. Sci 2018, 5, 1800100.

312. Choi MK; Park OK; Choi C; Qiao S; Ghaffari R; Kim J; Lee DJ; Kim M; Hyun W; Kim SJ Cephalopod-Inspired Miniaturized Suction Cups for Smart Medical Skin. Adv. Healthcare Mater 2016, 5, 80–87.

Author Manuscript Author Manuscript Author Manuscript Author Manuscript

313. Baik S; Lee HJ; Kim DW; Min H; Pang C.Capillarity-Enhanced Organ-Attachable Adhesive with Highly Drainable Wrinkled Octopus-Inspired Architectures. ACS Appl. Mater. Interfaces 2019, 11, 25674–25681. [PubMed: 31251017]

314. Lee H; Um DS; Lee Y; Lim S; Kim HJ; Ko H.Octopus-Inspired Smart Adhesive Pads for Transfer Printing of Semiconducting Nanomembranes. Adv. Mater 2016, 28, 7457–7465. [PubMed: 27322886]

315. Chen Y-C; Yang H.Octopus-Inspired Assembly of Nanosucker Arrays for Dry/Wet Adhesion. ACS Nano 2017, 11, 5332–5338. [PubMed: 28448714]

316. Langowski JK; Dodou D; Kamperman M; Van Leeuwen JL Tree Frog Attachment: Mechanisms, Challenges, and Perspectives. Front. Zool 2018, 15, 1–21. [PubMed: 29434647]

317. Xue L; Sanz B; Luo A; Turner KT; Wang X; Tan D; Zhang R; Du H; Steinhart M; Mijangos C.Hybrid Surface Patterns Mimicking the Design of the Adhesive Toe Pad of Tree Frog. ACS Nano 2017, 11, 9711–9719. [PubMed: 28885831]

318. Kim DW; Baik S; Min H; Chun S; Lee HJ; Kim KH; Lee JY; Pang C.Highly Permeable Skin Patch with Conductive Hierarchical Architectures Inspired by Amphibians and Octopi for Omnidirectionally Enhanced Wet Adhesion. Adv. Funct. Mater 2019, 29, 1807614.

319. Iturri J; Xue L; Kappl M; García-Fernández L; Barnes WJP; Butt HJ; Del Campo A.Torrent Frog-Inspired Adhesives: Attachment to Flooded Surfaces. Adv. Funct. Mater 2015, 25, 1499–1505.

320. Autumn K; Peattie AM Mechanisms of Adhesion in Geckos. Integr. Comp. Biol 2002, 42, 1081–1090. [PubMed: 21680391]

321. Autumn K; Sitti M; Liang YA; Peattie AM; Hansen WR; Sponberg S; Kenny TW; Fearing R; Israelachvili JN; Full RJ Evidence for Van der Waals Adhesion in Gecko Setae. Proc. Natl. Acad. Sci. U.S.A 2002, 99, 12252–12256. [PubMed: 12198184]

322. Huber G; Mantz H; Spolenak R; Mecke K; Jacobs K; Gorb SN; Arzt E.Evidence for Capillarity Contributions to Gecko Adhesion from Single Spatula Nanomechanical Measurements. Proc. Natl. Acad. Sci. U.S.A 2005, 102, 16293–16296. [PubMed: 16260737]

323. Glick P; Suresh SA; Ruffatto D; Cutkosky M; Tolley MT; Parness A.A Soft Robotic Gripper with Gecko-Inspired Adhesive. IEEE Rob. Autom. Lett 2018, 3, 903–910.

324. Jiang H; Hawkes EW; Fuller C; Estrada MA; Suresh SA; Abcouwer N; Han AK; Wang S; Ploch CJ; Parness A.A Robotic Device Using Gecko-Inspired Adhesives Can Grasp and Manipulate Large Objects in Microgravity. Sci. Rob 2017, 2, eaan4545.

325. Raut HK; Baji A; Hariri HH; Parveen H; Soh GS; Low HY; Wood KL Gecko-Inspired Dry Adhesive Based on Micro–Nanoscale Hierarchical Arrays for Application in Climbing Devices. ACS Appl. Mater. Interfaces 2017, 10, 1288–1296. [PubMed: 29214798]

326. Zhang Y; Qu S; Cheng X; Gao X; Guo X.Fabrication and Characterization of Gecko-Inspired Dry Adhesion, Superhydrophobicity and Wet Self-Cleaning Surfaces. J. Bionic Eng 2016, 13, 132–142.

327. Jin K; Cremaldi JC; Erickson JS; Tian Y; Israelachvili JN; Pesika NS Biomimetic Bidirectional Switchable Adhesive Inspired by the Gecko. Adv. Funct. Mater 2014, 24, 574–579.

328. Ma S; Wang D; Liang Y; Sun B; Gorb SN; Zhou F.Gecko-Inspired but Chemically Switched Friction and Adhesion on Nanofibrillar Surfaces. Small 2015, 11, 1131–1137. [PubMed: 25331382]

329. Frost SJ; Mawad D; Higgins MJ; Ruprai H; Kuchel R; Tilley RD; Myers S; Hook JM; Lauto A.Gecko-Inspired Chitosan Adhesive for Tissue Repair. NPG Asia Mater. 2016, 8, e280.

330. Dayan CB; Chun S; Krishna-Subbaiah N; Drotlef DM; Akolpoglu MB; Sitti M.3D Printing of Elastomeric Bioinspired Complex Adhesive Microstructures. Adv. Mater 2021, 33, 2103826.

331. Wang Y; Hensel R.Bioinspired Underwater Adhesion to Rough Substrates by Cavity Collapse of Cupped Microstructures. Adv. Funct. Mater 2021, 31, 2101787.

332. Han D; Morde RS; Mariani S; La Mattina AA; Vignali E; Yang C; Barillaro G; Lee H.4D Printing of a Bioinspired Microneedle Array with Backward-Facing Barbs for Enhanced Tissue Adhesion. Adv. Funct. Mater 2020, 30, 1909197.

333. Park H-H; Seong M; Sun K; Ko H; Kim SM; Jeong HE Flexible and Shape-Reconfigurable Hydrogel Interlocking Adhesives for High Adhesion in Wet Environments Based on Anisotropic

Author Manuscript Author Manuscript Author Manuscript Author Manuscript

Swelling of Hydrogel Microstructures. ACS Macro Lett. 2017, 6, 1325–1330. [PubMed: 35650811]

334. Yang SY; O'Cearbhaill ED; Sisk GC; Park KM; Cho WK; Villiger M; Bouma BE; Pomahac B; Karp JM A Bio-Inspired Swellable Microneedle Adhesive for Mechanical Interlocking with Tissue. Nat. Commun 2013, 4, 1702. [PubMed: 23591869]

Author Manuscript Author Manuscript Author Manuscript Author Manuscript

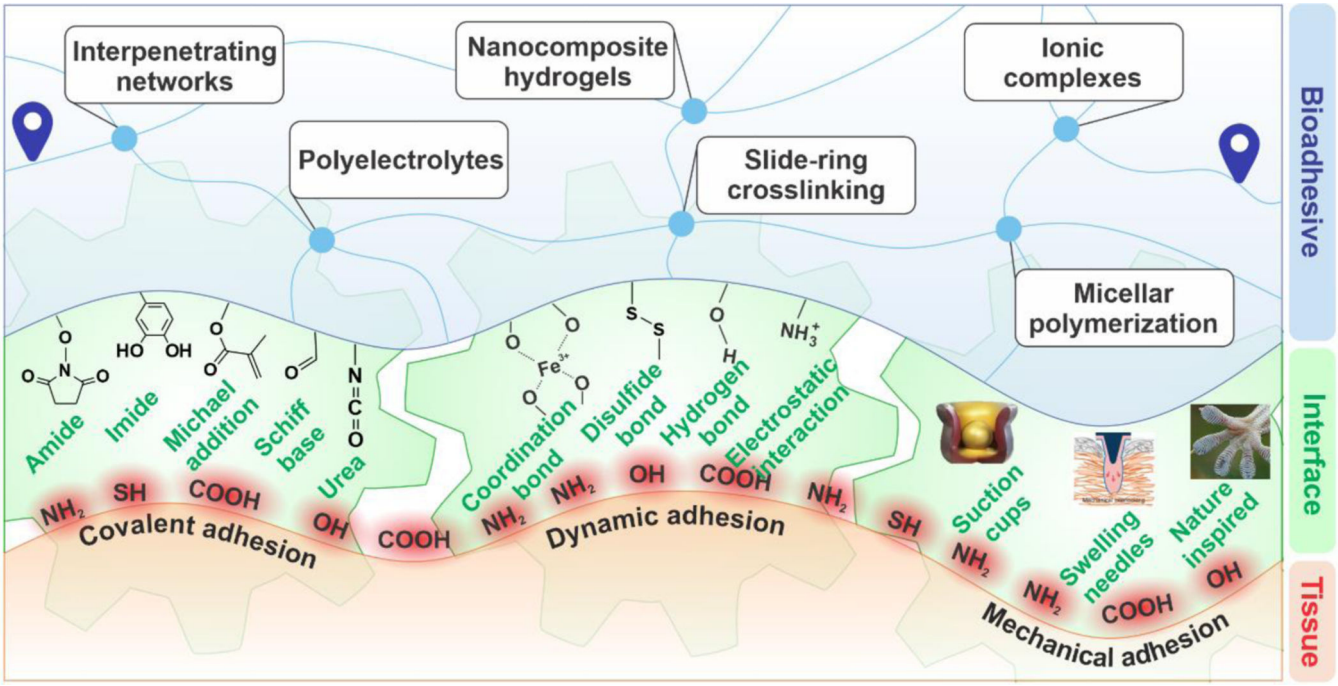

Figure 1. An overview of the material design roadmap for tough bioadhesives.

Development of bioadhesive materials involves: (i) design for cohesion where a combination of the polymer backbone and crosslinking strategy is selected to ensure mechanical durability in a tough hydrogel, and (ii) design for bioadhesion where a mixture of covalent and dynamic interactions, as well as mechanical interlocks, are incorporated into the material design.

Author Manuscript Author Manuscript Author Manuscript Author Manuscript

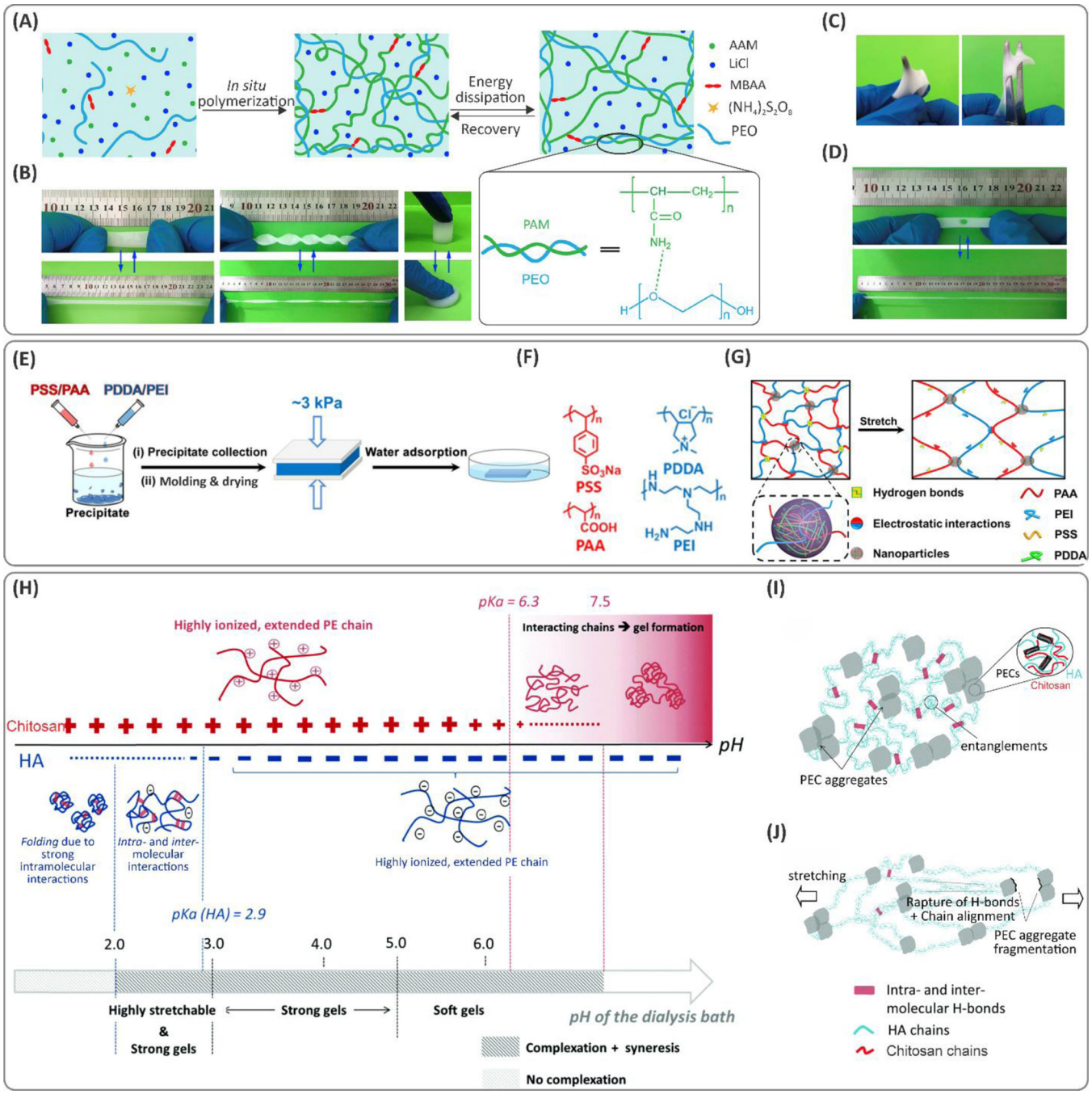

Figure 2. Examples of interpenetrating hydrogel networks (IPN) with improved toughness.

(A) Schematic of components and interactions in an IPN of poly(acrylamide) (PAM)/ poly(ethylene oxide) (PEO) hydrogel crosslinked by *N,N'*-methylene-bis(acrylamide) (MBAA) toughened due to the synergy between hydrogen-bonding and covalent networks. (B) Hydrogel resistance against tensile, compressive, and torsion deformations. The hydrogels were able to stretch by ~8.8×. (C) Hydrogels showed anti-puncturing characteristics. (D) The punctured hydrogels still maintained their stretchability. Reproduced with permission from ref [57]. Copyright 2019, Elsevier. (E) Schematic of processing

Author Manuscript Author Manuscript Author Manuscript Author Manuscript

poly(diallyldimethylammonium chloride) (PDDA)-poly(sodium 4-styrenesulfonate) (PSS)/branched poly(ethylenimine) (PEI)-poly(acrylic acid) (PAA) hydrogels. (F) Chemical structure of PSS, PAA, PEI, and PDDA components. (G) Toughening mechanism of the hydrogels: the effect of electrostatic interactions and hydrogen bonding. Reprinted with permission from ref [59]. Copyright 2019 American Chemical Society. (H) Effect of pH on the conformation of polyelectrolytes (PE). At low pH, chitosan is ionized resulting in polyelectrolyte repulsion. Hyaluronic acid (HA), on the other hand, tends to fold due to intramolecular interactions. As the pH increases (above pK_a of chitosan), a random coil conformation is formed by chitosan. Any further increase above pK_a of HA leads to its extended conformation. Schematic of molecular reformation of the chains before (I) and after (J) the application of stretching loads. The dissipative process stems from the interchain hydrogen bonding and crosslinking through the polyelectrolyte complex (PEC) aggregates and hydrogen bonding. Reproduced with permission from ref [60]. Copyright 2017, Royal Society of Chemistry.

Author Manuscript Author Manuscript Author Manuscript Author Manuscript

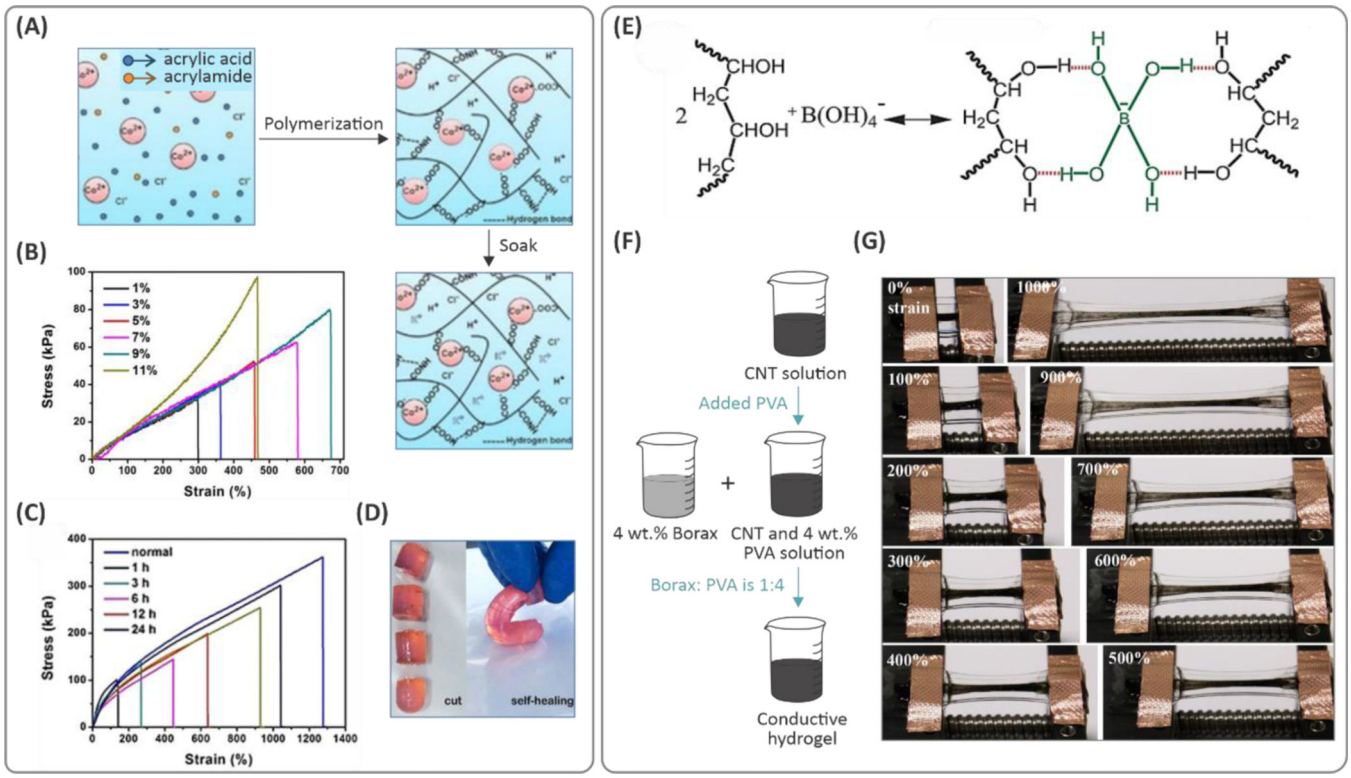

Figure 3. Engineering tough and stretchable ionic hydrogels.

(A) Processing scheme for the ionic hydrogels based on poly(acrylic acid-*co*-acrylamide)/$CoCl_2$ composition. (B) Effect of the Co^{2+} concentration on the tensile mechanical properties of the hydrogels. (C, D) Self-healing properties of the hydrogels and mechanical properties of the healed hydrogels at different time points. Reprinted with permission from ref [68]. Copyright 2019 American Chemical Societ€(E) Fabrication procedure of the carbon nanotubes (CNT)/poly(vinyl alcohol) (PVA) hydrogels with borax to form the PVA complex through (F) attraction of borax to the hydroxyl groups of the PVA chain. (G) Tensile deformation of the hydrogel by 1000%. Reproduced with permission from ref [71]. Copyright 2017, Wiley-VCH Verlag GmbH & Co. KGaA, Weinheim.

Author Manuscript Author Manuscript Author Manuscript Author Manuscript

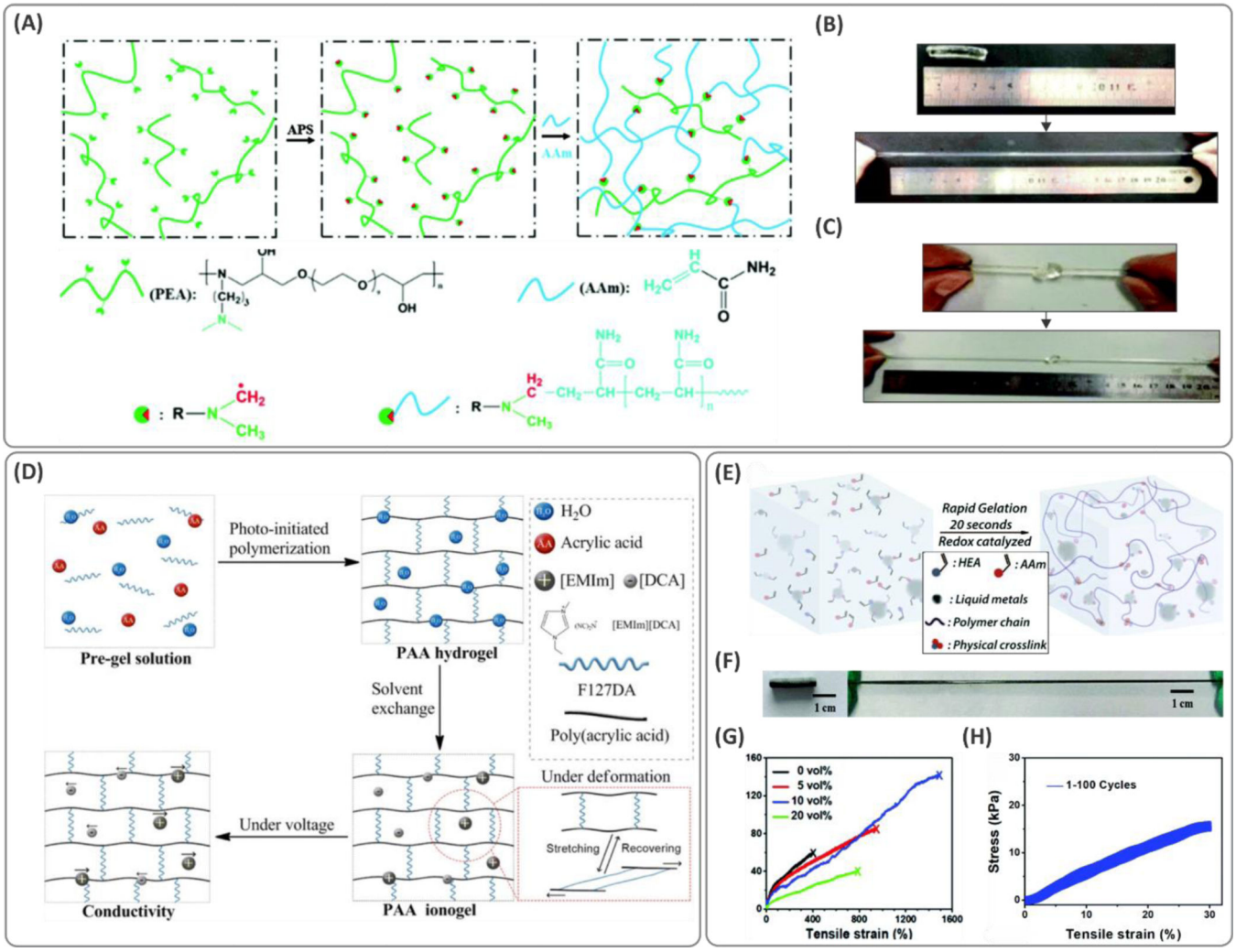

Figure 4. Creating tougher hydrogels through functionalization of the crosslinker and polymeric backbone.

(A) Functionalization of polyetheramine (PEA) with tertiary amines allowed the polymeric backbone to act as both the initiator and crosslinker during the radical polymerization in the presence of poly(acrylamide) (PAM) network. (B, C) Tough and stretchable hydrogels were obtained with stretchability of up to 2000%. Reproduced with permission from ref [75]. Copyright 2016, Royal Society of Chemistry. (D) Schematic illustration of the synthesis and deformation mechanism of poly(acrylic acid) (PAA) hydrogels crosslinked with Pluronic F127 (F127DA). Ionogels were fabricated by adding ionic liquid 1-ethyl-3-methylimidazolium dicyanamide ([EMIm][DCA]) through a solvent exchange process. The hydrogel showed high fatigue resistance for strains of up to 850%. Reprinted with permission from ref [66]. Copyright 2019 American Chemical Society. (E) Rapid synthesis procedure of the liquid metal-based hydrogels acrylamide (AAm) and 2-hydroxyethyl acrylate (HEA) formed *via* a redox catalyzed reaction. (F) Elasticity of the hydrogel and (G) the stress-strain curves showing stretchability at the optimized concentration of liquid metal (up to ~1500%). (H) Cyclic stress-strain curves of the hydrogel for 100 cycles. Reproduced with permission from ref [79]. Copyright 2019, Royal Society of Chemistry.

Author Manuscript Author Manuscript Author Manuscript Author Manuscript

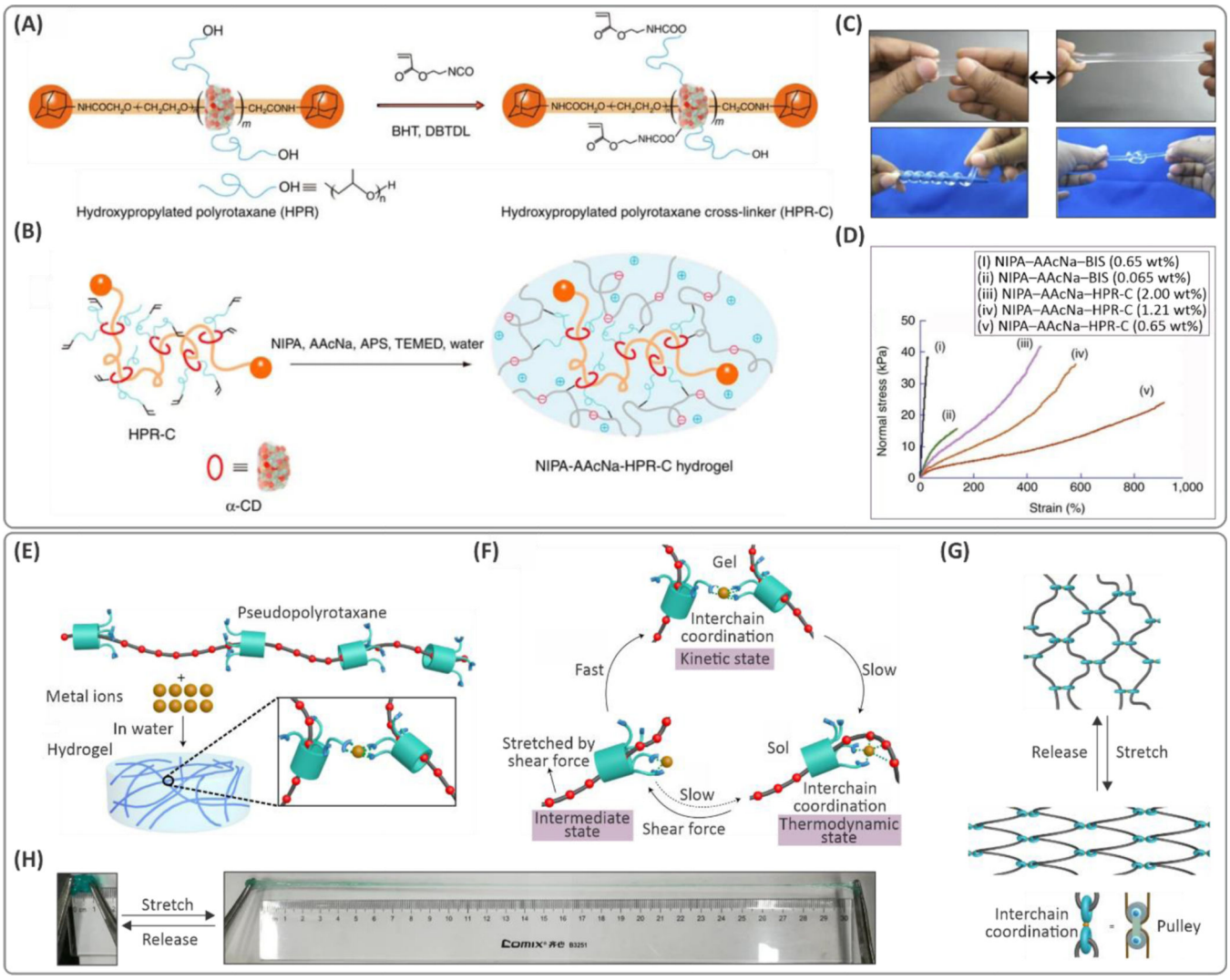

Figure 5. Examples of slide-ring polymers to form hydrogels with improved toughness.

(A) Molecular design of a hydroxypropylated polyrotaxane (HPR) crosslinker (HPR-C) based on α-cyclodextrin (α-CD) and (B) schematic of free radical copolymerization of *N*-isopropyl(acrylamide) (NIPA) and sodium acrylic acid (AAcNa) using the developed crosslinker. (C) Demonstration of highly stretchable and deformable hydrogels. (D) Stress-strain curves for (i) NIPA–AAcNa–*N,N*′-methylene-bis(acrylamide) (BIS) (0.65 wt%), (ii) NIPA–AAcNa–BIS (0.065 wt%), (iii) NIPA–AAcNa–HPR-C (2.00 wt%), (iv) NIPA–AAcNa–HPR-C (1.21 wt%) and (v) NIPA–AAcNa–HPR-C (0.65 wt%) shows the hydrogels containing the same amount of crosslinkers but different amounts of HPR-C crosslinker can stretch up to 912%, which is significantly higher than that of BIS crosslinker, (*i.e.*, 29%). Reprinted by permission from ref [81]. Nature Publishing Group, Copyright 2014. (E) Schematic illustration of the gelation *via* metal coordination through pseudo-polyrotaxanes. (F) The mechanism proposed for the thermal relaxation and shear-induced gelation effects. (G) Chain conformation changes with stretching the hydrogel, and (H) digital photographs of the hydrogel stretched by ~30×. Reprinted by permission from ref [84]. Nature Publishing Group, Copyright 2019.

Author Manuscript Author Manuscript Author Manuscript Author Manuscript

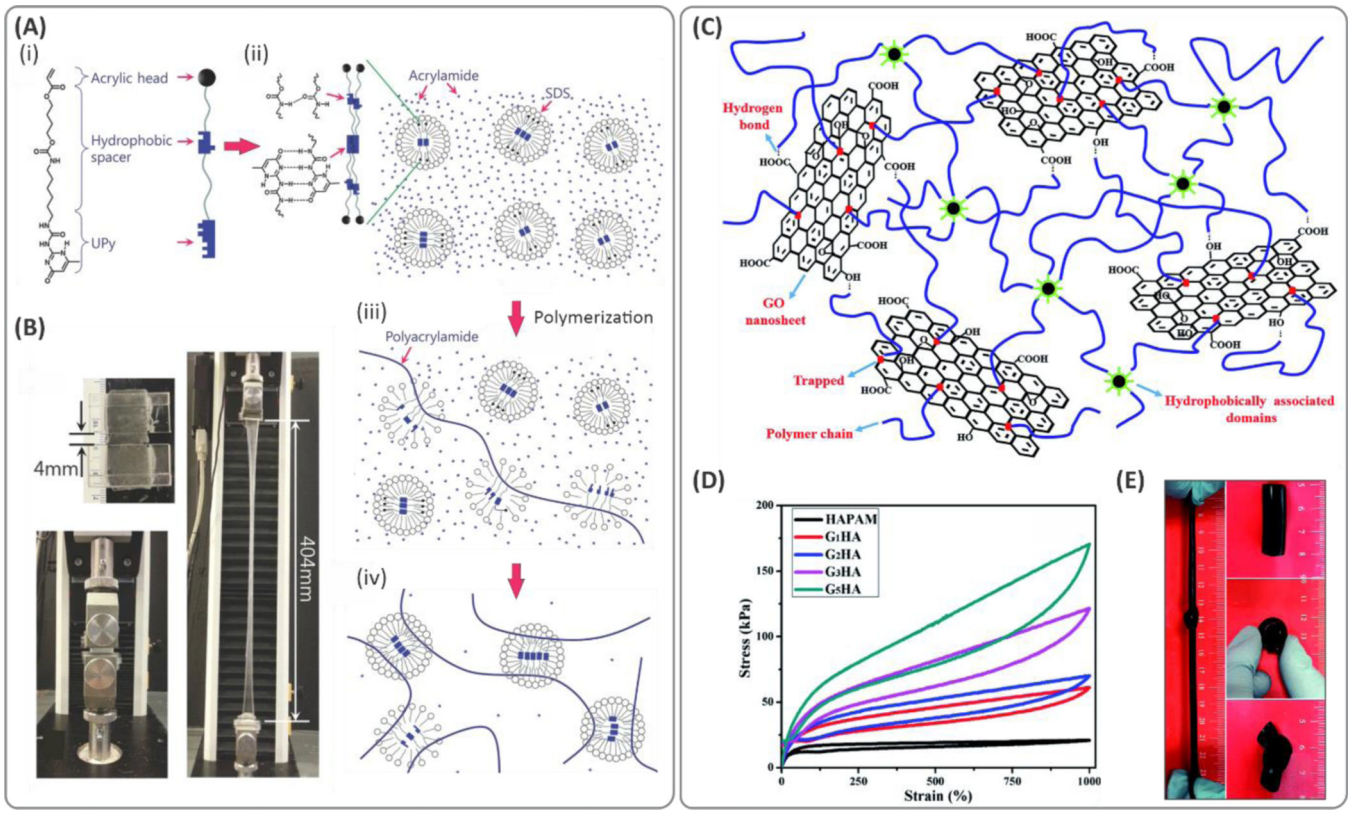

Figure 6. Examples of tough hydrogels created by micellar polymers.

(A) (i) Schematic illustration of the crosslinker based on hydrophobic interactions. (ii) A crosslinker that consists of an acrylic head, a hydrophobic alkyl spacer connected by carbamate, and a 2-ureido-4-pyrimidone (UPy) tail (UPyHCBA) and the micelles loaded with UPyHCBA in an acrylamide solution. (iii, iv) micellar copolymerization of acrylamide using the developed hydrophobic crosslinkers. (B) Demonstration of the stretchability of tough acrylamide hydrogels stretched by 100×. Reproduced with permission.[87] Copyright 2016, Wiley-VCH Verlag GmbH & Co. KGaA, Weinheim. (C) Dual crosslinking mechanism in the hydrophobically crosslinked polyacrylamide (PAM)/GO composite hydrogel. Hydrophobic domains formed by the interactions between hydrophobic sides of stearyl methacrylate (SMA) and sodium dodecyl benzene sulfonate (SDBS), which led to abundant dynamic crosslinking points well dispersed within the polymer network. (D) The stress-strain curves under cyclic loads demonstrating elasticity and strain-recovery of the hydrogels. (E) Digital photographs of the hydrogel under bending, knotting, and stretching conditions. Reproduced with permission from ref [88]. Copyright 2015, Royal Society of Chemistry.

Author Manuscript Author Manuscript Author Manuscript Author Manuscript

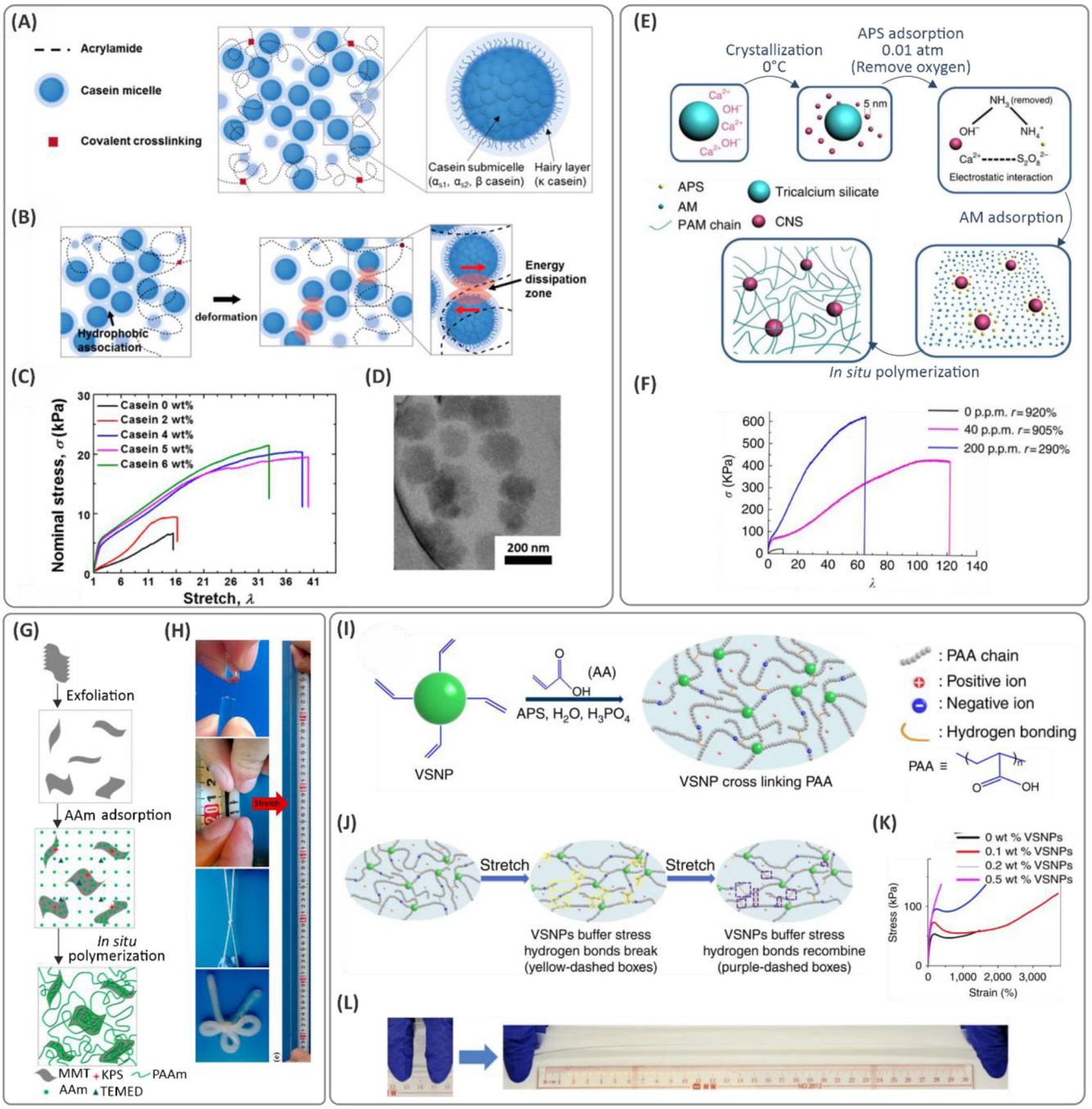

Figure 7. Examples of nanocomposite (NC) hydrogels.

(A) Internal components of a casein-reinforced polyacrylamide (PAM) hydrogel, and (B) schematic illustration of the toughening mechanism of casein additives due to energy dissipation through hydrophobic interactions. (C) The tensile mechanical properties, and (D) transmission electron microscopy (TEM) images of casein micelles in the hydrogels (reprinted with permission from ref [94]). (E) Fabrication process of tough nanocomposites mediated by incorporating calcium hydroxide ($Ca(OH)_2$) nano-spherulites (CNS) in a PAM network. The Ca_3SiO_5 releases Ca^{2+} and OH^- in a hydration process during which

Author Manuscript Author Manuscript Author Manuscript Author Manuscript

the small-sized CNS particles (<5 nm in size) are crystallized at 0 °C. The persulfate ions from the ammonium persulfate (APS) initiator are attracted electrostatically to CNS and act as crosslinkers. (F) Significant improvement of stretchability in PAM networks with small amounts of CNS. Reprinted by permission from ref [96]. Nature Publishing Group, Copyright 2016. (G) Fabrication steps of montmorillonite (MMT)/PAM composite hydrogels. (H) Digital photographs of bow-tied hydrogel, and tensile stretching of the hydrogels over 12000%. Reprinted with permission from ref [99]. Copyright 2015 American Chemical Society. (I) Preparation of vinyl functionalized hybrid silica nanoparticles (VSNPs)-poly(acrylic acid) (PAA) hydrogels where VSNP nanoparticles act as crosslinking points. (J) The mechanism explaining the improved hydrogel stretchability and molecular mechanism of deformation. (K) Stress-strain characteristics of the hydrogels with different amounts of VSNP nanoparticles, and (L) illustration of manually stretched hydrogels. Reprinted by permission from ref [107]. Nature Publishing Group, Copyright 2015.

Author Manuscript Author Manuscript Author Manuscript Author Manuscript

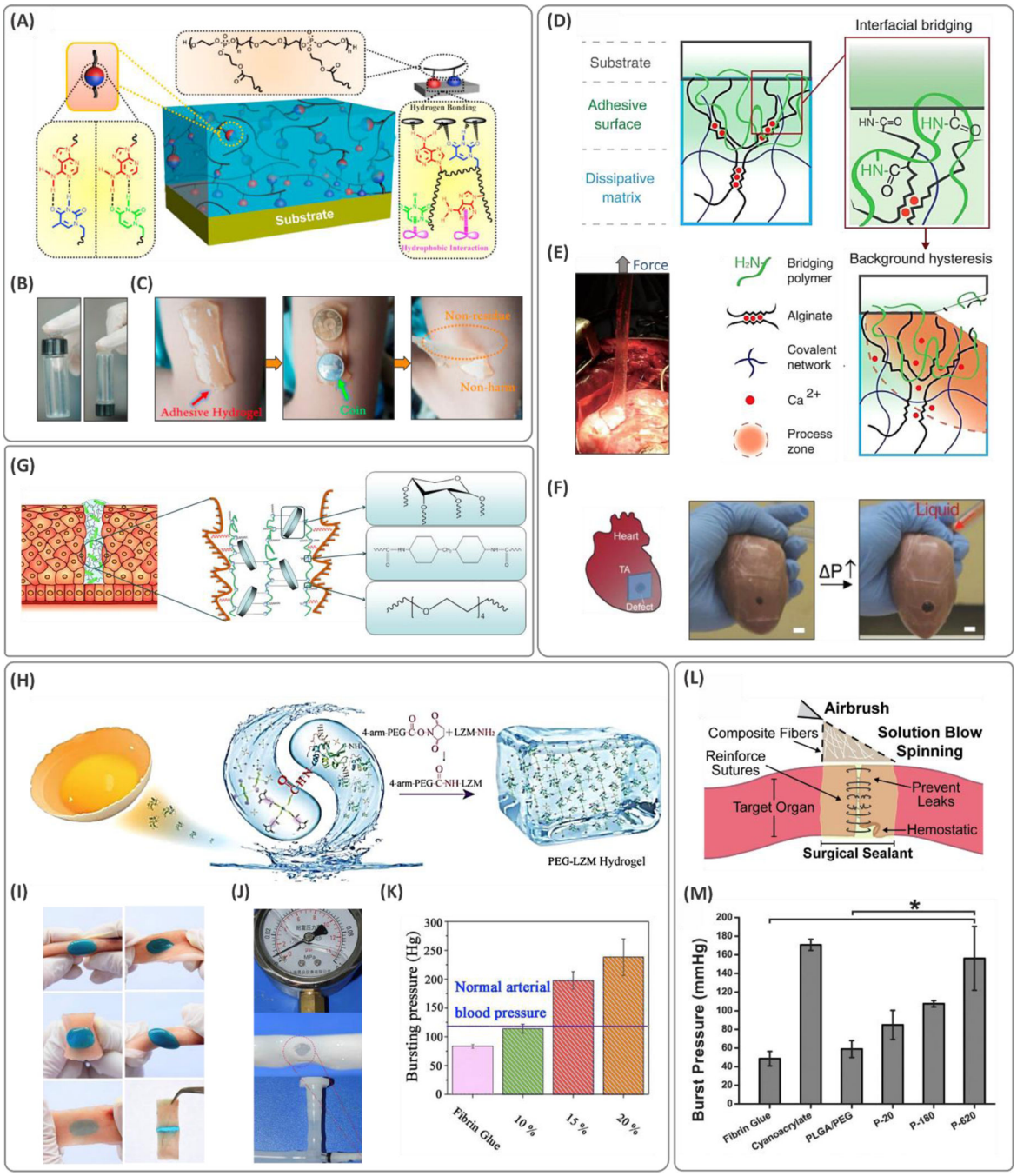

Figure 8. Methods and procedures for developing synthetic bioadhesives.

(A) Crosslinking mechanisms and the molecular interactions between the substrate leading to adhesion in nucleobase materials. (B) Demonstration of adhesion of polyphosphoesters to glass vials and (C) human skin. Reprinted with permission from ref [152]. Copyright 2019 American Chemical Society. (D) Schematic of the tough hydrogels comprised of a dissipative layer matrix and bridging polymers containing primary amines, which can diffuse into the substrate and the sealant. Propagation of a crack at the tissue interface is inhibited by the energy absorbed through the dynamic ionic bonds between the calcium ions

Author Manuscript Author Manuscript Author Manuscript Author Manuscript

and alginate chains. (E) Illustration of the tough adhesive adhered to the myocardium tissue while peeling off, and (F) under internal pressure. Reprinted with permission from ref [157]. Copyright AAAS. (G) Schematic of the xylose-based polyurethane (PU) sealant and their mechanism of adhesion. Reprinted with permission from ref [170]. Copyright 2016 American Chemical Society. (H) Chemistry of adhesion in the polyethylene glycol (PEG)-lysozyme (LZM) hydrogels formed *via* the amidation reaction between the egg-derived lysozyme protein and 4-arm-PEG-*N*-hydroxysuccinimide. (I) Demonstration of the conformation of hydrogels onto the tissue under different deformation scenarios. (J) *In vitro* analysis of the burst tests on the porcine vessels, and (K) the burst pressure results showing that the strength values are greater than those of the normal arterial blood pressure. Reproduced with permission from ref [17]. Copyright 2019, Elsevier. (L) Schematic of the composite fiber deposition on the wounded tissue using an airbrush acting as a surgical sealant. (M) Burst pressure data for the sealants show enhanced strength with increasing silica particle size in PEG/poly(lactic-*co*-glycolic acid) (PLGA)-based hydrogel. Reproduced with permission from ref [176]. Copyright 2019, Elsevier. *N*-hydroxysuccinimide, NHS.

Author Manuscript Author Manuscript Author Manuscript Author Manuscript

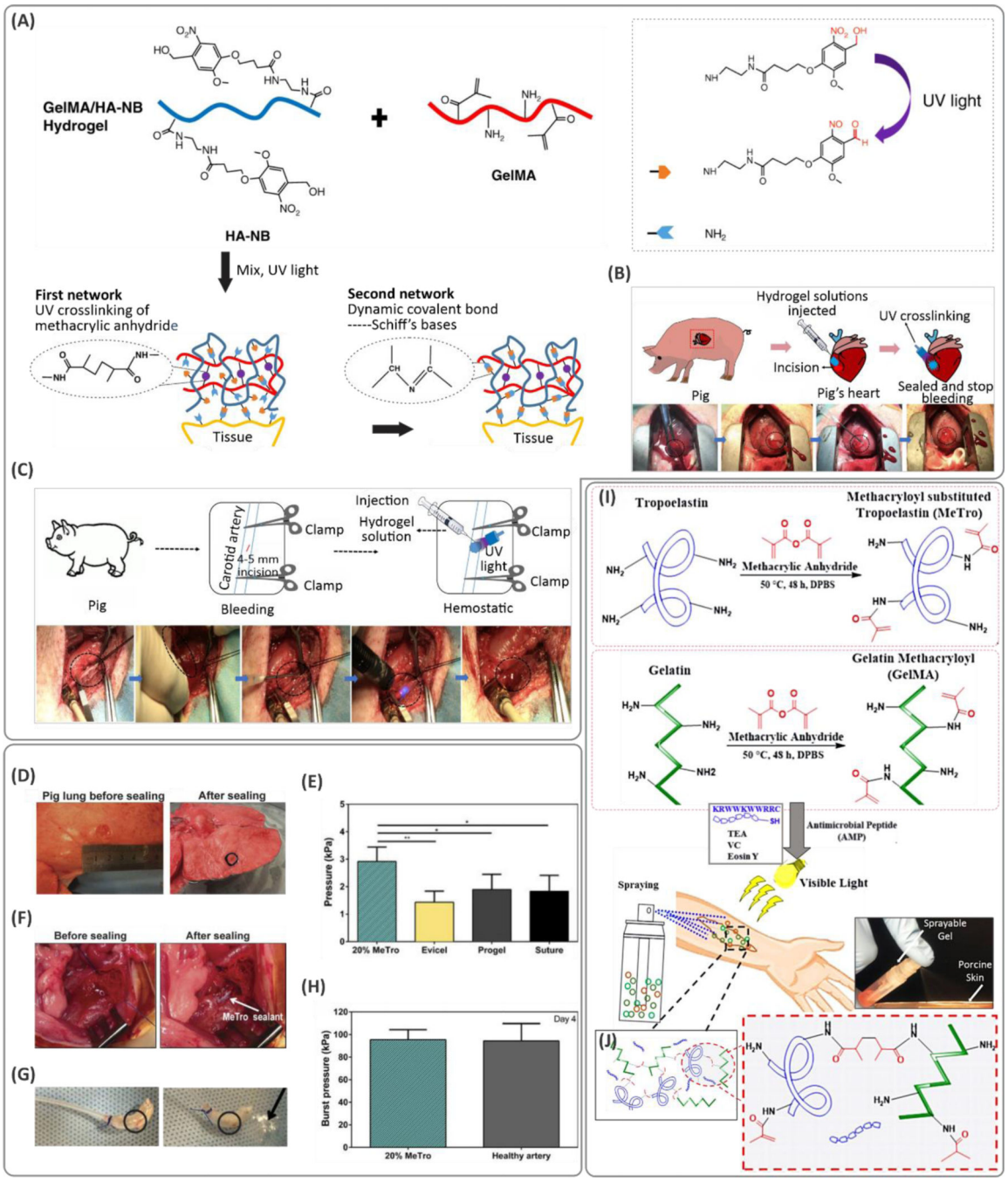

Figure 9. Different chemical modification strategies used to create gelatin-based bioadhesives.

(A) Chemical synthesis route for the development of highly adhesive and strong hydrogels based on modified hyaluronic acid (HA) and gelatin methacryloyl (GelMA) and its application in sealing (B) heart- and (C) arterial-related incisions. Reproduced with permission from ref [121]. Copyright 2019, Wiley-VCH Verlag GmbH & Co. KGaA, Weinheim. (D) *Ex vivo* evaluation of the methacryloyl-substituted tropoelastin (MeTro) sealant for sealing pig lung. (E) The sealing pressure was increased significantly using a MeTro hydrogel at 20 wt.% pre-polymer concentration. (F, G) Application of MeTro for

Author Manuscript Author Manuscript Author Manuscript Author Manuscript

sealing rat artery, and (H) the burst pressure suggesting the MeTro hydrogel is on the same order as a healthy artery. From ref [213]. Reprinted with permission from AAAS. (I) Synthesis of the MeTro and (J) GelMA pre-polymers for application on the wound site. (J) MeTro/GelMA hydrogels in a crosslinked network. Reproduced with permission from ref [230]. Copyright 2017, Elsevier.

Author Manuscript
Author Manuscript
Author Manuscript
Author Manuscript

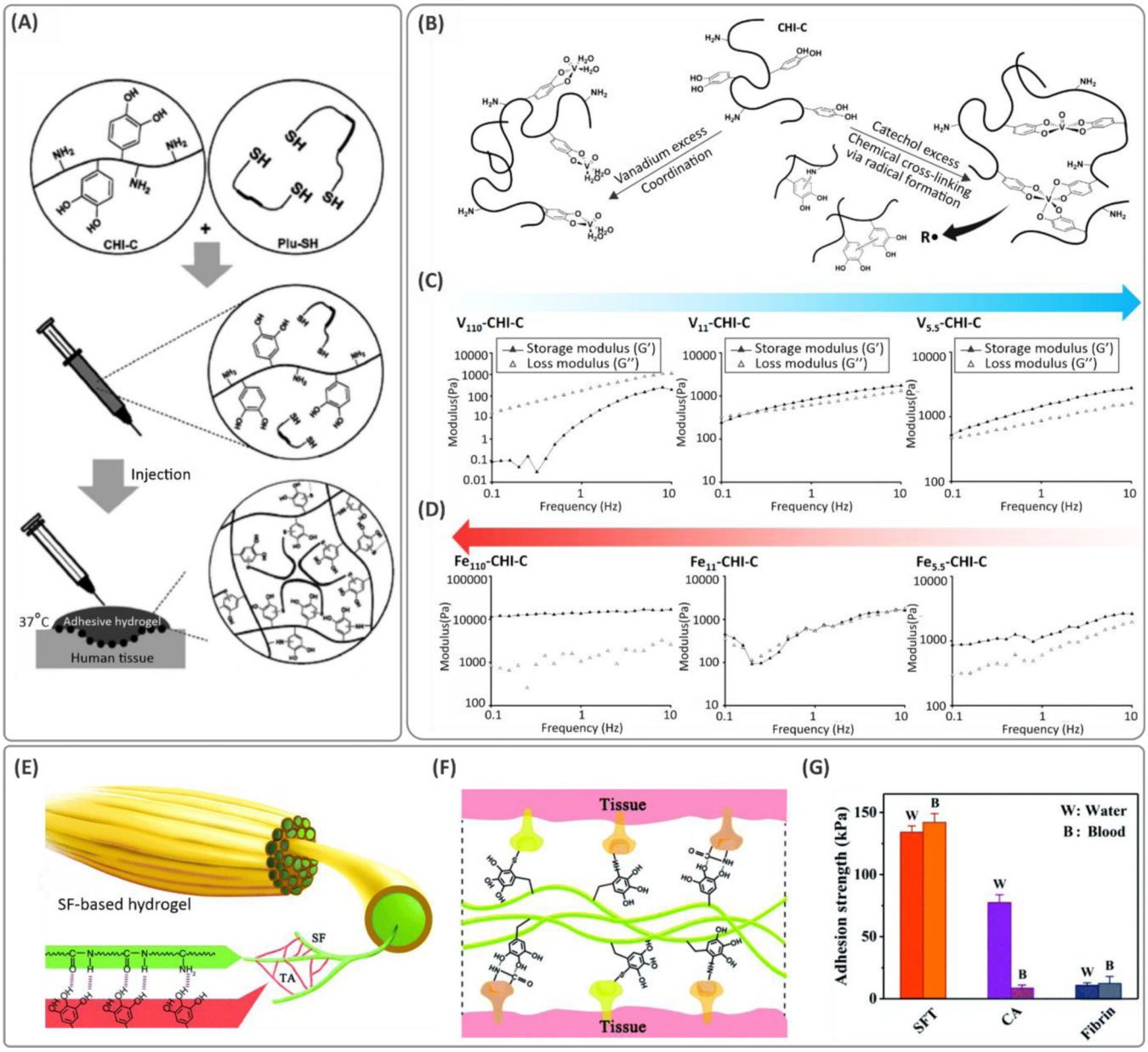

Figure 10. Mechanisms of introducing covalent and non-covalent interactions in catechol-terminated hydrogels.

(A) The crosslinking scheme of catechol functionalized chitosan (CHI-C) and thiolated Pluronic F127 (Plu-SH), resulting in thermosensitive *in situ* crosslinking at body temperature. Reprinted with permission from ref [259]. Copyright 2011 American Chemical Society. (B) Schematic of the crosslinking mechanism of catechol conjugated chitosan *via* vanadium. Rheological characterization of a pre-polymer containing 4 wt.% CHI-C with different compositions of (C) vanadium and (D) Fe^{3+} ions. Reprinted with permission from [265]. Copyright 2014 American Chemical Society. (E) Schematic of the mussel-inspired silk fibroin (SF)-based hydrogels, and (F) the different mechanisms of hydrogel-tissue adhesion. (G) Lap shear adhesive strength of the SF hydrogel sealant (SFT) is significantly higher

Author Manuscript Author Manuscript Author Manuscript Author Manuscript

than that of commercially available fibrin sealant. Reproduced with permission from ref [268]. Copyright 2019, Royal Society of Chemistry.

Author Manuscript Author Manuscript Author Manuscript Author Manuscript

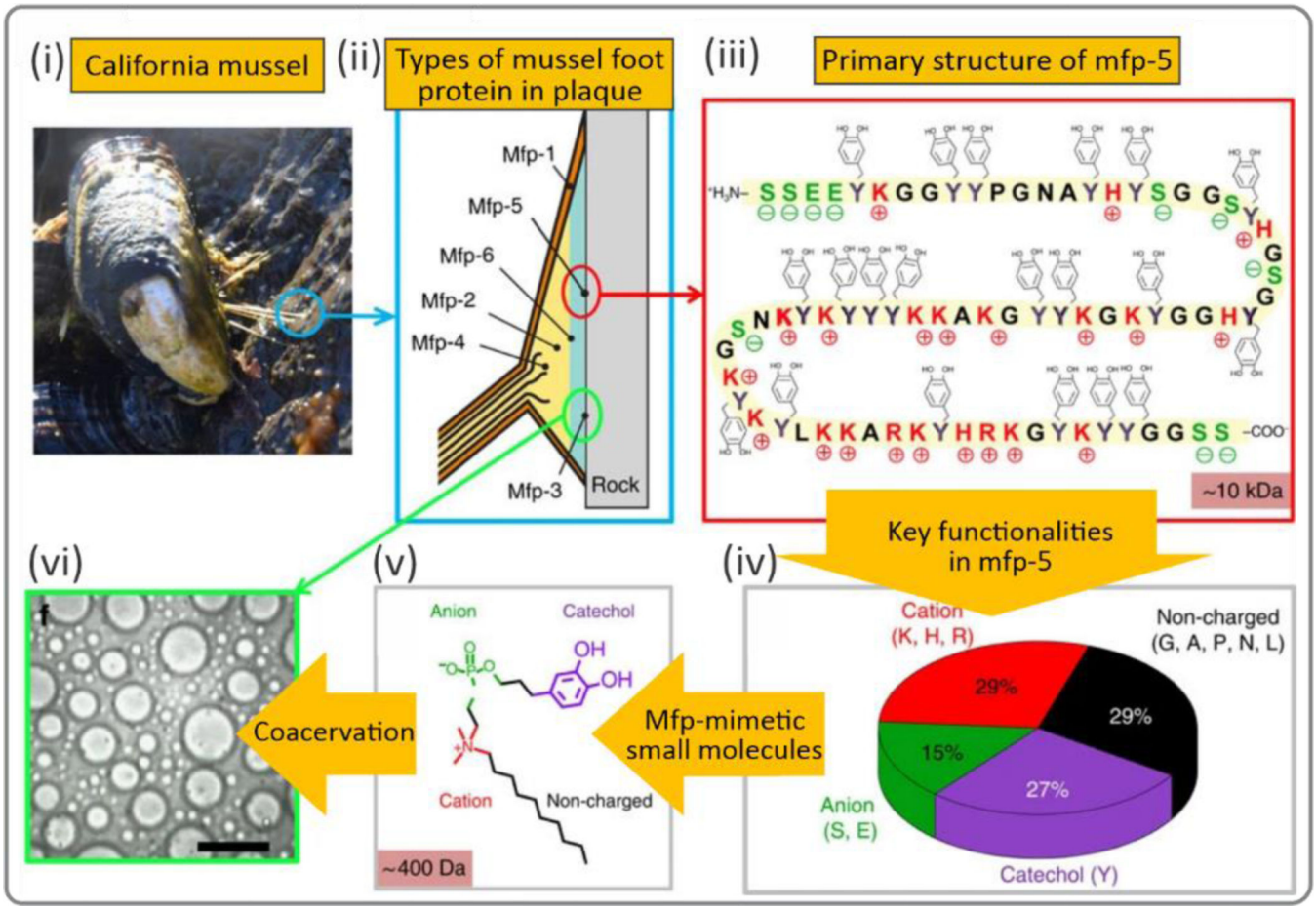

Figure 11. Mussel foot proteins (mfp)-inspired adhesive biomaterials.

(i) A mussel anchored by plaques and threads to a rock. (ii) Illustration of the mussel adhesive protein distribution within a plaque. (iii) The primary sequence of the mussel foot protein (mfp)-5, and (iv) distribution of the functionalities in mfp-5. (v) A polymer design based on small molecules to mimic the functionalities inside mfp-5, and (vi) micrograph photo of the liquid phase-separated zwitterionic surfactant (scale bar = 200 μm). Reprinted by permission from ref [274]. Nature Publishing Group, Copyright 2015.

Author Manuscript Author Manuscript Author Manuscript Author Manuscript

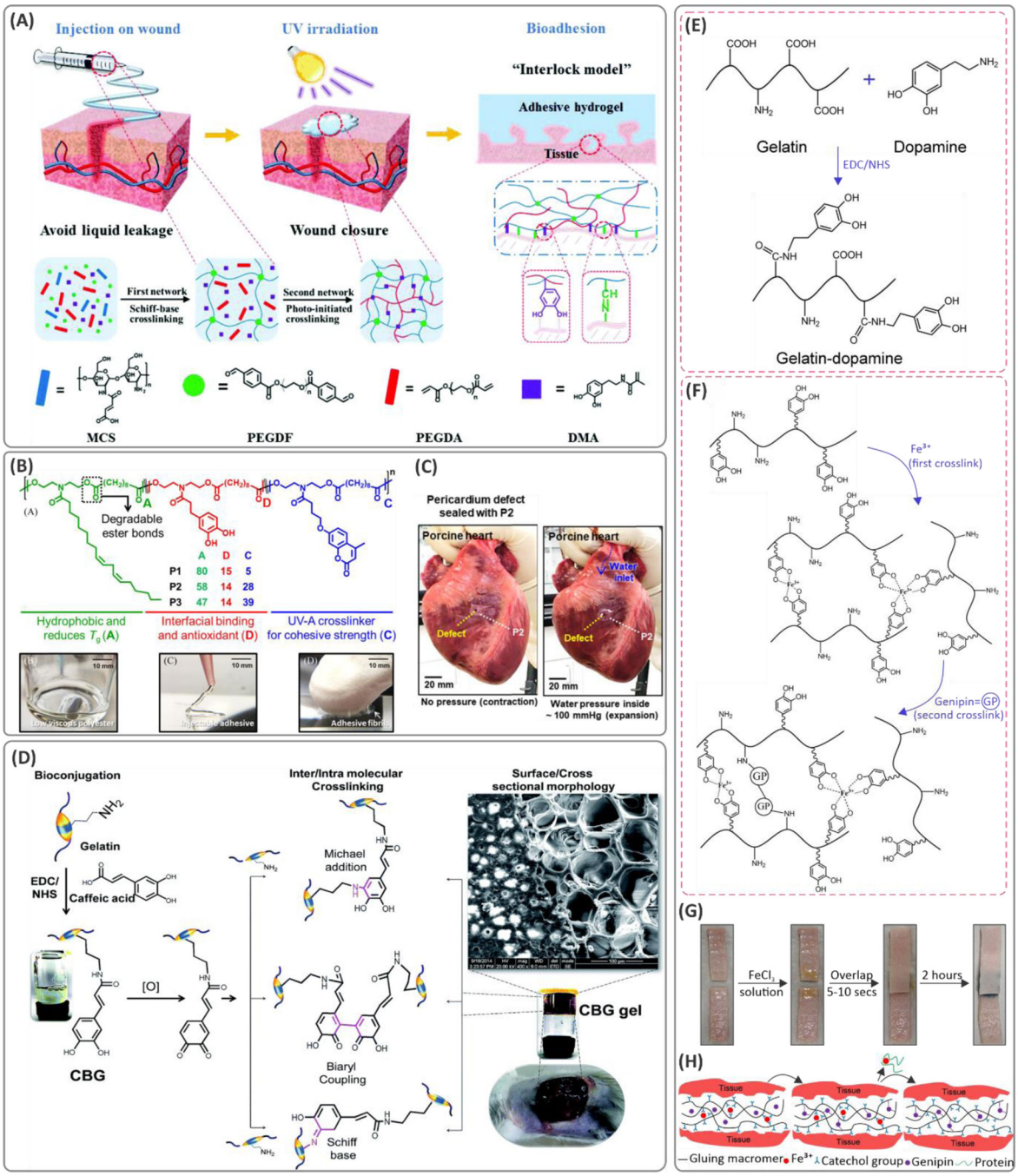

Figure 12. Examples of copolymerization of catechol-containing monomers, and conjugating catechol groups to the hydrogel polymer backbones for enhancing adhesion.

(A) Schematic of the fit-to-shape photocurable sealants and underlying mechanisms of crosslinking and adhesion to the tissue in wound-closure applications. The hydrogel is composed of PEGDF, maleic-modified chitosan (MCS), dopamine methacrylate (DMA), and poly(ethylene glycol)diacrylate (PEGDA) components. Reproduced with permission from ref [18]. Copyright 2019, Royal Society of Chemistry. (B) Molecular design of statistical co-polymer adhesives consisting of hydrophobic, interfacial bonding region, and crosslinking portions. (C) Application of the hydrogel for sealing incision and defects on

Author Manuscript Author Manuscript Author Manuscript Author Manuscript

the myocardium tissue. Reprinted with permission from ref [286]. Copyright 2019 American Chemical Society. (D) Carbodiimide coupling of the caffeic acid to the gelatin backbone as a wound dressing material. The caffeic-acid-bioconjugated gel (CBG) was crosslinked through Michael addition, biaryl coupling, as well as Schiff base formation mechanisms. Reproduced with permission from ref [289]. Copyright 2015, Royal Society of Chemistry. (E) Chemical conjugation of the dopamine to the gelatin backbone using carbodiimide chemistry. (F) Mechanism of dual ionic and covalent crosslinking of the catechol conjugated gelatin using Fe^{3+} ions and genipin. (G) The lap shear adhesion test and (H) the molecular mechanisms of adhesion to the tissue substrates. Reproduced with permission from ref [219]. Copyright 2016, Elsevier.

Author Manuscript Author Manuscript Author Manuscript Author Manuscript

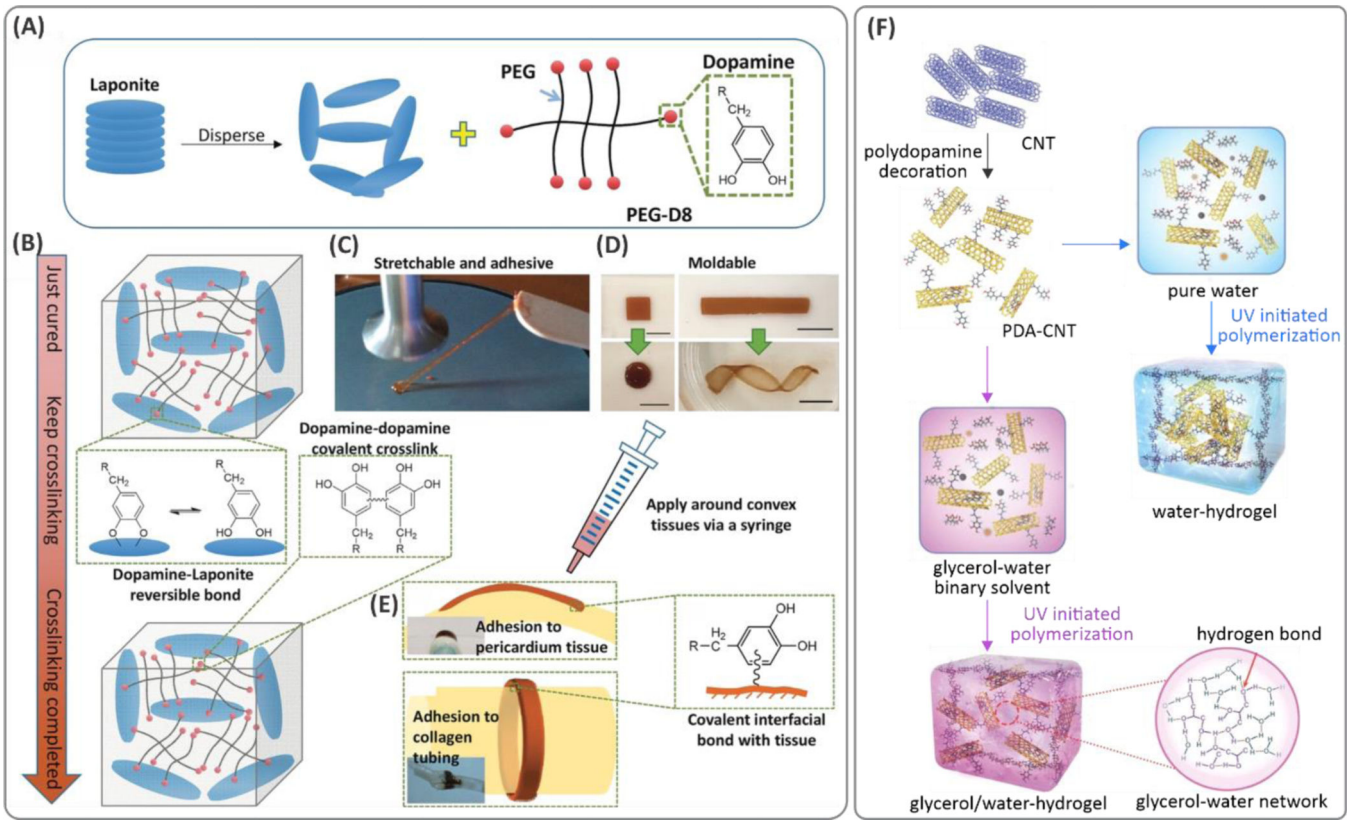

Figure 13. Coating nanoparticles with polydopamine (PDA) for nanocomposite (NC) hydrogel development and improvement in adhesion and cohesion.

(A) Design and processing of adhesive nanocomposite hydrogels based on Laponite® nanoclays. Multi-arm poly(ethylene glycol) (PEG) was capped with the catechol groups. (B) Curing occurred *via* a mixture of dynamic interactions and covalent bonds between the catechol-functionalized PEG and Laponite®. (C) Reversible and loose crosslinking as well as adhesion through catechol groups, and (D) moldability of the cured hydrogels. (E) Application of the adhesive hydrogel to the convex pericardium and collagen tubing and the mechanism of covalent bonding explaining adhesion. Reproduced with permission from ref [300]. Copyright 2017, Wiley-VCH Verlag GmbH & Co. KGaA, Weinheim. (F) Schematic of nanocomposite hydrogels based on PDA-coated carbon nanotubes (CNT). The UV-assisted crosslinking of the hydrogel network and internal strong hydrogen-bonding interactions between the polymer molecules led to gelation in the hydrogels. Reproduced with permission from ref [15]. Copyright 2018, WILEY-VCH Verlag GmbH & Co. KGaA, Weinheim.

Author Manuscript Author Manuscript Author Manuscript Author Manuscript

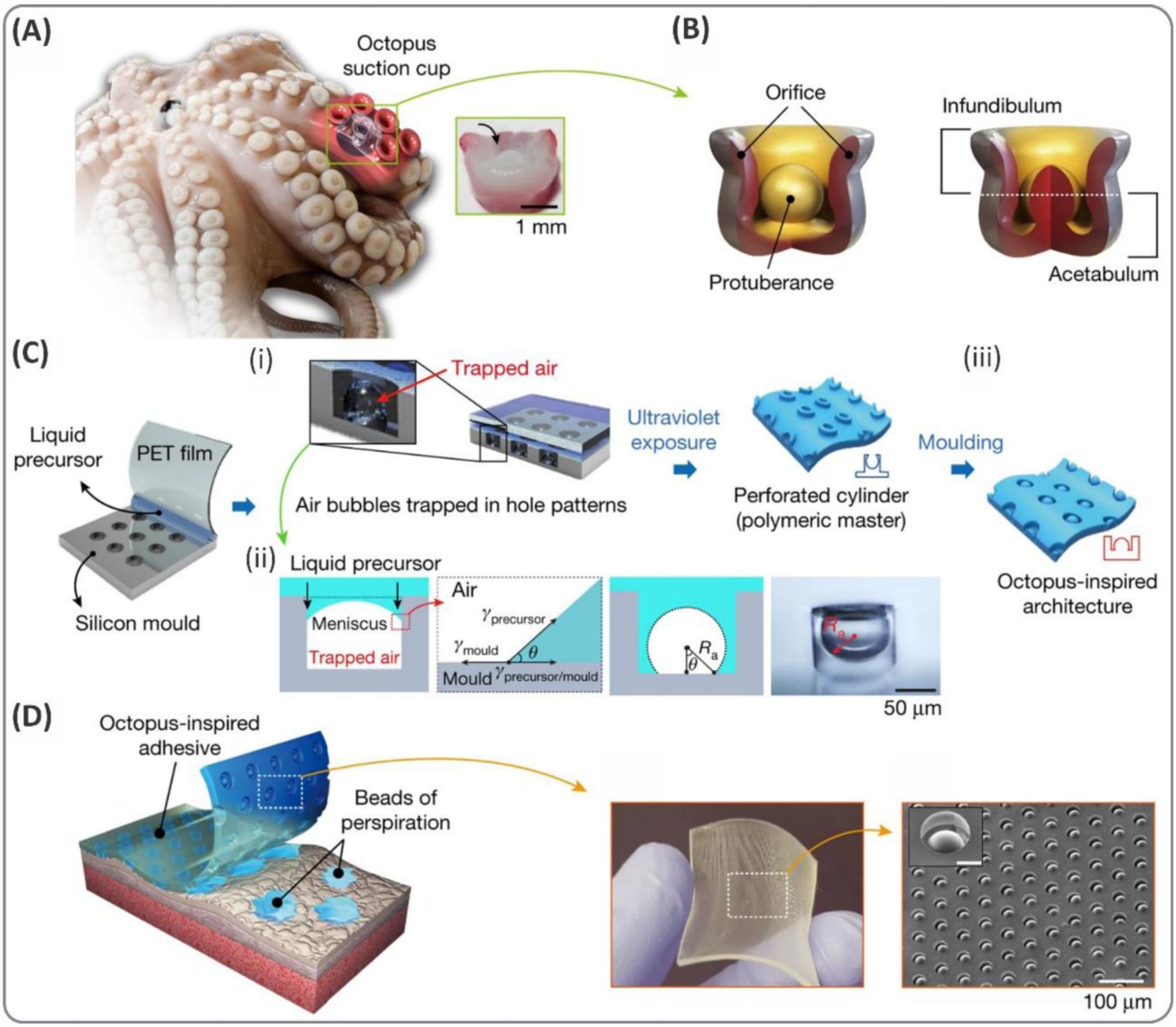

Figure 14. Illustration of octopus-inspired mechanical bioadhesives.

(A) Anatomical structure of *O. vulgaris tentacles.* (B) Suction cups on the *O. vulgaris* tentacles. (C) The fabrication process of the octopus-inspired adhesive tapes. (D) Illustration of the attachment mechanism of adhesive layers with octopus suction-inspired surface architecture. Reprinted by permission from ref [310]. Nature Publishing Group, Copyright 2017.

Author Manuscript Author Manuscript Author Manuscript Author Manuscript

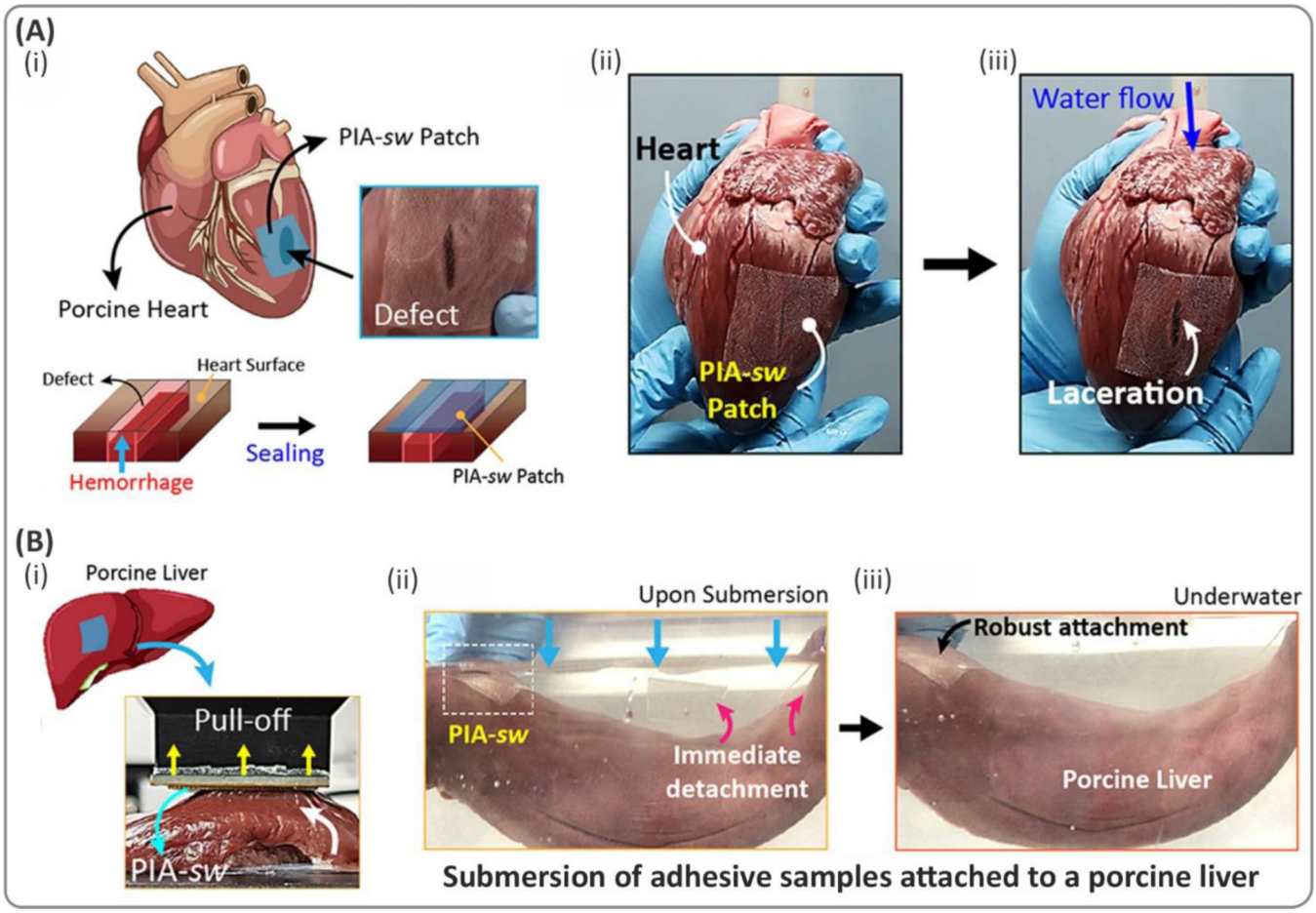

Figure 15. The application of organ-attachable wrinkled octopus-inspired adhesives for sealing incisions.

Demonstration of sealing wounds in (A) heart and (B) liver tissues using protuberance-inspired architectures (PIA) with soft wrinkles (*sw*). Reprinted with permission from ref [313]. Copyright 2019 American Chemical Society.

Author Manuscript Author Manuscript Author Manuscript Author Manuscript

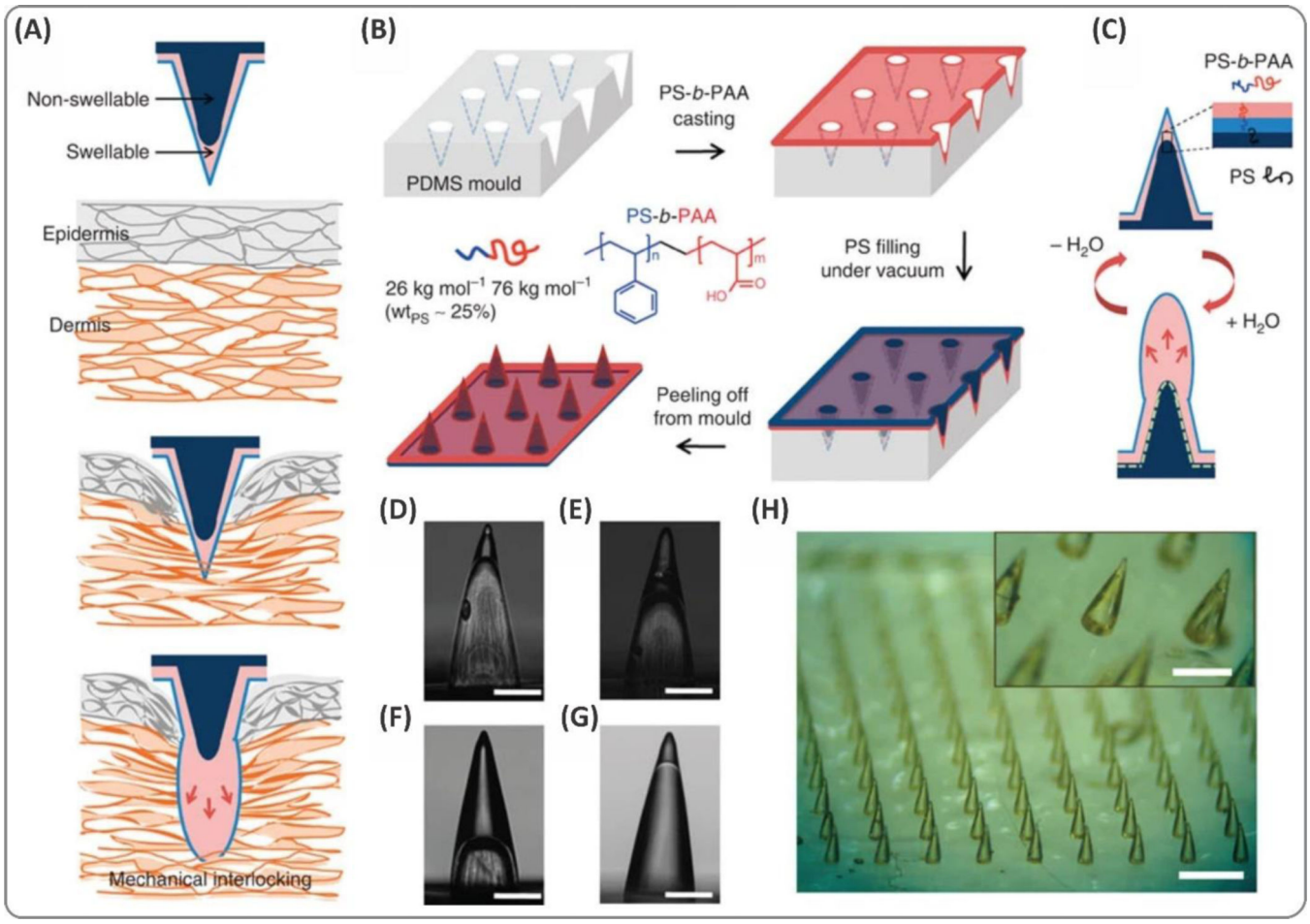

Figure 16. Swelling-mediated adhesive microneedles.

(A) Illustration of mechanical interlock adhesion enabled by swelling of the needle tip in the microneedle patches. (B) The fabrication process of the microneedle array using a polydimethylsiloxane (PDMS) mold and double-layered deposition of stiff PS core and swellable polystyrene-block-poly(acrylic acid) (PS-*b*-PAA) coating. (C) The mechanisms showing the swelling effect on the improved interlock with the tissue. (D-H) Magnified images of the fabricated needle tip on the microneedle arrays. Reprinted by permission from ref [334]. Nature Publishing Group, Copyright 2013.